

**ANALYSIS OF FRASER RIVER SOCKEYE SALMON COASTAL MIGRATION  
ROUTE VARIATION USING BAYESIAN ESTIMATION METHODS AND  
INDIVIDUAL-BASED MODELLING**

by  
**DALE SHAWN KOLODY**

B.Sc., University of Victoria, 1991

A thesis submitted in partial fulfillment of the  
requirements for the degree of  
Doctor of Philosophy  
in  
the Faculty of Graduate Studies  
(Department of Earth and Ocean Sciences)

We accept this thesis as conforming to the  
required standard

UNIVERSITY OF BRITISH COLUMBIA

1998

© Dale Kolody, 1998

In presenting this thesis in partial fulfilment of the requirements for an advanced degree at the University of British Columbia, I agree that the Library shall make it freely available for reference and study. I further agree that permission for extensive copying of this thesis for scholarly purposes may be granted by the head of my department or by his or her representatives. It is understood that copying or publication of this thesis for financial gain shall not be allowed without my written permission.

Department of EARTH AND OCEAN SCIENCES

The University of British Columbia  
Vancouver, Canada

Date 20 OCT 1998

## ABSTRACT

Sockeye salmon (*Oncorhynchus nerka*) can return from the Gulf of Alaska to the Fraser River by migrating around the north or south end of Vancouver Island and the proportion of fish using each route varies considerably among years. This thesis consists of three separate studies that contribute to the overall objective of understanding the migration route variation. The first two components are concerned with the estimation of migration routes from fisheries data, and potentially have additional practical implications for fisheries management. The third component examines some explicit interactions between individual behaviour and oceanographic variability that could potentially affect migration route selection.

The first study investigated how standard methods of estimating salmon fishery harvest rates introduce substantial errors because of violations to migration dynamics assumptions. This involved: 1) defining plausible stochastic salmon migration rate variability scenarios from observations of salmon migratory timing distributions and tagging studies, and 2) using Monte Carlo simulations of fisheries to examine how this variability affects harvest rate estimation when uniform migration rates are assumed during the process of run-reconstruction. A unique migration dynamics scenario could not be defined. Within the migration constraints that were identified, the simulations suggested that, in general, harvest rate estimates can be expected to be beta-distributed, and there is a potential underestimation bias for high harvest rates. The magnitude of the error variance and bias are dependent upon the migration dynamics, fishery temporal and spatial structure, and run-reconstruction method.

The second study presents methods for estimating harvest rates and migration routes in a multiple approach salmon fishery. The Bayesian approach explicitly admits uncertainty from 1) the confounded relationship between harvest rates and migration routes, 2) escapement estimation error that arises from run-reconstruction, and 3) the unknown relationship between harvest rates and effort. The resulting parameter uncertainty is reflected in posterior probability distributions. Potential advantages and disadvantages of adopting this method for the Fraser River sockeye fishery are examined.

The third study involved simulating adult sockeye salmon migration routes from the Gulf of Alaska to the coastal approaches of the Fraser River. A spatially-explicit individual-based model was used to explore potential mechanisms that could explain the observed interannual variation in migration routes. Assuming that sockeye are initially distributed throughout the central Gulf of Alaska and orient on a compass bearing, the following mechanisms were simulated to produce migration route variations among years in a physical environment described by dynamic surface temperatures and currents: 1) the distribution prior to homing was constrained by southern thermal limits, 2) sockeye were advected by currents during open ocean migration, and 3) sockeye tended to avoid high water temperatures. Optimization of the behavioral component of the model for a least squares fit between hindcast and observed coastal migration routes suggested that thermal limits and offshore-currents could not explain very much coastal migration route variability. Avoidance of high water temperature explained about 33% of the interannual variability and suggested that coastal processes (although poorly resolved in the model) could be more important than the offshore processes examined.

## TABLE OF CONTENTS

Abstract.....	ii
Table of Contents.....	iii
List of Tables.....	v
List of Figures.....	vi
Acknowledgements .....	viii
Chapter 1: General Introduction.....	1
Overview .....	1
Background .....	3
The migratory life history of Fraser River sockeye salmon.....	3
Fraser River sockeye fishery management: implications of coastal migration route variability .....	7
Review of previous studies examining the Fraser sockeye northern diversion rate ...	10
Chapter 2: Uniform Migration Rate Assumptions in Salmon Fishery Box Models Result in Beta-distributed, Biased, Reconstructed Harvest Rate Estimates .....	17
Abstract .....	18
Introduction .....	19
Box model representation of a gauntlet salmon fishery.....	21
Box Model Notation .....	21
Reconstruction of harvest rates.....	23
Violation of the order of movement assumption .....	26
Representing stochastic migration rate variability with a modified boxcar model....	28
Representing Fraser River sockeye salmon coastal migration dynamics with a modified boxcar model.....	31
Monte Carlo simulations of Fraser sockeye fisheries.....	37
Example (2.1).....	37
Harvest rate error distribution dependence on migration dynamics and fishery characteristics.....	42
Discussion .....	44
Chapter 3: A Bayesian Method for Estimating Harvest Rates and Migration Routes in The Fraser River Sockeye Salmon Fishery.....	55
Abstract .....	56
Introduction .....	57
Fishery notation.....	58
Problems associated with estimating harvest rates and migration routes in a multiple approach fishery.....	60

Overview of the Bayesian estimation method.....	62
Example (3.1): simultaneous estimation of migration routes and harvest rates in a hypothetical fishery with two approach routes.....	66
The Relationship between harvest rates and fleet size.....	67
The likelihood calculation.....	69
Specification of priors.....	74
Posteriors for example (3.1).....	76
Discussion .....	78
Chapter 4: Numerical Simulations of Fraser River Sockeye Salmon Homing Migration Routes in a Dynamic Marine Environment.....	91
Abstract .....	92
Introduction .....	93
Methods.....	95
Numerical representation of the physical oceanography of the north-east Pacific Ocean .....	95
Numerical representation of sockeye salmon homing migration behaviour.....	96
Optimization with a floating point genetic algorithm.....	99
Stepwise assessment of mechanisms potentially affecting coastal migration routes	104
Results .....	104
Effects of thermal constraints on the sockeye distribution prior to homing.....	105
Effects of current advection.....	106
Effects of a behavioural tendency to avoid high SST during homing migration.....	106
Effects of combined mechanisms .....	107
Discussion .....	108
Chapter 5: General Discussion .....	119
References .....	127

## LIST OF TABLES

Table 2.1. Qualitative summary of how the bias and error variance of harvest rate estimates are dependent on fish migration dynamics and fishery characteristics.....	47
Table 3.1. Temporal and spatial structure of northern and southern approach route fisheries defined in example (3.1).....	82
Table 3.2. A hypothetical time series of observations from the fishery with two approach routes in example (3.1).....	83
Table 4.1. Range of valid parameter values in the spatially-explicit individual-based migration model.....	113
Table 4.2. Goodness of fit between modelled and observed Fraser River sockeye salmon coastal migration routes (1982-94).....	114

## LIST OF FIGURES

Figure 1.1. Map of the coastal approaches to the Fraser River showing important locations. ....	15
Figure 1.2. Time series of the Fraser sockeye northern diversion rate.....	16
Figure 2.1. Illustration of how variable salmon migration dynamics affect harvest rate estimation. ....	48
Figure 2.2. Illustration of salmon migratory timing anomaly indices.....	49
Figure 2.3. Anomaly indices observed for various Fraser sockeye runs 1992- 94. ....	50
Figure 2.4. Comparison of observed and simulated salmon migration rate distributions. ....	51
Figure 2.5. Error distributions of estimated harvest rates produced by Monte Carlo simulations.....	52
Figure 2.6. Comparison of harvest rate error distributions from Monte Carlo simulations and the likelihood model.....	53
Figure 2.7. Harvest rate posteriors.....	54
Figure 3.1. Relationships between elemental harvest rate and fleet size.....	84
Figure 3.2. Joint distribution for $L(E'_n, E'_s   C_n, C_s, \theta_k, \phi_k)$ illustrating the calculation of $L(E'_{n+s}   C_n, C_s, \theta_k, \phi_k)$ .....	85
Figure 3.3. Priors for the parameters in example (3.1).....	86
Figure 3.4. Implicit prior for harvest rates in example (3.1). ....	87
Figure 3.5. Northern diversion rate posteriors for example (3.1).....	88
Figure 3.6. $\phi$ posteriors for example (3.1). ....	89
Figure 3.7. Implicit posteriors for harvest rates in example (3.1). ....	90
Figure 4.1. Range of sockeye salmon initial distributions that resulted when the migration model was optimized with thermal limit constraints on the initial distribution. ....	115

Figure 4.2. Initial distribution and mean migration trajectories that resulted when the model was optimized with offshore current variability. ....	116
Figure 4.3. Typical trajectories that resulted when the model was optimized with a behavioural tendency to avoid high SST. ....	117
Figure 4.4. Comparison of simulated and observed annual northern diversion rates (1982-94).....	118



## ACKNOWLEDGEMENTS

I wish to thank numerous people for their support and contributions to this project. I am greatly indebted to Michael Healey, my supervisor, for many productive discussions, encouragement and his perspectives that seemed at times to be both broader and more focused than my own. I also thank my committee members Paul Leblond, Jim Woodey, Keith Thomson and William Hsieh. Thanks to Jim Cave for providing a considerable amount of data and patient explanation of the Fraser salmon fishery. Other members of the biophysical controls of salmon migration and production group were very helpful, particularly Sean Cox, Leonardo Huato, Ian Jardine, James Scandol, Peter Rand and Scott Hinch. Don Ludwig provided useful criticism to key parts of this thesis. Carl Walters was an important influence on this work in direct and indirect ways. This work was funded by an NSERC strategic grant.

Without the continuous encouragement, amusing correspondence, and welcome diversion of family and friends it is unlikely that this task would have been completed. To my parents, John and Mildred, and cohort members, Brenda and Brian I am very grateful. Many friends made more of an impact than they can imagine, including Christine Adkins, Michael Baumann, Kim Carr, Ana Carrasco, Steven Dokken, Pierre Dubeau, Maya Evenden, Brian Grant, John Grant, Gertjan Hofman, Maria Morlin, Derek Nishimura, Daniel Ricard, Corinne Rocchini, Joel Sawada, Andrew Thomson and Lisa Thompson. I attribute many of my happier memories during the darkest months to Sarah Bunce.

Finally, I thank Kim Hyatt, whose timely influence rekindled my interest in aquatic biology.

## CHAPTER 1: GENERAL INTRODUCTION

### OVERVIEW

Sockeye salmon (*Oncorhynchus nerka*) have a complex life history characterized by extensive freshwater and marine migrations. Spawners demonstrate the remarkable ability to return to their natal streams after migrating for thousands of kilometers in the north Pacific Ocean, and the consistency of their migration routes and return timing is an integral part of the fisheries and fisheries management tactics that have developed for this species. The sensory and navigational processes that guide these migrations are of considerable theoretical interest to biologists from evolutionary, behavioural and physiological perspectives, but remain poorly understood. This thesis describes my attempts to improve the understanding of Fraser River sockeye salmon homing migration dynamics, and was motivated jointly by theoretical interest in the interactions between fish behaviour and oceanographic variability, and by the practical relevance for fisheries management.

A number of features contributed to the selection of Fraser River sockeye for this study, including multiple homing migration routes, a history of fisheries data collection, and prior migration studies on these stocks. Adult sockeye salmon can return from the

Gulf of Alaska to the Fraser River by migrating around either the north or south end of Vancouver Island (fig. 1.1), and the proportion of fish using each route varies considerably among years (fig. 1.2). This observational contrast provides the means with which interactions between salmon migration behaviour and oceanographic variability may be explored.

Uncertainty in the proportion of fish migrating via the northern route around Vancouver Island (northern diversion rate) complicates the task of fisheries managers attempting to meet complex harvest allocation goals and confounds the estimation of harvest rates that are important for in-season stock assessment and scheduling fishery openings. The migration route estimates are generated from fisheries observations, and a long historical time series is present, the collection of which would have been impossible for a typical research program. However, fisheries data are rarely collected with ideal sampling procedures, and this led to the first two studies presented in this thesis that were aimed at understanding the error structure of fisheries harvest rates, and developing formal methods of estimating coastal migration routes from these data. These studies thus have implications for theoretical pursuits that rely on fisheries observations, and have additional relevance for fisheries management.

The final study examined some explicit interactions between hypothesized individual behaviour and actual oceanographic variability that could potentially affect Fraser sockeye migration routes. The ability to explain and reliably predict coastal

migration route variation would also be of considerable use to managers, but the final study represented only an incremental step towards attainment of that ambitious goal.

This thesis is structured in 5 chapters. The remainder of this introductory chapter (1) describes the relevant background material and places the research into a theoretical ecological and practical management context. Chapter (2) describes how harvest rates are estimated in salmon fisheries and examines how simplifying assumptions about migration dynamics can be expected to introduce systematic errors. Chapter (3) builds on the results of chapter (2), and presents a Bayesian method for estimating confounded harvest rates and migration routes in a multiple approach salmon fishery. Chapter (4) describes my attempt to model the observed historical salmon migration route variability by simulating salmon behaviour on temporal and spatial scales that are relevant to the decision process of individuals in a dynamic marine environment. The final chapter (5) provides a general discussion, suggesting avenues for future research and additional applications for the methods presented here.

## **BACKGROUND**

### *THE MIGRATORY LIFE HISTORY OF FRASER RIVER SOCKEYE SALMON*

Fish communities of the central subarctic domain of the NE Pacific Ocean are dominated by sockeye, pink and chum salmon (Ware and McFarlane 1989),

demonstrating the evolutionary success of the anadromous life history. Of these species, sockeye exhibit the most complicated life cycle, with substantial marine and freshwater phases. Large lifetime energy expenditures, specialized sensory abilities, and precise regulatory mechanisms are required to ensure that individuals complete the final, spawning phase of the migration at an extremely precise point in space and time. The selective advantages of migration must have been substantial for this life history strategy to have evolved in spite of these costs and constraints. However, the biological processes controlling the migration remain poorly understood, and the temporal and spatial characteristics of the abundance distributions are poorly described, particularly in the marine environment.

The Fraser River is the largest and most valuable sockeye salmon producing system in British Columbia (Starr et al. 1984), consisting of more than 50 stocks, and supporting important aboriginal, commercial and recreational fisheries. The majority of these fish follow a similar 4 year life history, beginning as fertilized eggs in the autumn. The eggs generally hatch in tributaries near lake systems in the following spring, and fry migrate into nearby lakes where they begin feeding and growing. After one year (occasionally two) in the nursery lake, most of the yearlings migrate downstream, through the Fraser River and into the Strait of Georgia during April-June. The smolts migrate north along the coast of British Columbia and SE Alaska, and eventually move offshore and spread across vast areas of the NE Pacific Ocean (French et al. 1976). After spending approximately two years (1 or 3 years for a small proportion) in the Gulf of Alaska, maturing sockeye engage in a rapid, well-timed and directionally precise homing

migration (Groot and Quinn 1987). The adult fish are exposed to a gauntlet of sequential fisheries as they migrate along the coastal approaches to the Fraser River, and a number of additional fish are taken by aboriginal fisheries within the river. Those that escape the fisheries return to their natal streams with remarkable fidelity and spawn.

Many different guidance mechanisms may be active during the marine phase of the salmon homing migration. Direction-finding mechanisms are commonly divided into three categories originally defined by Griffin (1955): piloting, compass-orientation, and bi-coordinate navigation. Piloting is defined as the ability to reach a goal by recognizing familiar landmarks. It has been demonstrated fairly conclusively that many salmonids recognize odours from their natal streams, and rely on odour detection as a form of piloting during upstream migrations (e.g. Cooper and Scholz 1976, Groot et al. 1986, Shimizu 1993). However there is no evidence to suggest that salmon are following odours or other familiar landmarks during the marine phase of migration. It has also been shown that returning adults can use migration routes that differ from those experienced as juveniles (Groot and Cooke 1987). This indicates that piloting is not a sufficient navigational scheme for the marine homing migration. Compass orientation is defined as the ability to reach a goal by orienting to particular compass directions irrespective of local landmarks. It has been demonstrated that salmon can discriminate celestial patterns (Quinn and Brannon 1982, Hawryshyn and Bolger 1990) and geomagnetic fields (Quinn 1980, Quinn and Brannon 1982), all of which provide a compass bearing. Numerical simulations have suggested that compass orientation is sufficient to explain the offshore marine phase of Fraser sockeye homing migrations provided that the bearing varies

depending on the initial position (Dat et al. 1995). Bi-coordinate navigation is the most complex direction-finding mechanism, and is defined as the ability to orient toward a fixed goal from different geographic locations, which are not necessarily familiar to the organism (i.e. the organism has behavioural and sensory abilities analogous to not only a compass, but also a map). Healey and Groot (1987) have argued that bi-coordinate navigation is required for certain salmon stocks in which individuals can reach a common goal from vastly different initial positions. While this mechanism has not been demonstrated in salmonids, there is evidence that sea turtles (Lohman and Lohman 1996), and pigeons (see Moore 1980) may use geomagnetic fields as maps for bi-coordinate navigation. It is generally believed that sockeye salmon are using compass orientation or bi-coordinate navigation during marine migrations.

Saila and Shappy (1963) and Patten (1964) used numerical simulations to suggest that only a low degree of directional precision was required to explain the homing ability of Pacific salmon. However, Groot and Quinn (1987) re-examined the biological assumptions of these models and demonstrated that high directional precision was required. While the migration model of Patten (1964) was incorrect in its biological assumptions, it did lead to a generalized model of migration behaviour summarized in Leggett (1977). This model suggests that fish do not perceive or strive for the long term objective of migration, but rather, they are continuously attempting to maximize instantaneous 'comfort'. In this case, maximum comfort is achieved by optimizing physiological and/or neurological states. The perception of the optimal state depends on a compromise among conditions perceived simultaneously by different senses, and likely

depends on neuro-endocrine factors that change seasonally and ontogenetically. This generalized model suggests that multiple factors could be guiding the migration, and balancing potentially conflicting urges to migrate, forage and avoid predation.

The emerging understanding of salmon migration represents a slow accumulation of knowledge from a number of disciplines. The importance of migration to salmon fisheries results in the fortuitous collection of data that may contribute to some of these research objectives. In particular, Fraser River sockeye fisheries provide coarse resolution observations of temporal and spatial distributions that can potentially provide insight into the selection of migration routes. The primary direction-finding mechanisms that have been proposed for salmon are based on celestial and geomagnetic patterns that are stable among years (on relevant time scales). So the introduction of migration route variability is likely driven by secondary orientation processes that are dependent on oceanographic features that vary among years. One of the primary objectives of this research, described in chapter (4), was to explore how coastal migration route variation might arise from individual salmon decision processes in a dynamic marine environment.

#### *FRASER RIVER SOCKEYE FISHERY MANAGEMENT: IMPLICATIONS OF COASTAL MIGRATION ROUTE VARIABILITY*

Management of the Fraser River sockeye fishery is a complex task, involving numerous user groups in Canada and the United States (Woodey 1987). Fisheries are



regulated to meet the first priority of escapement to ensure future production, and second, to meet international allocation goals, provided that there is an agreement between Canada and the United States. The domestic catch of each country is further subdivided between aboriginal, commercial and sport fisheries. There are numerous aboriginal groups with independent allocations that are given priority over the sport and commercial fisheries. The commercial catch in turn is also subdivided among trollers, seiners and gillnetters. The allocation goals have become increasingly complex in recent years, and there is a major concern that the regulatory agencies no longer have the ability to ensure equitable harvest allocations and spawning objectives (Fraser 1995). The available stock assessment methods contain too much uncertainty, and the fishery does not have enough scheduling flexibility to meet the present demands. Additional management failures such as the late-run escapement shortfall of 1994 (PSC 1995, Fraser 1995) seem to be inevitable within the fishery and management structure as it exists at this time.

In addition to theoretical interest, this thesis research was motivated by the practical importance to fisheries management of quantifying stock assessment uncertainty, and estimating/predicting coastal migration route variability. Adult sockeye salmon can return from the Gulf of Alaska to the Fraser River by migrating around either the north or south end of Vancouver Island (fig. 1.1) and the annual proportion of fish using each route varies considerably among years (fig. 1.2). Uncertainty in the proportion of fish using the northern route (northern diversion rate) complicates the task of fisheries managers in two ways: 1) it is difficult to estimate the historical exploitation rates in the individual approach route fisheries because harvest rates and migration routes are

confounded, and hence it is difficult to schedule approach route fisheries with specific exploitation objectives, and 2) it is difficult to meet harvest allocation goals among user-groups because not all users have equal access to the resource (e.g. fishers from the United States cannot fish the northern approach route). Conceivably, migration route variability would be irrelevant if 1) the northern and southern approach route fisheries were always opened simultaneously, 2) the same proportion of the run migrating via each route was vulnerable to fishing, and 3) all users had equal access to both routes. Since this is not the case, the northern diversion rate cannot be ignored. The importance was exemplified by the serious under-escapement of late-run stocks in 1994. This was partially attributed to the high northern diversion (PSC 1995). Within the existing management system, improved estimation and prediction of the northern diversion rate would assist in the attainment of equitable allocations and reduce overfishing risk.

Fraser River sockeye fisheries provide a considerable amount of information about coastal distributions that could not be collected for economically insignificant stocks. This information is invaluable for effective fisheries management, and has been opportunistically applied to studies of salmon migration such as those described in the section below. However, these data are generally not collected with the sort of consistent sampling that would optimize the information content. Important fishery parameters may be expeditiously estimated with *ad hoc* methods for in-season stock assessment, without full consideration of the statistical properties of the estimates. One of the primary objectives of my research was to examine the error distribution of harvest rate estimates that can be expected when traditional estimation methods are used, as described in

Chapter (2). These results were then used to develop formal methods for estimating proportions of fish using each coastal migration route, described in Chapter (3). So these two chapters have direct implications for both fisheries management, and theoretical studies of coastal migration routes, both of which have largely ignored potential errors in migration route estimates.

#### *REVIEW OF PREVIOUS STUDIES EXAMINING THE FRASER SOCKEYE NORTHERN DIVERSION RATE*

The northern diversion rate has intrigued biologists and oceanographers for several decades. Numerous hypotheses have been advanced to explain and predict migration route variability among years, but none of the models has been shown to be consistent over the entire historical record. Most commonly, the published studies have demonstrated a correlation between time series of the northern diversion rate and some environmental index, but failed to define explicit causal mechanisms. Subsequent to publication, the relationship breaks down, indicating that it was wrong or at least incomplete. This section briefly summarizes these studies, and suggests how an alternative dynamic modelling approach might provide new insight.

The most consistent environmental index correlated with the northern diversion rate in recent years has been late spring Kains Island lighthouse sea surface temperature (SST), on the NW coast of Vancouver Island (indicated in fig 1.1). Numerous simple and multiple regression analyses have included significant Kains Island SST terms indexed

over various time intervals (Hamilton 1985, Groot and Quinn 1987, Xie and Hsieh 1989). Various studies have also demonstrated a significant correlation or non-statistical association between the diversion rate and SST from other coastal and offshore locations (Wickett 1977, Hsieh et al. 1991, Groot and Quinn 1987, Royal and Tully 1961, Tully et al. 1960). The mechanisms by which high SST supposedly causes high northern diversion rate is usually described only vaguely, and it cannot be distinguished whether coastal or offshore processes are involved. In warm years, the sockeye distribution on the high seas could be further north relative to cooler years, so that a greater proportion of homing migrants could arrive on the coast north of Vancouver Island. In turn, this may result in a higher proportion of sockeye using the northern route around the island. Alternatively, the majority of sockeye might always arrive north of Vancouver Island, and may simply be avoiding high water temperatures during the coastal migration. This latter mechanism would be consistent with the low observed diversion in 1990 despite high SST at Kains Island, because Queen Charlotte Strait was also exceptionally warm (David Blackburn, Pacific Biological Station, Nanaimo, B.C., V9R 5K6, pers. comm.).

Variability in the distribution of salinity or Fraser River water, particularly around the north end of Vancouver Island, has also been suggested as a mechanism influencing migration route variability. This theory has been advanced on the basis of offshore salinity observations (Favorite 1961), and observed correlations between the diversion rate and Fraser River discharge indices (Groot and Quinn 1987, Hamilton 1985, Wickett 1977, Xie and Hsieh 1989). Thomson (1981) suggests that interannual variability in the flow of Fraser River water northward through Johnstone Strait would be the link between

discharge and the northern diversion rate. It is well established that salmonids use odours near the river mouth and within freshwater systems to identify spawning grounds, but it is not known what role olfaction plays in open ocean and coastal migrations. There is a long time series of salinity observations measured at coastal lighthouse stations, but presumably there is no simple relationship between lighthouse salinity and migration routes or a correlation would have been published. The distribution of Fraser River water seems like a reasonable factor that may affect migration routes, but there is no direct means of accurately estimating the concentration of Fraser water outside the Georgia and Juan de Fuca Straits (see LeBlond et al. 1994). It has also been suggested that the northward flow of Fraser River water along the west coast of Vancouver Island may be important for migrating salmon, especially as this flow is only intermittently observed north of Brooks Peninsula (Richard Thomson, Institute of Ocean Sciences, Sidney B.C. V8L 4B2, pers. comm.); however there is presently no evidence to support or refute this idea.

I consider the third most viable hypothesis explaining diversion rate variability to be large scale ocean circulation patterns. Thomson et al. (1992) demonstrated the viability of ocean circulation as a mechanism for affecting the latitude of landfall of migrating salmon, while Hsieh et al. (1991) found a correlation between diversion rates and NE Pacific circulation indices. However, the published relationships were weak, and Wickett (1977) and Groot and Quinn (1987) failed to find any relationship with other circulation time series.

A few other theories have been suggested regarding northern diversion variability, and some have been shown to be incorrect. Groot and Cooke (1987) suggested that adults might return via the same route they used as juveniles, while Groot et al. (1986) suggested that adult fish might follow population-specific odours produced by out-migrating juveniles. Both of these theories were disproved when juvenile sampling indicated that most or all smolts migrated north via Johnstone Strait (Groot and Cooke 1987). Barber (1983) suggested that sockeye homing involves the following of pink and chum fry odour trails. Xie and Hsieh (1989) included an auto-regressive term (diversion rate 2 years earlier) in a multiple regression model and suggested that smolts and adults that migrate in the same year (i.e. originate from brood years separated by two years) may be affected by the same (unspecified) oceanographic factors. Gilhousen (1960) observed that high northern diversion events corresponded with high sunspot abundance. Hamilton (1985) found no evidence of a 4 year diversion pattern that would have suggested a stock-specific or cycle-specific migration pattern.

As an alternative investigative approach, I was interested in exploring explicitly-defined mechanisms on scales relevant to the decision process of individuals. The correlation approach, which has been used extensively in previous studies, could in principle, yield a reasonable predictive relationship for the northern diversion rate if the underlying mechanism was governed by simple linear dynamics. However, by itself, this approach could not be used to elucidate the salmon migration decision processes and resultant trajectories at a satisfying temporal or spatial resolution. The northern diversion

rate is a cumulative result of the migration trajectories of millions of individuals, broadly distributed in a dynamic heterogeneous environment, each making independent migration decision rules according to their own unique sensory input and developmental history; so there is no reason to believe that the system should be governed by simple linear dynamics. Tyler and Rose (1994) review process-based modelling studies in fisheries on the basis of three defining characteristics: spatial heterogeneity, individual variability and individual movement. They emphasize that spatially-explicit individual-based models provide a means of combining all three of these characteristics into a single framework. Chapter (4) describes my efforts to consolidate data on sockeye distributions and orientation behaviours, and represent the spatial and temporal heterogeneity of the physical environment of the NE Pacific, so that key mechanisms potentially driving the northern diversion rate could be examined with a spatially-explicit, individual-based migration model.

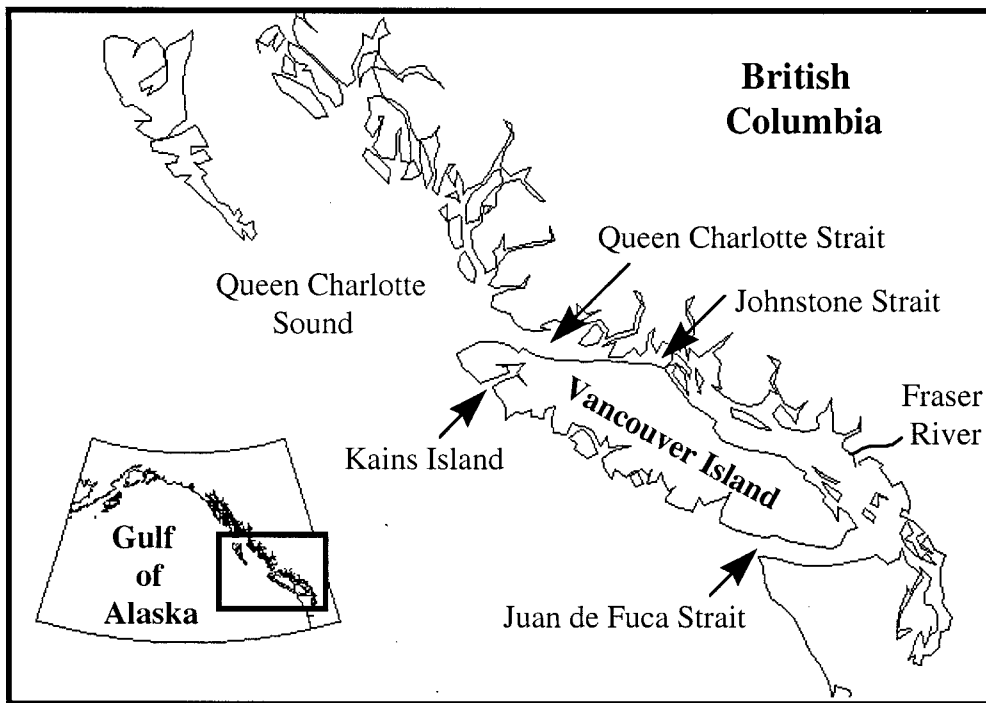


Fig. 1.1. Map of the coastal approaches to the Fraser River showing important locations referred to in the text.



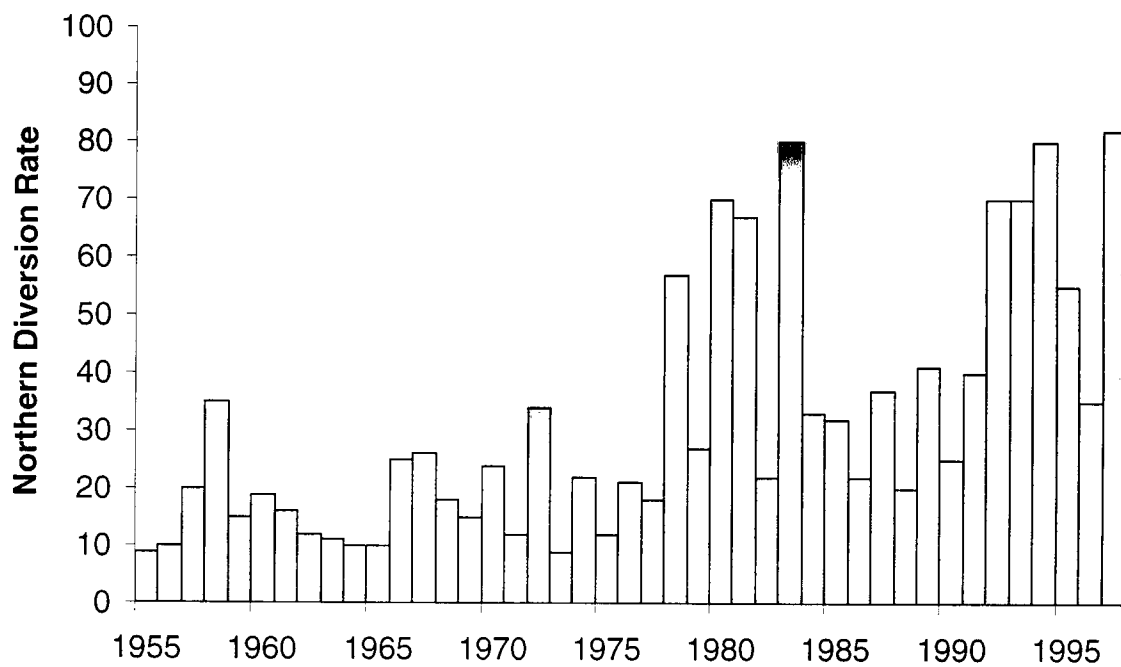


Fig. 1.2. Time series of the estimated annual proportion of sockeye salmon returning to the Fraser River via Johnstone Strait (northern diversion rate), (James Cave, Pacific Salmon Commission, pers. comm.).

**CHAPTER 2: UNIFORM MIGRATION RATE ASSUMPTIONS IN SALMON  
FISHERY BOX MODELS RESULT IN BETA-DISTRIBUTED, BIASED,  
RECONSTRUCTED HARVEST RATE ESTIMATES**

## ABSTRACT

Box models are an important stock assessment tool used to represent the dynamic spatial distribution of mature salmon as they migrate through a gauntlet of fisheries. In these models, it is generally assumed that all individuals maintain their position in the run relative to each other, and implications of violating this assumption have not been previously examined in detail. The objectives of this chapter were to 1) define plausible stochastic salmon migration rate variability scenarios that are consistent with Fraser River tagging studies and observed migratory timing distributions, and 2) use Monte Carlo simulations of fisheries to examine how this variability affects harvest rate estimation under the assumption of uniform migration rates. A unique migration dynamics scenario could not be defined. Observations were consistent with a range of plausible scenarios that represented a compromise between independent individual migration rate variability (causing diffusion), and migration rate variability that covaries among individuals (causing aggregation and polymodal timing distributions). The Monte Carlo simulations suggested that harvest rate errors can be expected to follow a beta distribution, with substantial underestimation bias at high harvest rates. Harvest rate error distributions are described in detail for a single example, while the expected effects over a range of alternative migration dynamics and fishery temporal/spatial characteristics are described qualitatively.

## INTRODUCTION

Simple box models (or boxcar models) are used to represent salmon abundance in time and space as returning adults migrate through a gauntlet of fisheries en route to spawning grounds. At a fixed point in time during the migration, a typical salmon run is spread out along the migration route with a roughly bell-shaped abundance distribution. At each point along the migration route, the run is observed as a bell-shaped abundance distribution that passes over time. In principle, an efficient fishing fleet could harvest the whole run in a single opening if there were no spatial restrictions, or alternatively, if the fleet was restricted to a very small area it could harvest the whole run if there were no temporal restrictions. Effective management of these fisheries is achieved by the careful selection of fishery temporal and spatial openings. Box models provide the means with which fish and fishery dynamics can be described in temporal and spatial units that are appropriate for this purpose. However, these models require very restrictive assumptions about migration dynamics, and implications of violating these assumptions have not been described.

Box models are used in a variety of salmon management tools, including pre-season planning, in-season stock assessment and post-season run-reconstruction. The pre-season planning model (Cave and Gazey 1994) is used primarily to explore alternative patterns of fishery openings in time and space and plan harvest allocation targets under different scenarios. The in-season model (Carl Walters, University of British Columbia, Fisheries Centre, pers. comm.) is used to provide updated stock

abundance estimates at frequent intervals during a fishing season. This model provides Bayesian stock size estimates in-season by calculating the likelihood of observing catch and test fishery observations given the historical observations. The run-reconstruction model (Starr et al. 1984, Starr and Hilborn 1988) iterates the boxcar model backwards in time after the fishery is over, and provides a post-season assessment of harvest rates and migratory timing characteristics.

Boxcar models are dependent on the assumption that all fish from a given stock migrate at the same rate, maintaining their position in relation to the rest of the stock. This assumption is known to be violated, but to date there has not been much work done to quantify the effects of this problem. The objectives of this chapter were to: 1) define stochastic salmon migration dynamics scenarios that are consistent with observations from Fraser River sockeye salmon tagging studies and migratory timing distributions, and 2) use Monte Carlo simulations to describe how salmon migration dynamics affect reconstructed harvest rate estimates when uniform migration rates are assumed. Harvest rate error distributions are described in detail for a single example, while the expected effects over a range of alternative migration dynamics and fishery temporal/spatial characteristics are described qualitatively.

## BOX MODEL REPRESENTATION OF A GAUNTLET SALMON FISHERY

### *BOX MODEL NOTATION*

The notation presented here is a simplified version of Starr and Hilborn (1988) and Cave and Gazey (1994), but describes the same process. Box models are used to represent salmon abundance in space and time, and partition catch and escapement for individual fisheries to calculate harvest rates. As Starr and Hilborn (1988) described, this is accomplished using the relationships:

$$(2.1) \quad \begin{aligned} N_{t,l} &= C_{t,l} + E_{t,l} \\ h &= C_{t,l} / N_{t,l} \end{aligned}$$

where  $N$  (abundance),  $C$  (fishery catch) and  $E$  (escapement) are divided into discrete units by  $t$  (time) and  $l$  (location), and  $h$  is the harvest rate. Additional subscripts may be used to describe the stock or approach route, but these were not relevant to this study. Temporal and spatial units are chosen so that the mean migration distance in one time unit corresponds to one spatial unit (a fishery may contain multiple spatial units). The fish in one unit of space and time may be visualized as one boxcar of a train, which consists of a series of distinct boxcars progressing along the migration route, hence the term boxcar model. The units usually represent some trade-off between temporal resolution requirements and the estimation error that is likely to arise from errors in catch reporting and escapement partitioning. The model used was iterated on a daily time step,

so that multiple-day openings in multiple-spatial unit fisheries could be modelled, and the effects of calculating harvest rates over a range of summation intervals could be explored.

During the fishing season, salmon migrate in a fairly consistent pattern toward their natal streams, and harvesting at one location affects the abundance available for harvesting in subsequent fisheries along the migration route. For two adjacent fisheries ( $i = 1$  and  $i = 2$ ) located at  $l$  and  $l + 1$ , with sequential openings at  $t$  and  $t + 1$ , respectively, the catch in the first fishery is  $C_{t,l} = h_1 N_{t,l}$ . The catch in the second fishery, which occurs during the next time step, is  $C_{t+1,l+1} = h_2 N_{t+1,l+1}$ , and because of migration,  $N_{t+1,l+1} = N_{t,l}(1-h_1)$ .

In the case of a fishery with a duration greater than one day, it is useful to distinguish between the total fishery harvest rate  $h$ , and the elemental exploitation rate,  $u$ , adopted from Cave and Gazey (1994). Using the elemental exploitation rate is equivalent to an exponential model of harvest with an instantaneous fishing mortality rate ( $F$ ) applied for 24 hours ( $u = \exp(-24F)$ ). Cave and Gazey (1994) used a slightly more complicated version of  $u$  to account for fish movement during a fishery, but this added complication was not included (it will become apparent that the magnitude of harvest rate estimation errors due to migration dynamics is likely very large relative to the error potentially introduced by the different definitions of  $u$ ). A fishery on two spatial units ( $l, l + 1$ ) with an elemental exploitation rate  $u$  for a duration of two days, affects three boxcars of fish. On the first day, two boxcars are harvested at  $u$ . On the second day, one of these boxcars moves out of the fishery (from  $l + 1$  to  $l + 2$ ), and another previously unexposed

boxcar moves into the fishery (from  $l - 1$  to  $l$ ), and is harvested at  $u$ ; the boxcar that remained in the fishery (moves from  $l$  to  $l + 1$ ) is harvested at  $u$  a second time, so that the total harvest rate on this boxcar is  $u + u(1-u)$ . Assuming that fish do not mix between boxcars, the three boxcars before the fishery,  $N_{t,l-1}$ ,  $N_{t,l}$ ,  $N_{t,l+1}$ , are observed three days later as  $N_{t+3,l+2}$ ,  $N_{t+3,l+3}$ ,  $N_{t+3,l+4}$ , where  $N_{t+3,l+2} = (1 - u)N_{t,l-1}$ ,  $N_{t+3,l+3} = (1 - (u+u(1-u)))N_{t,l}$ , and  $N_{t+3,l+4} = (1 - u)N_{t,l+1}$ , and the total harvest rate,  $h$ , for this fishery can be calculated:

$$h = 1 - (N_{t+3,l+2} + N_{t+3,l+3} + N_{t+3,l+4}) / (N_{t,l+1} + N_{t,l} + N_{t,l-1}).$$

Fisheries pre-season planning models are iterated forward in time in this manner (using historical harvest rate estimates) to game alternative fishery opening scenarios. The post-season run-reconstruction models are iterated backward in time after all fisheries have occurred, and are used to estimate stock and fishery characteristics including harvest rates, migratory timing, migration routes and stock composition in mixed-stock fisheries.

#### *RECONSTRUCTION OF HARVEST RATES*

Post-season estimation of harvest rates is important for the effective management of most salmon fisheries. Attainment of catch and escapement objectives can be extremely difficult and complicated especially in mixed-stock fisheries with multiple user groups (e.g. Woodey 1987). The harvest rate estimates from previous years are required to anticipate harvest rates for future fishery openings under consideration. Harvest rates



are also used to estimate the proportion of fish using different migration routes as detailed in chapter (3). In this chapter, I am primarily interested in exploring the errors in the estimated harvest rate,  $h'$ , for particular fisheries relative to the actual harvest rate,  $h$ . To invoke harvest rates in pre-season planning models as described above, it might be more useful to calculate the elemental harvest rate,  $u$ , from  $h$ , however, errors in  $h$  have a simple direct interpretation and remain the focus of this chapter.

Harvest rates are calculated from equation (2.1). Catch is generally measured fairly well from landings or observations of hailed vessels. Escapement is usually measured in-river and is much more uncertain than catch. Assuming for the moment that escapement data are known at a boxcar resolution in space and time, then given the total catch from a fishery  $C_i = \sum C_{t,l}$  (the sum of the catch across all temporal and spatial units for fishery  $i$ ), and the total escapement  $E_i = \sum E_{t,l}$  (the sum of all fish exposed to fishery  $i$ , but not caught), the harvest rate for each fishery  $i$  is calculated:  $h_i = C_i / (C_i + E_i)$ . This calculation can be complicated for an actual fishery (see Cave and Gazey 1994), particularly if individual boxcars are exposed to more than one fishery during the same opening (i.e. if fisheries are spatially close together and the opening is long enough for fish to migrate out of one fishery into the adjacent one). Since boxcars may be exposed to multiple fisheries (whether or not they overlap in time), the run must be reconstructed in reverse temporal order from  $t = T$  to  $t = 1$ , such that for all  $t$ :  $E_{t,l} = E_{t+1,l+1} + C_{t+1,l+1}$  (i.e. the migratory timing distribution at time  $t = 1$  (prior to any fisheries) is recreated by simulating the migration backward in time from the river at  $t = T$ , and adding the catch from all fisheries back onto the escapement timing distribution at the appropriate points

in time and space). In the multiple fishery case, complications arise if  $C_{i,l}$  must be partitioned by boxcar and temporal unit, but for the simulations described here, this is not required. In some cases, it is useful to define the harvest rate over a time/space interval that exceeds the fishery interval (e.g. if catch and escapement data cannot be resolved at the same resolution) and this is simply accomplished by expanding  $\Sigma E_{i,l}$  to include additional boxcars not exposed to the fishery.

Depending on the migration characteristics of particular stocks, and the escapement monitoring program, there are two different run-reconstruction methods that are used to estimate harvest rates after a fishing season. Both methods rely on equation (2.1) as described above, but they differ in the calculation of  $E_{i,l}$ . The first method, referred to here as backward-iterated, requires high temporal resolution escapement observations, such as the daily hydroacoustic surveys conducted in the Fraser River near Mission. With these observations, escapement can be 'backed out' from Mission through the various fisheries, and catch can be added back onto the run at the appropriate points in time and space, recreating the initial migratory timing curve as it appeared before fishery exploitation. The second approach, referred to here as forward-iterated (PSC 1995), is used when escapement observations are not available at a high resolution (e.g. a single abundance estimate from spawning bed counts), or when migration rates are known to be inconsistent (e.g. late-run Fraser stocks usually reside in the Strait of Georgia for 3-5 weeks before migrating through the escapement monitoring site). In this case, it is assumed that the migratory timing distribution prior to the fishery is a normal distribution. The fishery is then simulated forward in time, as though it was being used

for pre-season planning. Fish are removed from this normal distribution according to the actual fishery schedule and harvest rates calculated from previous years, and a final escapement timing distribution is simulated. The daily abundance of the simulated escapement distribution is then uniformly scaled so that the total abundance equals the total observed escapement for the year. This scaled distribution is then assumed to be representative of the actual escapement timing distribution at the fishery. The run is reconstructed by iterating this estimated escapement timing curve backward in time and adding the fishery catch back in at the appropriate times and locations as in the first method.

#### *VIOLATION OF THE ORDER OF MOVEMENT ASSUMPTION*

In boxcar models, it is usually assumed that all fish from a particular stock maintain their position in the run relative to the other fish (and that the migration rate is constant or varies in a known way). If this order of movement assumption is realized, then the shape of the migratory timing distribution is conserved, and the harvest rate for a particular fishery can be calculated perfectly from the escapement timing distribution observed at any subsequent location along the migration route (fig. 2.1A). In this case, the fish abundance in each boxcar remains constant with time, except for when the fishery 'carves a hole' in the run. At the escapement monitoring site, the fishery 'hole' is observed exactly as it would have been observed at the fishery. So during backward-iterated run-reconstruction, the escapement timing distribution is backed up to the fishery

according to the estimated migration rate, and the hole is filled in to reproduce the original migratory timing distribution prior to the fishery.

Unfortunately, observations suggest that there is substantial variability in migration rates within stocks. If individual salmon exhibit random, independent variations in migration rates (due to swimming speed and orientation differences), then there will be a continuous diffusive mixing of individuals along the migration route. If a boxcar structure is imposed on these escapement observations, and harvest rates are estimated with backward-iterated run-reconstruction under the order of movement assumption, then this diffusion results in a tendency to underestimate harvest rates (fig. 2.1B) and this has been observed in actual fisheries (PSC 1995). Each fishery carves a hole in the migratory timing distribution, and with time, the hole partially fills with fish from adjacent boxcars. When the run is reconstructed post-season, catch is added back onto an escapement timing distribution that is smoothed out relative to the actual escapement distribution that was present at the fishery. The escapement that was estimated to have occurred during the fishery is overestimated, and results in underestimation of the harvest rate.

In addition to diffusive processes, there seem to be substantial migration rate variations that covary among large groups of individuals. Salmon migratory timing distributions are generally observed to be polymodal when observed on a fine time scale, with abundance peaks and troughs of one to several days duration. The irregularity of these timing curves cannot be easily explained by measurement errors, or fishery effects

on the timing distribution. Diffusion would tend to smooth out this polymodal structure, so there must be additional processes at work. The observed peaks and troughs are probably the result of independent fish responses to fairly large scale, dynamic oceanographic features (e.g. frontal systems or surface currents). These features probably cause spatial aggregation as many fish experience similar conditions and exhibit similar migration delay responses. These migration delays are common at river mouths, but since polymodal timing distributions are also observed in coastal areas, it suggests that migration delays also occur in the ocean. If diffusion and aggregation processes occur, then reconstructed harvest rates could be severely overestimated or underestimated depending on the particular pattern of migration rate variability that the run experienced (fig. 2.1C).

#### *REPRESENTING STOCHASTIC MIGRATION RATE VARIABILITY WITH A MODIFIED BOXCAR MODEL*

The Monte Carlo fishery simulations (described below) required a numerically efficient means of describing independent and co-varying salmon migration rate variability and this was achieved with a modified boxcar model. The traditional boxcar model requires that a spatial unit is equal in length to the distance a salmon migrates in one unit of time. To simulate non-uniform migration rates, the fish in a given boxcar were subdivided into proportions that migrated 0, 1, and 2 boxcars per timestep, and these proportions varied in space and time.

Independent migration rate variability was implemented as a constant proportion of fish migrating 0 and 2 boxcars, defined as the diffusion rate,  $M$ , ( $0 \leq M \leq 1$ ). During one timestep of the model with a 20% diffusion rate ( $M = 0.2$ ), 10% of the fish in a boxcar do not move, 80% migrate forward one boxcar, and 10% migrate forward two boxcars. The actual migration rate distribution that results is a function of the diffusion rate, boxcar length and timestep.

Migration rates that co-vary among individuals were implemented by adding migration delays at random locations in time and space. The delays were independent and randomly distributed, so some boxcars could be affected by multiple delays that overlapped in time and space resulting in compounded delays. In the boxcar model, delays are described by a migration rate reduction factor,  $B$ , ( $0 < B \leq 1$ ) relative to the mean migration rate. On any given timestep, most boxcars are not affected by delays ( $B = 1$ ), while  $B < 1$  causes fish to aggregate in certain areas, and thin out in adjacent areas forward of the migration blockage.

With uniform migration dynamics, the number of fish moving from one boxcar to the next is calculated  $N_{t+1,l+1} = N_{t,l}$ . With non-uniform dynamics, if we assume for the sake of example that at time  $t$ ,  $N_{t,l}$  is the only boxcar with any fish in it, then:

$$N_{t+1,l} = p_0 N_{t,l},$$

$$N_{t+1,l+1} = p_1 N_{t,l},$$

$$N_{t+1,l+2} = p_2 N_{t,l}.$$

where  $p_0$ ,  $p_1$ , and  $p_2$  are the proportion of fish that migrate 0, 1 and 2 boxes respectively ( $p_0 + p_1 + p_2 = 1$ ; each of  $p_0$ ,  $p_1$ ,  $p_2 \geq 0$ ). These proportions are dependent upon  $M$  and  $B$ :

$$p_2 = B(M/2) ,$$

$$p_1 = B - 2(p_2) = B(1 - M)$$

$$p_0 = 1 - p_1 - p_2 = 1 - B(1 - M/2)$$

This representation of migration rates ensures that: 1) provided that  $B > 0$  and  $M > 0$ , there are always some fish migrating 2 boxcar lengths, and 2) the mean migration rate is reduced by the intended factor  $B$ , regardless of  $M$ . However, this representation of migration rate variation is only an approximation of what would be observed if individuals were distributed in continuous space and experienced migration rate variations according to a continuous frequency distribution. This boxcar representation produced results that were very similar to an individual-based model with continuous spatial structure and continuous migration rate distributions (with mean and variance comparable with the boxcar rate frequency distribution dictated by  $M$ ) for the fish and fishery dynamics examined in example (2.1).

In the Monte Carlo simulations described below, fishery harvesting is included in the model as a discrete time process as in the simpler model with uniform migration

dynamics. So harvest rates are only dependent upon abundance in fishery areas at the end of the migration step, not migration rates during the time step.

### **REPRESENTING FRASER RIVER SOCKEYE SALMON COASTAL MIGRATION DYNAMICS WITH A MODIFIED BOXCAR MODEL**

To examine the potential impact of non-uniform salmon migration dynamics on harvest rate estimates, it was necessary to quantify the migration rate variability that exists, and implement this variability in the modified boxcar model presented above. Fraser River sockeye salmon were selected for this study because chapters (3) and (4) focus on this system, and there is a lot of data available from fisheries and tagging studies. These observations suggest that there is considerable migration rate variability, but were not sufficient to define a unique stochastic migration dynamics scenario.

Mark and recapture studies in the coastal approaches to the Fraser River describe individual migration rates on a scale relevant to fishery management. Verhoeven and Davidoff (1962) (VD) provide details of several marine tagging studies carried out between 1938-48; results of two typical studies are mentioned here. The mean migration rate for sockeye tagged in Johnstone Strait and recovered at the mouth and lower reaches of the Fraser River (approximately 260 km) was  $24 \pm 13 \text{ km} \cdot \text{d}^{-1}$  (SD), from approximately 200 recoveries (estimated from VD fig. 10, Mouth of Fraser and North Arm). Variability in migration rates within and among years was demonstrated by fish



tagged at Sooke and recovered at the mouth of the Fraser River (approximately 170 km), estimated from VD Table 17. The mean migration rate for fish tagged in July (1938-41) was  $22 \text{ km}\cdot\text{d}^{-1}$  (242 recoveries), while the mean rate for fish tagged in August during the same years was  $15 \text{ km}\cdot\text{d}^{-1}$  (229 recoveries). Annual migration rates for July ranged from  $15 - 26 \text{ km}\cdot\text{d}^{-1}$  (57 and 80 tag recoveries respectively), while August rates ranged from  $9 - 24 \text{ km}\cdot\text{d}^{-1}$  (51 and 46 tag recoveries respectively). This clearly demonstrates that there is considerable migration rate variability among individuals, and within and among years, unfortunately these studies did not distinguish variability among stocks.

An alternative method of estimating mean migration rates is based on migratory timing distributions. The mean migration rate of a stock can be estimated by calculating the mean of the migratory timing distribution observed at different locations, and dividing the distance between locations by the difference in mean timing. In practice, the displacement of a distinct characteristic of the timing distribution (either a sharp peak or deep trough) may be easier to identify than the distribution mean, because tails of the run are often poorly described. Fraser sockeye coastal migration rate estimates used by the Pacific Salmon Commission in their forward simulation models are  $40\text{-}55 \text{ km}\cdot\text{d}^{-1}$ , with late-summer stocks delaying off the river mouth for a period of days to weeks (inferred from Cave and Gazey (1994) Table 3). The exact years and methods used to generate these estimates have not been reported, but given enough observations, this approach should provide a reasonable estimate of mean migration rates, even with relatively coarse abundance estimates such as test fishery catch per unit effort.

Mean migration rates estimated from migratory timing distributions are likely more accurate than the mark and recapture studies because the latter are affected by several potential errors. Verhoeven and Davidoff (1962) provide a comprehensive list of tagging study problems, including: 1) tags recovered in fisheries may not always be reported immediately, 2) late-summer stocks tend to delay in the Strait of Georgia before migrating into the Fraser River, 3) the act of tagging may disorient or otherwise delay the fish, and 4) dates of tag recovery are restricted to fishery openings. The first three of these errors would result in underestimation of migration rates. Conversely, it is not clear how migratory timing distribution displacement could consistently overestimate migration rates by a factor of two.

The distribution of migration rates observed from mark and recapture studies indicated that there is considerable variability in migration rates among individuals; however, given that the mean migration rate seems to be underestimated, it is impossible to know how well the variance of the distribution is represented. The tagging studies indicated that the fastest sustained migration rate observed was about  $90 \text{ km}\cdot\text{d}^{-1}$ . This rate is very close to the fastest sustained swimming speeds observed by ultrasonic telemetry studies of sockeye in this region (Quinn 1988), although the telemetry studies would only be representative of migration rates if orientation was nearly perfect. On this basis, a boxcar length of 45 km (base migration rate  $45 \text{ km}\cdot\text{d}^{-1}$ ) was selected for the fishery model. Thus fish migrating two boxcars per timestep (when  $M > 0$ ) attain the maximum rate of  $90 \text{ km}\cdot\text{d}^{-1}$ .

The frequency and intensity of co-varying migration rate changes cannot be measured directly from the available data, but the polymodal structure of Fraser sockeye migratory timing distributions can be used to define constraints to which valid migration scenarios must adhere. This was accomplished by comparing each actual timing distribution (reconstructed through all fisheries) to a normal distribution with the same mean and variance (fig. 2.2). Two indices were developed to characterize the deviations from normality: 1) the Number of Anomaly Stanzas (NAS) in which the absolute value of the difference between the observed and normal distributions on at least one day was  $>1\%$  of the total run size, (a stanza consists of all consecutive days in which the observed deviations are either all positive, or all negative), and 2) the Summed Absolute Values (SAV) of the anomalies across the entire distribution. NAS and SAV from 6 backward-iterated reconstructions from 1993, and 33 forward-iterated reconstructions from 1992-94 (provided by James Cave, Pacific Salmon Commission, 600 - 1155 Robson St., Vancouver, B.C., Canada) show a range of timing anomaly characteristics (fig. 2.3). The migratory timing anomaly structure is potentially dependent upon the fishery harvesting pattern, so migration scenarios were defined such that the NAV and SAV distributions of backward-iterated reconstructed runs approximated the observed runs in the absence of fisheries, or with three equally-spaced, high harvest rate fisheries as defined in example (2.1) below. If forward-iterated reconstructions were used to define migration dynamics, the Monte Carlo simulations would have to approximate the complexity of the Fraser River fishery. Hence the validity of migration dynamics scenarios was assessed only on the basis of backward-iterated reconstructions, while forward-iterated reconstructions are

included in fig. 2.3 because they were available for more years and stocks, and suggest that 1993 was not unusual. The standard deviations of the backward-iterated timing distributions ranged from 6.5 - 9 d, with a mean of 7.8 d.

All of these observations of salmon migration rate variability were not sufficient to define a unique salmon migration dynamics scenario for the Monte Carlo simulations. However, on the basis of these data I defined some criteria for migration rates and migratory timing distributions that plausible migration dynamics scenarios should reproduce:

- 1) reconstructed migratory timing distribution standard deviation 7.0 - 8.5 d,
- 2) standard deviation of individual migration rates (260 km interval):  $<12 \text{ km}\cdot\text{d}^{-1}$ ,
- 3) mean migration rate  $38\text{-}42 \text{ km}\cdot\text{d}^{-1}$ ,
- 4) maximum migration rate  $90 \text{ km}\cdot\text{d}^{-1}$ ,
- 5) NAS: 3 - 11,
- 6) SAV: 30 - 90 %.

It may be argued that some of these criteria are excessively restrictive and do not allow for extreme events, but these constraints do admit a considerable range of migration dynamics scenarios. The two sources of migration rate variation are not directly constrained by these criteria, so there is a compromise in the relationship between diffusion rates and migration delays, such that these criteria can be satisfied in different ways. To increase the diffusion rate and still maintain consistency with SAV and NAS

criteria, the frequency and/or intensity of migration delays can be increased, or migration delays can be invoked closer to the escapement monitoring site. An upper bound on the magnitude of these processes is only realized indirectly because of constraints on the other criteria.

The following migration dynamics scenario defined for the Monte Carlo simulations is only one that can be justified from the available data. The baseline scenario consists of a 20% diffusion rate ( $M = 0.2$ ), and total migration delays resulting in a mean migration rate of 90% of the mean migration rate that would be observed in the absence of delays (40 instead of 45  $\text{km}\cdot\text{d}^{-1}$ , mean over >100 simulated runs). These migration delays were randomly distributed in the 400 km region immediately preceding the escapement monitoring site. Delays (magnitude randomly drawn from a uniform distribution  $B \sim U[0.2, 0.8]$ ) of 1-3 days duration, were introduced to the simulated run at random times (probability of a delay event = 0.4 / day, maximum of 5 simultaneous events), and affected areas of width 45-90 km. Two additional migration delay scenarios were tested in which the mean migration rate was decreased to 0.85 (38  $\text{km}\cdot\text{d}^{-1}$ ) and increased to 0.95 (42  $\text{km}\cdot\text{d}^{-1}$ ). The distribution of migration rates from the Johnstone Strait tagging study is compared with simulated distributions resulting from the three migration delay scenarios of 0.85, 0.9 and 0.95 in fig. 2.4. This comparison illustrates how the migration dynamics scenarios translate into individual migration rate variability over a fixed distance (260 km). The simulated rates are 14 - 18  $\text{km}\cdot\text{d}^{-1}$  faster than the observed rates, while the variance is somewhat lower.

## MONTE CARLO SIMULATIONS OF FRASER SOCKEYE FISHERIES

Monte Carlo simulations were used to generate a model of the harvest rate estimate error structure that can be expected for a specific fishery (example (2.1)), given the migration dynamics defined above. The process consisted of: 1) simulating fish migration through the fishery, 2) recording the simulated catch and escapement data in a manner comparable with actual fisheries, 3) using run-reconstruction to estimate the harvest rates, and 4) comparing the known simulation harvest rates with the estimated harvest rates. A brief qualitative description of how the error structure of example (2.1) changed with different migration dynamics and different fishery characteristics is provided .

### *EXAMPLE (2.1)*

The fishery in example (2.1) approximately corresponds to a Juan de Fuca Strait (Canadian statistical Area 20) sockeye purse seine fishery. The fisheries were of one day duration, spatial length 135 km (3 boxcars), with a proximal border 180 km from the escapement monitoring site. Each run was exposed to three fishery openings, scheduled approximately 7 days before the peak of the run, at the peak, and 7 days after the peak. Harvest rates were defined over the exact fishery interval (i.e. catch divided by the number of fish exposed to the fishery). A total of 1000 salmon runs were simulated (3000 fishery openings). One hundred runs were simulated for each harvest rate value between 0.05 - 0.95 in intervals of 0.1, resulting in 300 harvest rate estimates for each

known harvest rate. For the estimation of harvest rates, it was assumed that catch, total escapement, and the mean migration rate were measured without error. Therefore, the harvest rate estimation errors were introduced solely from the stochastic migration dynamics.

The Monte Carlo simulation results indicate that violations of the order of movement assumption result in substantial harvest rate estimation error, with a clear underestimation bias at high harvest rates (fig. 2.5). At low harvest rates, the error distribution is positively skewed, at intermediate harvest rates the distribution is fairly symmetrical and at high harvest rates the error distribution is negatively skewed. Forward-iterated run-reconstruction resulted in similar harvest rate error distributions, though slightly more biased and less precise than the backward-iterated reconstructions. Because of the similarity, results for the backward-iterated method are emphasized for clarity.

The beta distribution approximates the shape of the simulated harvest rate error distributions very well, as it can accommodate positive and negative skew, and is defined over the domain  $[0, 1]$ . For any fishery with an actual harvest rate of  $h$ , the reconstructed harvest rates,  $h'$ , are approximately distributed:

$$(2.2) \quad h' \sim \text{Beta}(\alpha, \beta) = \frac{\Gamma(\alpha)\Gamma(\beta)}{\Gamma(\alpha + \beta)} h^{\alpha-1} (1-h)^{\beta-1} \quad ; 0 \leq h \leq 1$$

where  $\alpha$  and  $\beta$  are related to the mean ( $\bar{h}'$ ) and variance ( $s^2$ ) of the error distribution:

$$\bar{h}' = \alpha / (\alpha + \beta),$$

$$s^2 = \frac{\alpha\beta}{(\alpha + \beta)^2(\alpha + \beta + 1)},$$

or conversely:

$$\alpha = -\frac{\bar{h}'^3}{s^2} + \frac{\bar{h}'^2}{s^2} - \bar{h}',$$

$$\beta = \alpha \frac{(1 - \bar{h}')}{\bar{h}'}$$

The reconstructed harvest rate bias,  $\Delta h$  is equal to the difference between the mean estimated and actual harvest rate ( $\Delta h = \bar{h}' - h$ ). The beta distribution approximated the Monte Carlo simulation results over a range of harvest rates so well that other probability distributions were not considered (a plot comparing the harvest rate error distributions with the best fit beta distribution was not included because the curves were essentially identical). The quality of the fit is perhaps not surprising when one considers the structure of the fishery simulation model. Since catch data was assumed to be error free, the harvest rate error distribution is only dependent on the reconstructed escapement distribution. As fish from  $E_i$  migrate toward the escapement monitoring site, they diffuse and experience random delays that produce errors in  $E'_i$ . These errors result in  $E'_i$  estimates that are approximately log-normally distributed. When  $h'_i$  is calculated



$h'_i = C_i / (C_i + E'_i)$ , and  $E'_i \sim \text{LogNormal}()$ , then it is a reasonable approximation that  $h'_i \sim \text{Beta}()$ .

A general model for the harvest rate error distribution observed for example (2.1) is provided by equation (2.3), where  $\alpha$  and  $\beta$  were estimated by a least squares fit to all error distributions (excluding  $h = 0.05$ , which was a consistently poor fit):

$$\begin{aligned} h' &\sim \text{Beta}(\alpha, \beta), \\ (2.3) \quad \alpha &= 17.7, \\ \beta &= 208 \exp(-4.751h) + 4.13. \end{aligned}$$

This general relationship describes most of the error distributions well (fig. 2.6), with the exception of the very low harvest rates, which were problematic in all the models considered. A more complicated, better fitting model describing the  $\alpha$  and  $\beta$  parameters could easily be developed, but equation (2.3) describes the essential bias and error variance features well enough to be useful as a likelihood function. The fitting errors could only be reduced a trivial amount relative to the uncertainty that exists due to the plausibility of alternative migration dynamics scenarios. The low harvest rate fisheries are not a big concern in this chapter or chapter (3), so the poor fit of the generalized model to the low harvest rates is ignored.

Equation (2.3) describes the distribution of harvest rate estimates  $h'$ , which may be expected for a known harvest rate  $h$ , however in practice,  $h$  is unknown, and the real

problem is describing the uncertainty in  $h$  associated with the estimate,  $h'$ . Provided that relationship (2.3) is defined, this can be achieved in a Bayesian framework (e.g. Gelman et al. 1995):

$$(2.4) \quad P(\text{parameters}|\text{data}) = \frac{L(\text{data}|\text{parameters}) \times P_0(\text{parameters})}{\sum L(\text{data}|\text{all parameters}) \times P_0(\text{all parameters})},$$

where the posterior probability,  $P()$ , for a particular parameter combination given the data, is equal to the product of the likelihood,  $L()$ , of observing the data given the parameters, and the prior probability,  $P_0()$ , of the parameters, normalized by dividing by the probability of observing the data summed over all parameter combinations considered. In this case, the only parameter to be estimated is  $h$ , and the data consists of a single observation,  $h'$ . Assuming that all values of  $h$  are initially equally likely (uniform prior probability  $P_0(h) \sim U[0,1]$ ), equation (2.4) is reduced to:

$$(2.5) \quad P(h|h') = \frac{L(h'|h)}{\sum_j L(h'|h)}.$$

where, the likelihood of observing  $h'$ ,  $L(h'|h)$ , is calculated from equation (2.3). The denominator of equation (2.4) is the sum of the likelihood of observing  $h'$  over all  $h$  (a grid of  $h$  in  $j$  intervals). The posterior probability distributions for  $h$  for example (2.1) are shown in fig. 2.7. The posteriors demonstrate that with perfect knowledge of the error distributions, the highest uncertainty in  $h$  is observed at intermediate values of  $h'$ .

#### *HARVEST RATE ERROR DISTRIBUTION DEPENDENCE ON MIGRATION DYNAMICS AND FISHERY CHARACTERISTICS*

Example (2.1) provides a detailed description of the harvest rate error structure that can be expected under very specific conditions. For these error structures to be applied to an actual fishery, it would be useful to know how the distributions depend on the fish migration dynamics assumptions, and the temporal and spatial characteristics of the fishery. Ideally, it would have been useful to expand the generalized model of equation (2.3) to describe error distributions as a result of all of these characteristics, but there are too many dimensions to justify doing this. Instead, I only describe how the bias and error variance change when individual characteristics are perturbed away from the baseline conditions of example (2.1).

The simulations suggested that the harvest rate error distributions follow the same general form as example (2.1), regardless of the specific details. The errors always follow a beta-distribution and differ primarily in the magnitude of the bias and error variance as described qualitatively in Table 2.1 (for fisheries with  $u = 0.85$ ). The errors follow patterns that are intuitively consistent. Since harvest rate errors arise as a consequence of errors in partitioning escapement, factors that increase the magnitude of escapement errors (relative to catch) increase the magnitude of harvest rate errors. Violation of the order of movement assumption produces escapement errors as fish exposed to the fishery migrate out of the exposed boxcars, or as fish not exposed to the fishery migrate into the

exposed boxcars. Increased frequency/intensity of migration delays and higher diffusion rates result in larger violations to the order of movement assumption and larger errors in escapement partitioning. Similarly, increasing the distance between the fishery and the escapement monitoring site allows more time for the variable migration dynamics to operate, and increases the errors in escapement partitioning. Conversely, increasing the spatial area and duration of a fishery tends to decrease the harvest rate errors because the magnitude of escapement errors relative to catch is decreased. This arises because larger fisheries (greater area or duration) affect more boxcars, and movements between boxcars within the summation interval do not affect the final summed escapement. Only movements into and out of the terminal fishery boxcars affect the summed escapement. If a greater number of boxcars are included in the summation interval, the terminal boxcar movement violations, which produce errors, account for a smaller proportion of the total calculated escapement. In the extreme case, if the fishery affects the whole run, then violations to the order of movement assumption are irrelevant because the summed escapement is correct (even if escapement in the individual boxcars cannot be properly partitioned). This also explains why the harvest rate bias decreases if the calculation interval is redefined to include boxcars that were not exposed to the fishery. In the scenario defined in example (2.1), the harvest rate estimation bias is essentially eliminated by simply expanding the summation interval from the 3 boxcar fishery width to 7 boxcars (although the error variance remains substantial).

## DISCUSSION

The objectives of this chapter were to define plausible stochastic salmon migration dynamics scenarios, and describe how harvest rate estimates are affected by violations of the order of movement assumption. The first objective was successful in that criteria were identified to constrain the range of plausible migration dynamics scenarios. However, within the constraints identified, there still remains considerable latitude for alternative scenarios. The second objective was successful in describing the general form for harvest rate estimation errors under a range of conditions, but specific descriptions were limited by the description of migration dynamics. These results provided the methods for generating harvest rate likelihood functions that are required for the estimation of migration routes as described in chapter 3, while additional implications for fisheries management are examined in this section.

The variance of the simulated harvest rate error distributions for the baseline migration dynamics defined may seem high (fig. 2.6), and there are several reasons why these errors might be overstated. Since there is presently not enough information to adequately describe the migration dynamics scenario, it is possible that the variability is exaggerated. There is evidence suggesting that the estimation bias of high harvest rate fisheries does occur (PSC 1995), however there are problems with the quantification of this bias in the Fraser River system because harvest rate estimates are confounded with migration route estimates (see chapter 3). The ability of managers to make subjective adjustments during run-reconstruction may also reduce the expected error variance. e.g. It

may be possible to constrain  $E'_i$  based on other fisheries targeting the same run in the same year. Fisheries in close temporal and spatial proximity will not be independent, and during run-reconstruction, efforts are made to reconcile total catch and escapement observations, so higher overall exploitation rates should result in lower harvest rate errors for individual fisheries. Unfortunately, the simulations described here assumed that the fisheries were independent. However, it is conceivable that the harvest rate errors could also be understated in the examples, because the migration dynamics could be more variable than the scenario defined, and catch, escapement and mean migration rate errors were not considered in the simulations.

Harvest rate uncertainty can be attributed to several sources. Estimation errors arise from violations of the order of movement assumption, and other factors mentioned above. Actual harvest rate variability arises from variation in fishing effort and catchability, where catchability is dependent on behaviour (e.g. choice of migration rates, depths and routes). Harvest rate can be defined in different ways, and the definition can affect the uncertainty (i.e. a fixed elemental harvest rate  $u$  can produce different  $h$  values depending on the fishery duration and shape of the migratory timing distribution). Harvest rate definitions and methods of accounting for harvest rate uncertainty will differ depending on the particular application. Pre-season fishery planning models may require fine temporal resolution of harvest rates for the simulation of numerous small fisheries, while in-season stock assessment often depends on harvest rates expressed as a proportion of the total run (e.g. total run size may be estimated from the historical

relationship between total run size and the maximum weekly catch per unit effort, PSC 1995).

Forward simulation models used for pre-season fishery scheduling should ideally incorporate harvest rate uncertainty as an additional factor for assessing alternative plans. Simulations of alternative schedules with stochastic harvest rate variability would help to identify the sensitivity of different fishing plans to this uncertainty. Fine temporal resolution harvest rate error distributions for the simulations cannot be well-defined presently. However, the insight provided by this study, combined with historical estimates, should help to define distributions that are more meaningful than point estimates. The precautionary approach would be to assume the most variable salmon migration dynamics that can be justified from the observations and simulations.

There are two obvious avenues for additional research that could help define harvest rate error distributions. The first would be to try to improve the understanding of salmon coastal migration dynamics through field studies. This could involve new tagging studies, or detailed sampling of temporal and spatial distributions. The second avenue would be to examine the interdependence of harvest rates from different fisheries within years. Conceivably, the extra catch and escapement information generated within a year could provide substantial constraints to individual harvest rate estimates, and this data might already provide substantial limits to the harvest rate errors that have been generated historically, such that the importance of migration dynamics knowledge might be overstated in this study.

Table 2.1. Qualitative summary of how the bias and error variance of harvest rate estimates (derived from backward-iterated run-reconstruction) are dependent on fish migration dynamics and fishery characteristics. Each result represents Monte Carlo simulations of 150 fisheries with the indicated factors perturbed away from the baseline conditions of example (2.1). Bias and variance responses are indicated by increase (+) and decrease (-). Simulations describe a fishery with  $u = h = 0.85$  (except in the case of the fishery duration change, where  $0.8 < h < 0.9$ , and in the case of the boxcar summation interval change, where  $u = 0.85$ , and  $0.35 < h < 0.55$  depending on the interval).

As ... increases:	$h'$ underestimation bias	$h'$ error variance
Frequency/intensity of migration delays	+	+
Diffusion rate ( $M$ )	+	+
fishing area distance from river mouth	+	+
fishing area*	-	-
fishing duration*	-	-
number of boxcars in summation interval*	-	+

\* Note that changes in these factors affect the number of boxcars over which the harvest rate is calculated, and the temporal/spatial nature of fishing exposure, so the comparison with the baseline scenario is not exactly a case of 'all other things being equal'.



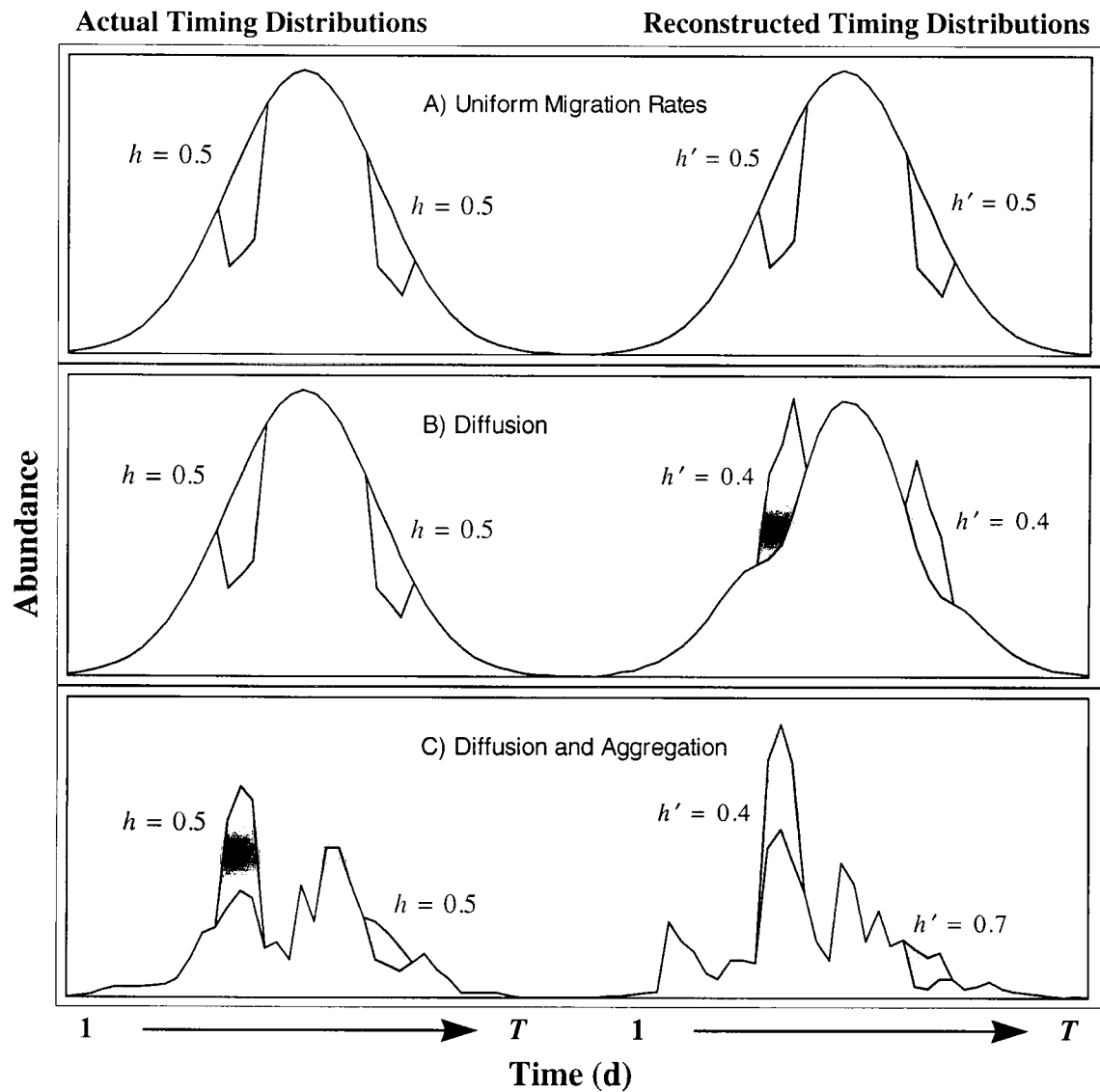


Fig. 2.1. Hypothetical salmon migratory timing distributions showing actual and reconstructed run timing at a fishery under three salmon migration dynamics scenarios: A) uniform migration rates, B) consistent diffusion rates, and C) diffusion and stochastic migration delays. The hollow portion of the curves represents the escapement timing distribution and the shaded portions represent the fishery catch. The reconstructed curve is generated under the 'order of movement' assumption, such that the escapement timing distribution observed 200 km from the fishery is assumed to be identical to the escapement distribution at the fishery (except for a time shift corresponding to the 200 km travel time that is accounted for in the reconstruction). Observed ( $h$ ) and reconstructed ( $h'$ ) harvest rates are indicated for each fishery.

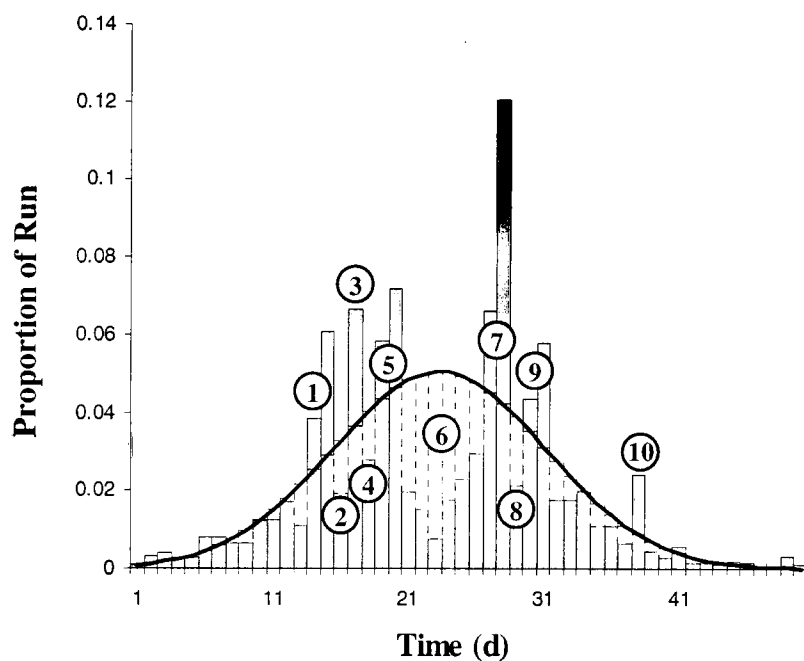


Fig. 2.2. Backward-iterated reconstructed migratory timing distribution from the 1993 Horsefly River sockeye run, showing deviations from a normal distribution with the same mean and variance. NAS is the Number of Anomaly Stanzas in which the abundance on at least one day exceeds 1 % of the total run size (a stanza consists of all consecutive days that the observed abundance is either all greater than or all less than the normal distribution). Positive anomalies are indicated by grey bars above the normal curve, and negative anomalies are indicated by white bars beneath the curve; numbers indicate anomalies sufficiently large to be counted. SAV is the Summed Absolute Value of all the anomalies. NAS and SAV of this run are shown relative to other runs in fig. 2.3.

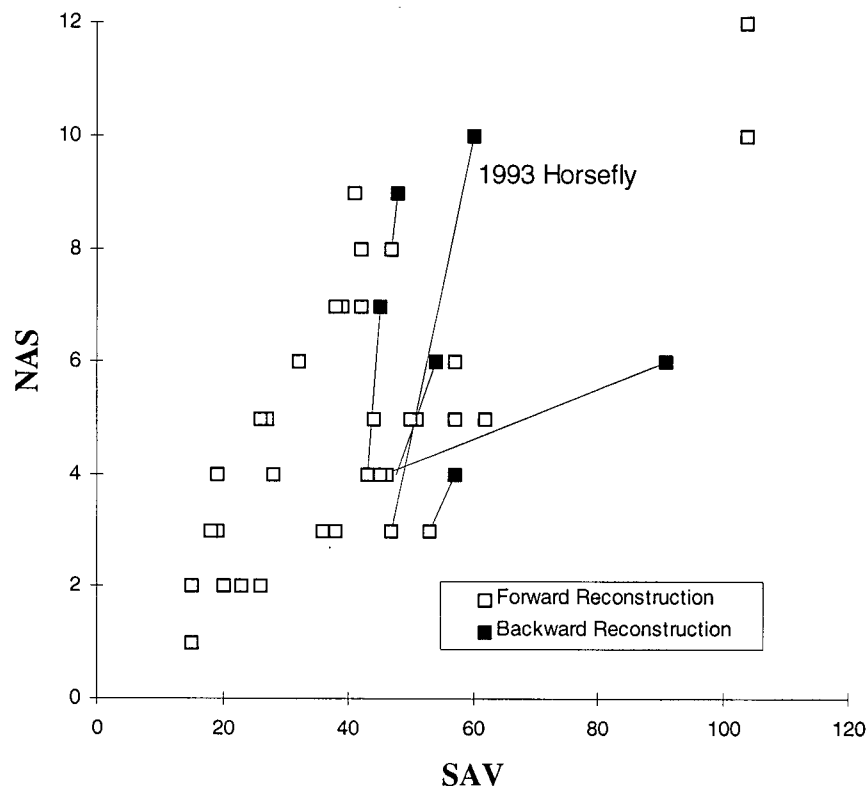


Fig. 2.3. Migratory timing anomaly indices of reconstructed Fraser River sockeye salmon runs (provided by James Cave, Pacific Salmon Commission). Solid squares represent indices for 1993 timing distributions reconstructed with the backward-iterated method; hollow squares indicate indices for forward-iterated reconstructions from 1992-94. Lines connect the indices from the same run reconstructed with both methods. NAS is the Number of Anomaly Stanzas (a stanza consists of all consecutive days that the observed abundance is either all greater than or all less than the normal distribution) in which at least one day exceeds 1 % of the total run size. SAV is the Summed Absolute Value of all the anomalies. The timing distribution of the 1993 Horsefly run is shown in fig. 2.2.

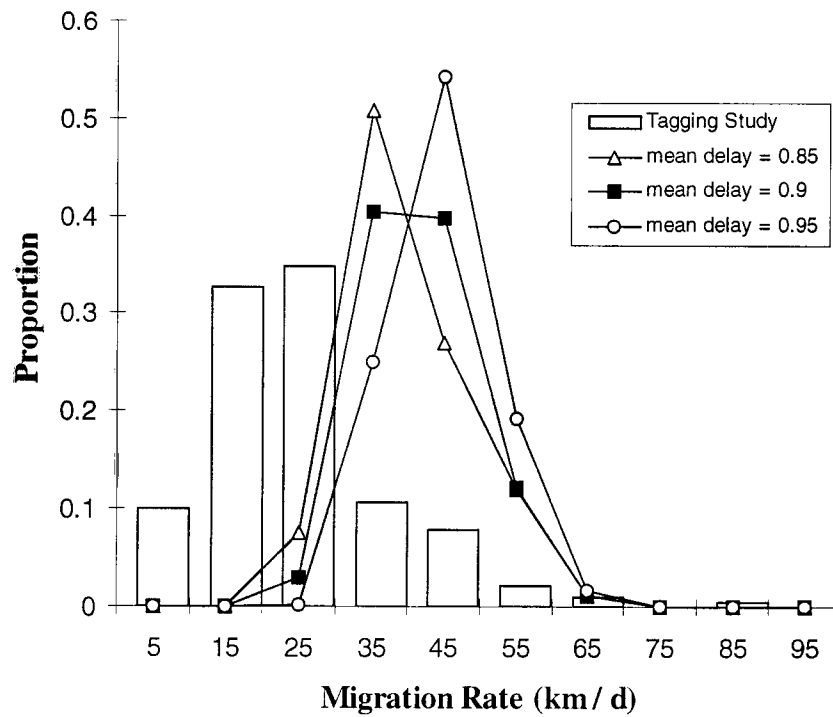


Fig. 2.4. Comparison of individual migration rate distributions (over 260 km) from Johnstone Strait sockeye tagging studies (estimated from Verhoeven and Davidoff (1962)) and simulated migration dynamics scenarios with a diffusion rate of 0.2, and migration delays resulting in mean rate reductions of 0.85, 0.9 and 0.95 of the baseline migration rate.

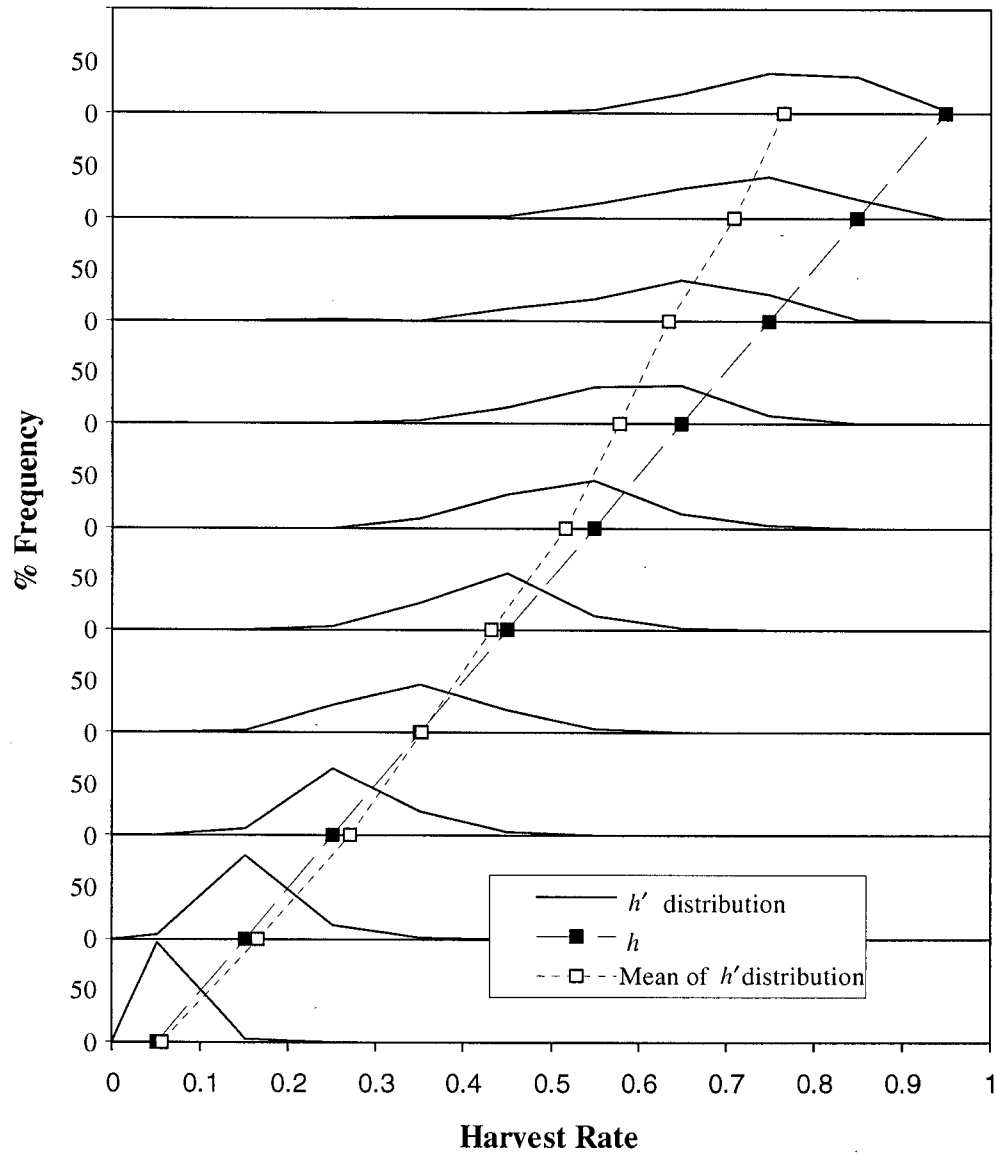


Fig. 2.5. Error distributions of (backward-iterated) reconstructed harvest rates produced by Monte Carlo simulations of a Juan de Fuca Strait (Canadian statistical Area 20) purse seine fishery with stochastic salmon migration dynamics described in example (2.1). Each panel shows the frequency distribution of harvest rate estimates ( $h'$ ) corresponding to the known harvest rate ( $h$ ) that is indicated by the solid square at the base of each panel. Hollow squares at the base of each panel indicate the mean of each  $h'$  distribution. The difference between the solid and hollow squares represents the harvest rate estimation bias.

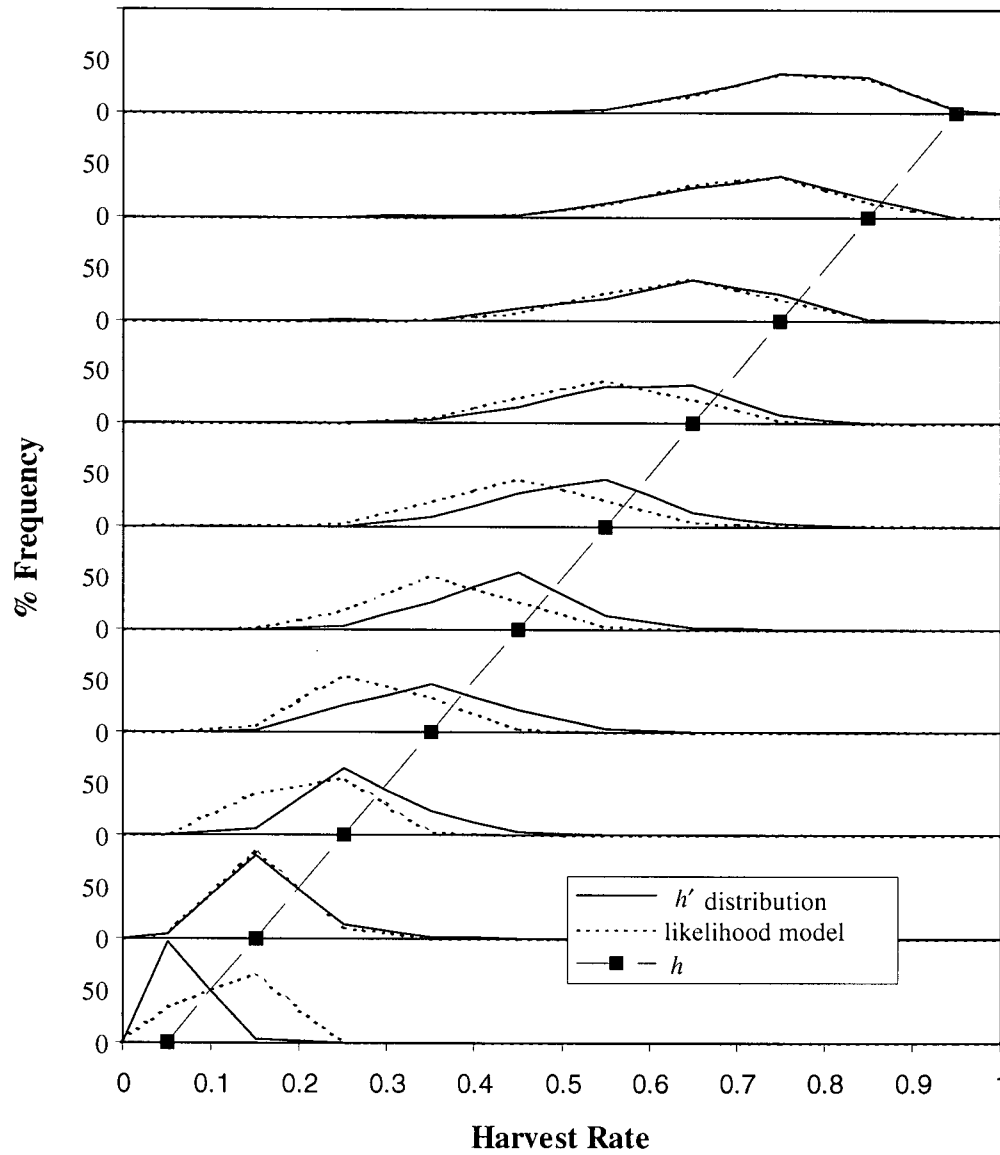


Fig. 2.6. Comparison of harvest rate error distributions (solid lines) produced by the Monte Carlo simulations of example (2.1), with distributions from the best fit likelihood model, equation (2.3), overlaid (broken lines). Each panel represents the distributions that correspond to the actual harvest rates,  $h$ , indicated by the solid square at the base of each panel.

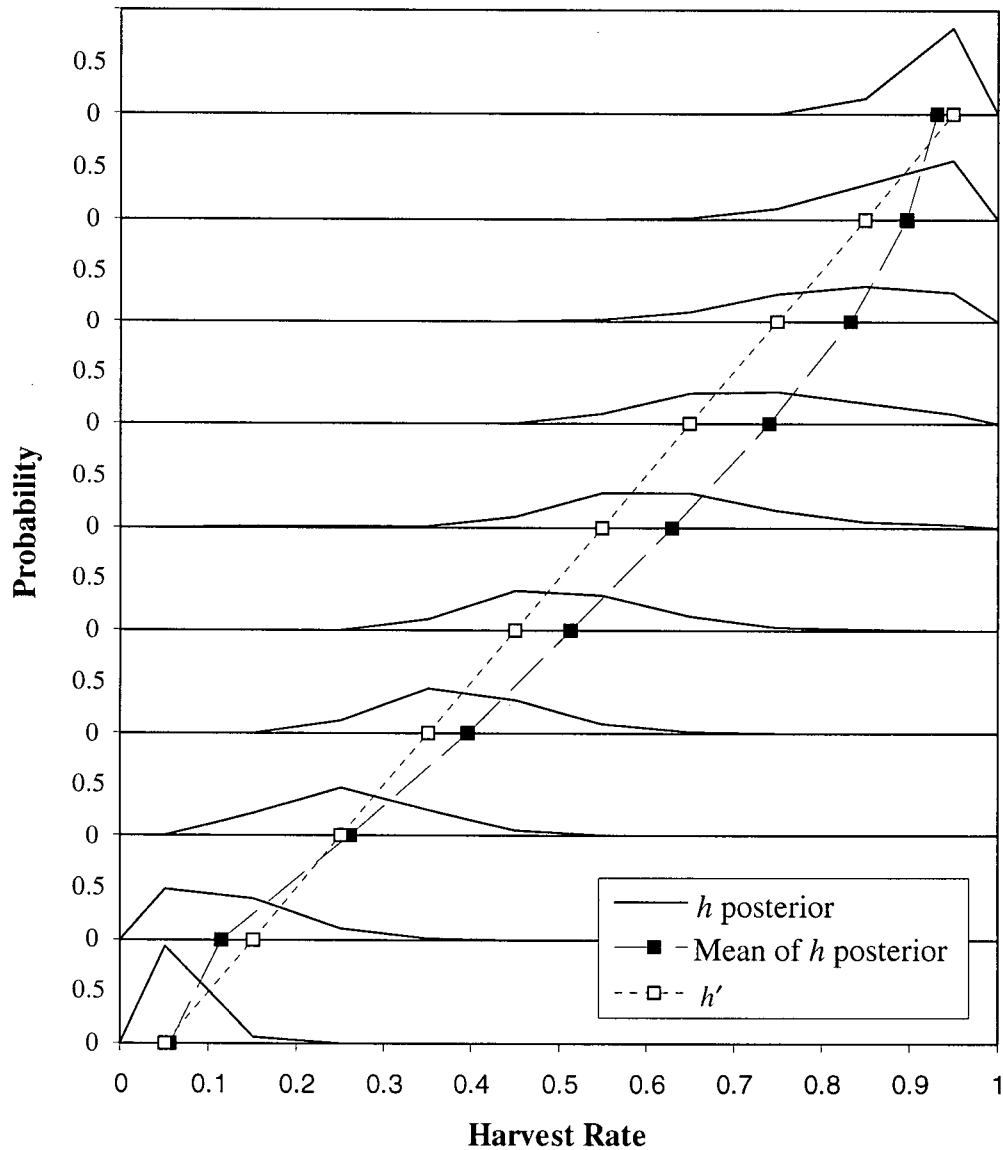


Fig. 2.7. Posterior probability distributions for harvest rates,  $h$ , (likelihoods approximated by equation (2.3)) which correspond to harvest rates estimated by run reconstruction,  $h'$ , in example (2.1). Each panel shows the posterior for  $h$  given the estimated  $h'$  indicated by the hollow square at the base of each panel. The solid squares indicate the mean of the  $h$  posterior distribution. The difference between the solid and hollow squares in each panel emphasizes the estimation bias that can be expected if  $h'$  is accepted as the best estimate of  $h$ .

### **CHAPTER 3: A BAYESIAN METHOD FOR ESTIMATING HARVEST RATES AND MIGRATION ROUTES IN THE FRASER RIVER SOCKEYE SALMON FISHERY**



## **ABSTRACT**

Maturing sockeye salmon can return to the Fraser River by migrating around either the north or south end of Vancouver Island, and the estimation of approach route harvest rates and the proportion of fish using each route is complicated because 1) the combined escapement through the two fisheries is monitored in-river and cannot be directly partitioned by route of origin, 2) there is likely considerable error in the escapement estimates, and 3) harvest rates probably vary with fishing effort. This chapter describes how a Bayesian framework can be used to quantify the relationships between harvest rates, fishing effort, and migration routes, such that these uncertainties are explicitly admitted and reflected in posterior probability distributions. A hypothetical example is used to illustrate the estimation process and the potential advantages and disadvantages of adopting this procedure are examined.

## INTRODUCTION

Maturing sockeye salmon can return from the Gulf of Alaska to the Fraser River either by migrating via the northern route around Vancouver Island, through Queen Charlotte and Johnstone Straits, or via the southern route through Juan de Fuca Strait (fig. 1.1), and the proportion of fish using each route varies considerably among years (fig. 1.2). The estimation of harvest rates and migration routes is complicated in this system, and there has never been any formal estimation method published that explicitly accounts for the major sources of error. As a result, existing time series have been used in fisheries management and numerous studies of salmon migration without much consideration of the statistical properties of the estimates.

Ideally, one could estimate migration routes knowing the harvest rates, or one could estimate harvest rates knowing the migration routes. Since both are unknown, this joint uncertainty should be recognized. Estimation of migration routes and harvest rates involves combining catch and escapement data to reconstruct the abundance in each approach route that was present during the fishery. Commercial fishery catch data from these fisheries is believed to be fairly accurate, however, potentially serious problems affect the escapement data. There is considerable uncertainty in the escapement estimates because of the violation of migration dynamics assumptions that are required in the process of run-reconstruction (described in chapter 2). Furthermore, escapement is monitored in the Fraser River after fish from both approach routes have merged, and harvest rate and migration route estimation requires that the escapement be partitioned by

the route of origin. Assuming that harvest rates remain fairly consistent over time, one can attempt to estimate harvest rates and migration routes by solving a system of simultaneous equations that combines data over a time series of fisheries with informative contrast. However, fishing effort also changes in both approach routes depending on fish abundance (and temporal and spatial fishery restrictions), and such an estimation scheme should also account for this variability. This chapter describes a Bayesian approach for estimating harvest rates and migration routes that formally admits uncertainty from these processes. The resulting posterior probability distributions for the parameters provide an indication of the uncertainty associated with each estimate. The method is described in detail for a hypothetical example, and some options for implementation with real data are examined.

#### *FISHERY NOTATION*

The proposed method for estimating harvest rates and migration routing focuses on the major commercial purse seine fisheries in the coastal approaches to the Fraser River. The notation used to describe these fisheries is adopted from the boxcar fishery model detailed in chapter (2), with a few modifications. In the Fraser River sockeye fishery, the relevant observations consist of:

$C$  = catch,

$E$  = escapement, and

$F$  = fishing effort (measured in standardized units of purse seine equivalents),

and a number of additional values can be calculated from these data:

$N = C + E$ , the total abundance,

$d$  = diversion rate (proportion of fish migrating via the indicated approach route),

$u$  = elemental (single boxcar daily) harvest rate, and

$h$  = the total harvest rate for a defined fishery interval ( $h$  is dependent on  $u$  and the spatial characteristics of the fishery, the fishery duration, the shape of the migratory timing distribution, and the temporal/spatial interval of interest). These variables are indexed to distinguish positions in space and time with the following subscripts:

$n$  = northern approach route (Queen Charlotte Strait and Johnstone Strait),

$s$  = southern approach route (Juan de Fuca Strait),

$i$  = fishery opening number (1 to  $I$ ),

Subscripts are sometimes omitted to improve readability, and these variables describe general relationships that are not specific to a fishery or approach route.

To simplify notation for a particular fishery which may encompass multiple days, and multiple boxcar units,  $i$  replaces a summation interval over  $t$  (day) and  $l$  (location in boxcar units away from the river escapement monitoring site). A fishery opening in this chapter refers to simultaneous openings in both the northern and southern approach routes. The actual time/space summation interval for  $i$  is defined over an interval that is large enough to encompass the boundaries of both approach route fisheries and thus includes some fish that were not actually exposed to harvesting. The total escapement associated with fishery  $i$ , is designated  $E_{n+s,i}$  ( $= E_{n,i} + E_{s,i}$ ). In the following equations, parameters are distinguished from parameter estimates and observations by a *prime* (e.g.

in example (3.1), arbitrarily selected values of  $h_n$ ,  $E_{n+s,i}$  are estimated by the values designated  $h'$ ,  $E'_{n+s}$ ).

An additional term  $h_u$ , is used to represent the harvest rate calculated for a particular fishery with elemental harvest rate  $u$ , assuming that the migratory timing distribution is uniform (described in Example 3.1 below). When referring to the proportion of fish migrating via each approach route in the Fraser system, it is customary to refer to the northern diversion rate,  $d_n$ , where  $d_n = N_n / (N_n + N_s) = 1 - d_s$ , and may refer to the total over the whole year, or a specific fishery.

To simplify the readability of the likelihood functions, additional parameter vectors are introduced:  $\theta$ ,  $\phi$ ,  $\psi$ , along with the matrix  $Y$  describing all the data. These are described in the overview below.

#### *PROBLEMS ASSOCIATED WITH ESTIMATING HARVEST RATES AND MIGRATION ROUTES IN A MULTIPLE APPROACH FISHERY*

The observations available for a given fishery consist of the total catch in each area, the fishing effort (standardized across gear types), and the estimated escapement from both fisheries combined. The components of a single approach route fishery  $i$ , are related by equation (2.1):  $N_i = C_i + E_i = C_i / h_i$ . Expressing  $E_i$  in terms of catch and harvest rate yields

$$E_i = C_i \left( \frac{1}{h_i} - 1 \right),$$

and it is easy to solve for  $h_i$  given  $C_i$  and  $E_i$ . In the Fraser River system, there are two approach routes and two components of escapement  $E_{n,i}$  and  $E_{s,i}$ , however, only the combined escapement in-river is monitored,  $E_{n+s,i}$  ( $= E_{n,i} + E_{s,i}$ ). So the observed escapement from simultaneous fisheries in the northern and southern approach routes are related by:

$$E_{n+s,i} = C_{n,i} \left( \frac{1}{h_{n,i}} - 1 \right) + C_{s,i} \left( \frac{1}{h_{s,i}} - 1 \right).$$

In this multiple approach case, estimates of  $h_{n,i}$  and  $h_{s,i}$  are confounded by the requirement to partition  $E_{n+s,i}$ , such that for a single fishery  $i$ , there is no unique solution (i.e.  $E_{n+s,i}$  could be the result of a relatively low  $h_{n,i}$ , and high  $h_{s,i}$ ,  $d_{n,i}$  or high  $h_{n,i}$  and low  $h_{s,i}$ ,  $d_{n,i}$ ). If harvest rates were stationary over time, then this equation would yield a unique solution for  $h_{n,i}$  and  $h_{s,i}$ , provided that high resolution, error-free data from multiple fisheries with informative contrast were available. However, harvest rate variability is introduced into the system in (at least) three important ways. First, harvest rates vary with fishing effort, and variability in the number of boats and fishery areas and durations must be considered. Second, migratory timing distributions are polymodal, and even though a precise relationship between harvest rates and fleet sizes could exist, the coarse resolution definitions required to examine north and south fisheries simultaneously introduces error into this relationship, as fish not exposed to harvesting must be incorporated into the calculation. So for the harvest rate definitions required, there is considerable noise around the relationship between fleet size and effort. Third, there are potentially large

errors in the measured escapement,  $E'_{n+s,i}$ , due to the separation of the fishery and the escapement monitoring site. Reconstruction of the run in space and time is required to align the escapement with the corresponding catch for a fishery. Since salmon migration dynamics are poorly understood, assumptions during this reconstruction process potentially introduce substantial errors as described in chapter (2). This chapter describes my attempt to develop a method for estimating harvest rates and diversion rates within a framework that accounts for these sources of uncertainty.

## OVERVIEW OF THE BAYESIAN ESTIMATION METHOD

The approach presented here attempts to account for three major sources of uncertainty that exist in this system, and it will become apparent that the level of complication may not be justifiable in terms of improved estimation accuracy or ease of interpreting results. Possible directions for simplification are suggested in the discussion. The interdependence of the quantities of interest is such that the problem can be defined in different ways, and the approach presented here is the most intuitively easy to follow in my opinion.

Assuming that salmon migration rate variability can be adequately constrained, the process of estimating harvest rates and migration routes amounts to defining a model that describes the system interactions, and comparing the relative credibility of the possible model parameter combinations given the observations. Bayes' theorem (equation (2.4)) provides a framework for accomplishing this comparison such that the

relative credibility of the parameter values are reflected by posterior probability distributions.

The likelihood calculation for this system is broken down into a couple steps and some additional notation is introduced to aggregate data and parameters in an attempt to improve readability. The data from each fishery,  $Y_i$  consists of the catch,  $C_{n,i}$ ,  $C_{s,i}$ , and effort,  $F_{n,i}$ ,  $F_{s,i}$ , from each approach route, and the reconstructed escapement  $E'_{n+s,i}$  corresponding to both approach routes combined (catch and effort are assumed to be measured without error, e.g.  $C'_{s,i} = C_{s,i}$ ). Greek letters are used to distinguish between groups of related parameters,  $\psi$ ,  $\theta$ , and  $\phi$ . The migration dynamics parameters are all grouped into  $\psi$  and are assumed to be known for the calculations presented in this chapter.  $\psi$  contains the factors that affect harvest rate estimation errors in a single approach fishery as described in chapter (2), including: diffusion rates, probability of experiencing a migration delay, and the location/intensity of migration delays.  $\psi$  will be omitted in most subsequent equations, but remains implicit as the underlying conditions upon which all the probability density functions are based. In reality,  $\psi$  is poorly quantified and presently requires considerable subjective judgement as indicated in chapter (2).  $\theta$  includes the parameters that are assumed to be independent among fisheries:  $N$  and  $d_n$ .  $N$  is treated as a nuisance parameter because it is not directly of interest here (although it is of interest for in-season stock assessment).  $\phi$  quantifies the relationship between effort and harvest rates that is required to calculate expected harvest



rates for a range of fleet sizes, and fishery spatial/temporal characteristics.  $\phi$  is assumed to be stable among fisheries, and consists of 4 parameters in example (3.1).

With this notation, the posterior probability (equation (2.4)) for a particular parameter combination,  $k$ , is expressed:

$$(3.1) \quad P(\theta_k, \phi_k | Y) = \frac{L(Y | \theta_k, \phi_k) \times P_0(\theta_k, \phi_k)}{\sum_j L(Y | \theta_j, \phi_j) \times P_0(\theta_j, \phi_j)}.$$

Marginal posteriors for  $d_n$  and each element of  $\phi$  are calculated by summing the joint posterior over all other parameters, e.g.:

$$P(d_n | Y) = \iint P(\theta, \phi | Y) dN d\phi,$$

(the integral over  $d\phi$  being the integral over all elements of  $\phi$ ). For a single fishery, the likelihood of observing the data from fishery  $i$  given a parameter combination  $k$  is more explicitly defined:

$$\begin{aligned} L(Y_i | \theta_k, \phi_k) &= L(C_{n,i}, C_{s,i}, E'_{n+s,i} | \theta_k, \phi_k) \\ &= L(C_{n,i} | \theta_k, \phi_k) \cdot L(C_{s,i} | \theta_k, \phi_k) \cdot L(E'_{n+s,i} | C_{n,i}, C_{s,i}, \theta_k, \phi_k), \end{aligned}$$

and the additional conditioning factors  $F_{n,i}$ ,  $F_{s,i}$ , and  $\psi$  are implicitly included in the likelihoods. The individual likelihood density functions are derived from Monte Carlo simulations using the methods of chapter (2) and are detailed in example (3.1). I am assuming that the factors affecting catch variability act independently in the north and

south. Thus the likelihood of generating the catch observations is the product of the two. In a single approach fishery, for a given set of parameters,  $L(C) = L(E) = L(h)$  because of the simple relationships (2.1). In this chapter, it is generally more intuitively obvious to refer to  $L(C)$ , but the actual calculations are presented in terms of  $L(h)$ , consistent with the methods of chapter (2).

The escapement likelihood calculation is more complicated because the actual escapement,  $E_{n+s,i}$ , is the sum of the escapement from both approach routes, and the observed escapement  $E'_{n+s,i}$ , may have substantial measurement error introduced as a result of reconstructing abundance at the fishery from escapement measured at a distant in-river location.  $L(E'_{n+s,i} | C_{n,i}, C_{s,i}, \theta_k, \phi_k)$  is actually the sum of all possible combinations of  $L(E'_{n,i} | C_{n,i}, \theta_k, \phi_k) \cdot L(E'_{s,i} | C_{s,i}, \theta_k, \phi_k)$  that meet the constraint  $E'_{n+s,i} = E'_{n,i} + E'_{s,i}$ . The escapement likelihood calculations are also presented in terms of harvest rates, i.e.  $h' = C / (C + E')$ , and hence  $L(E' | C) = L(h' | h)$ .

The prior probability distributions,  $P_0(\theta, \phi)$  represent another area where subjective decisions enter into the estimation process. The method proposed here initially assumes uniform prior probability distributions for each element of  $\theta$  and  $\phi$ , ( $P_0(\theta, \phi) \sim U[]$ ). If data from only one fishery is available, each of  $P_0(\theta) \sim U[]$  and  $P_0(\phi) \sim U[]$ . One of the expected benefits of this method is the integration of data across fisheries with informative contrast, such that uncertainty in  $\phi$  can be reduced, and this can in turn be used to reduce uncertainty in  $\theta$ . This is accomplished by using an iterative process in

which the posterior of  $\phi$  (integrated over  $\theta$ ) from one subset of fisheries is used as the prior for  $\phi$  for another subset of fisheries. There is also potential for the use of informative priors and constraints when additional data from a particular run is considered (i.e. catch and escapement observations that are not encompassed by the specified  $l$  and  $t$  summation intervals), and some of the options are mentioned.

Example (3.1) illustrates the whole procedure with details of an assumed functional relationship between fleet size and harvest rate, the probability density functions generated with the methods of chapter (2), and the calculation process.

**EXAMPLE (3.1): SIMULTANEOUS ESTIMATION OF MIGRATION ROUTES AND HARVEST RATES IN A HYPOTHETICAL FISHERY WITH TWO APPROACH ROUTES**

The following example demonstrates how this approach could be used to estimate migration routes, harvest rates and the relationship between fleet sizes and harvest rates for the Fraser River sockeye fishery. Table 3.1 describes the spatial and temporal characteristics of two fisheries approximately corresponding to a Johnstone Strait (Canadian Statistical Area 12 and 13) purse seine opening (north), and a Juan de Fuca Strait (Area 20) purse seine opening (south). Table 3.2 describes the parameters and observations associated with a series of 5 hypothetical fishery openings. The migration routing,  $d_n$ , was selected to cover a broad range, while fishing effort,  $F$ , was divided so that the catch per unit effort in both approach routes was within a factor of 1.5 (i.e. it was assumed that the fleet approached the ideal free distribution in a manner suggested by

Gillis et al. 1993). The parameter values describing the relationships between effort and harvest rate were chosen arbitrarily.

#### *THE RELATIONSHIP BETWEEN HARVEST RATES AND FLEET SIZE*

If the fishing fleet has the freedom to move in a multiple approach fishery, it is expected that the number of fishing vessels in each area will vary as the proportion of fish using each route varies. Provided that there exist effort observations  $F_n$  and  $F_s$  corresponding to catch observations, one can attempt to account for this harvest rate variation. The function relating  $F$  and the elemental harvest rate,  $u$  in this system should satisfy some simple conditions: 1) it passes through the origin (if  $F = 0$  then  $u = 0$ ), 2)  $u$  increases as  $F$  increases, 3) the rate of increase in  $u$  decreases as  $F$  increases, and 4)  $0 \leq u \leq 1$ . A Michaelis-Menten type saturation curve is a simple function that meets these criteria:

$$(3.2) \quad u = \frac{aF}{b + F},$$

where the  $a$  and  $b$  parameters can take any positive value as long as  $0 \leq u \leq 1$ . This function can assume many forms. At one extreme,  $u$  is essentially constant over all  $F$ , at the other extreme,  $u$  is essentially directly proportional to  $F$  over the range of observed fleet sizes, and at intermediate values, with increasing  $F$ ,  $u$  increases toward an

asymptote. The net harvest rate for a particular fishery,  $h$ , depends not only on  $u$ , but also the specific fishery characteristics as detailed below and in chapter (2).

Since the fleet size-harvest rate relationships may differ between northern and southern fisheries, there are four unknown parameters ( $a_n, a_s, b_n, b_s$ ). However, the relationship between the  $a$  and  $b$  parameters is not compatible with any simple grid over which to calculate posteriors. To account for this problem, equation (3.2) was reparameterized in terms of  $u_{100}$  and  $u_{50}$ , where  $u_{100}$  equals the harvest rate at maximum fleet size,  $F_{max}$ :

$$u_{100} = \frac{aF_{max}}{b + F_{max}},$$

and  $u_{50}$  equals the harvest rate at one half of  $F_{max}$ , expressed as a proportion of  $u_{100}$ :

$$u_{50} = \frac{a(F_{max}/2)/(b + F_{max}/2)}{u_{100}}.$$

This corresponds to an elemental harvest rate of:

$$(3.3) \quad u = \frac{u_{100}u_{50}F}{F_{max}(1 - u_{50}) + F(2u_{50} - 1)}.$$

Using these relationships,  $\phi = (u_{100n}, u_{100s}, u_{50n}, u_{50s})$ , and posteriors can be calculated over convenient grids of  $0 < u_{100n}, u_{100s} \leq 1$  and  $0.5 < u_{50n}, u_{50s} < 1$ . The arbitrarily chosen relationships for the two fisheries of example (3.1) are shown in fig. 3.1.

#### *THE LIKELIHOOD CALCULATION*

This estimation method requires the assumption that harvest rate probability distributions can be adequately quantified. In fact this is not really the case, but the arguments of chapter 2 suggest how constraints to  $\psi$  can be estimated, and the precautionary approach would be to admit the greatest variability in  $\psi$  that can be justified. All components of the likelihood from equation (3.1):

$$L(Y_i|\theta_k, \phi_k) = L(C_{n,i}|\theta_k, \phi_k) \cdot L(C_{s,i}|\theta_k, \phi_k) \cdot L(E'_{n+s,i}|C_{n,i}, C_{s,i}, \theta_k, \phi_k),$$

can then be calculated from the relationships between expected, actual, and estimated harvest rates ( $h_u, h, h'$ ) as described below.

The elemental harvest rate,  $u$ , is used to make assertions about the relationship between fleet sizes and harvest rates, by calculating a harvest rate,  $h_u$ , that can be expected for a fishery with particular characteristics. There are a number of reasons why the actual harvest rate,  $h$ , is not equal to  $h_u$ , and the relationship between these values must be described. The boxcars of fish exposed to harvesting do not coincide perfectly in time and space between northern and southern routes. From Table 3.1, the combined escapement estimate,  $E'_{n+s}$ , should include 6 boxcars (located at  $l = 1$  through  $l = 6$

during the fishery) to include all boxcars from both approach routes that were exposed to harvesting. As a result, boxcars are included in the summation interval that are not exposed to the fishery, and the actual value of  $h$  is dependent upon not only  $u$ , but also the shape of the migratory timing distribution. Hence, even if  $u$  is constant within each approach route fishery,  $h$  varies among fisheries. A harvest rate summation interval of 7 boxcars was chosen for this example.

Since the shape of the migratory timing distribution during a fishery is not known, the expected harvest rate,  $h_u$ , is calculated under the assumption that the distribution is uniform (e.g. for a 7 boxcar interval corresponding to fishery  $i$  on day  $t$ , each of  $N_{t,t}, N_{t,t+1}, \dots, N_{t,t+6} = N_i / 7$ ). For a 1 d southern approach fishery (Table 3.1), 3 boxcars are harvested at an elemental harvest rate of  $u_s$  (which is in turn dependent upon  $u_{100s}$ ,  $u_{50s}$  and  $F_s$ ) and with the summation interval of 7 boxcars,  $h_u = \frac{3}{7} u$ . For fisheries of duration greater than one day,  $h_u$  is calculated in such a way that there is an exponential depletion of exposed fish over time (see the calculation of the pre-season planning model description of  $h$  in chapter (2)). The relationships between  $h$  and  $h_u$  described below were generated assuming that the variability in the migratory timing distribution was the only factor introducing noise. Undoubtedly other factors directly affect  $u$ , including the current economic incentive for fishing, and the fine scale migration route variability affecting vulnerability at established fishing sites. It is assumed here that these factors do not have a large effect on the qualitative nature of the relationship and can be ignored for the purposes of this chapter, by assuming that all factors are already accounted for within the admittedly uncertain  $\psi$ .

In a single approach fishery, it is relatively simple to calculate  $h'$  directly and describe the posterior probability of  $h$  given  $h'$  (e.g. using equations (2.3) and (2.5)). In the multiple approach case,  $h'_n$  and  $h'_s$  cannot be calculated directly. Instead, posterior calculations are dependent on two separate relationships for each approach route. Equations (3.4) and (3.5) are required to calculate the likelihood of observing the catch, and (3.6) and (3.7) are required to calculate the likelihood of observing the escapement. These relationships were estimated using the Monte Carlo methods of chapter (2) for the two fishery structures described in table 3.1 and a forward-iterated reconstruction process. Equations (3.4)-(3.7) are presented in terms of expected ( $h_u$ ), actual ( $h$ ), and estimated ( $h'$ ) harvest rates, and the conversion to catch and escapement likelihoods are described below.

Assuming that the processes that cause harvest rate variability (other than effort variability) are independent in the two approach routes, then the likelihood of the catch observations is the product of the likelihood of the catch in the two approach routes. For parameter combination  $k$ , this is expressed:

$$\begin{aligned} L(C_n, C_s | \theta_k, \phi_k) &= L(C_n | \theta_k, \phi_k) \cdot L(C_s | \theta_k, \phi_k) \\ &= L(h_n | \theta_k, h_{u,n}) \cdot L(h_s | \theta_k, h_{u,s}), \end{aligned}$$

where:

$$\begin{aligned} h_n &= C_n / (d_{n,k} N_k), \\ h_s &= C_s / ((1 - d_{n,k}) N_k), \end{aligned}$$



and  $h_u$  is a function of  $\phi$ ,  $F$ , and the fishery temporal and spatial characteristics. This likelihood is calculated from the relationships between actual harvest rates ( $h_n$ ,  $h_s$ ) and expected harvest rates ( $h_{u,n}$ ,  $h_{u,s}$ ) generated by the Monte Carlo simulations:

$$(3.4) \quad h_n \sim \text{Beta}(\alpha_n, \beta_n); \quad \alpha_n = 14.2, \text{ and } \beta_n = 252 \exp(-6.41h_{u,n}) + 9.46,$$

$$(3.5) \quad h_s \sim \text{Beta}(\alpha_s, \beta_s); \quad \alpha_s = 35.2, \text{ and } \beta_s = 641 \exp(-6.61h_{u,s}) + 12.0.$$

If the boxcar model order of movement assumption was valid ( $E'_{n+s} = E_{n+s}$ ) then  $N (= C_n + C_s + E_{n+s})$  would be known without error, and these equations would be sufficient for calculating  $P(d_n, \phi | Y)$ .

Admitting the violation of the order of movement assumption complicates the calculation. There is an actual (but unmeasured) escapement associated with each approach route fishery:

$$E_n = N(d_n) - C_n,$$

$$E_s = N(1 - d_n) - C_s,$$

but the escapement observed in the river,  $E'_n + E'_s$ , contains error because of the variable migration rates. Since  $h' = C/(C + E')$  for each approach route, it follows that  $L(E'|C, \theta_k) = L(h'|h, \theta_k)$ . The Monte Carlo simulations indicated the following relationships between  $h$  and  $h'$ :

$$(3.6) \quad h'_n \sim \text{Beta}(\alpha_n, \beta_n); \quad \alpha_n = 19.9, \text{ and } \beta_n = 333 \exp(-5.89h_n) + 13.0,$$

$$(3.7) \quad h'_s \sim \text{Beta}(\alpha_s, \beta_s); \quad \alpha_s = 15.4, \text{ and } \beta_s = 461 \exp(-11.1h_s) + 25.0.$$

The observed escapement is the sum of the escapement from both approach routes,  $E'_{n+s} = E'_n + E'_s$ . Assuming that the migration dynamics are independent for each approach route, the likelihood of observing a particular  $E'_{n+s}$  is:

$$L(E'_{n+s} | C_n, C_s, \theta_k, \phi_k) = \int_a L(E'_n, E'_s | C_n, C_s, \theta_k, \phi_k) ds,$$

where  $a$  is the line that satisfies  $E'_{n+s} = E'_n + E'_s$  through the joint distribution  $L(E'_n, E'_s | C_n, C_s, \theta_k, \phi_k)$ . This line integral represents all possible ways of obtaining  $E'_{n+s}$  as a sum of  $E'_n$  and  $E'_s$  (given the observed catch and specified parameters). For numerical integration, each point on the line  $a$  is calculated:

$$\begin{aligned} L(E'_n, E'_s | C_n, C_s, \theta_k, \phi_k) &= L(E'_n | C_n, \theta_k) \cdot L(E'_s | C_s, \theta_k) \\ &= L(h'_n | h_n, \theta_k) \cdot L(h'_s | h_s, \theta_k), \end{aligned}$$

and is calculated from equations (3.6) and (3.7), where

$$h'_n = C_n / (C_n + E'_n),$$

$$h'_s = C_s / (C_s + E'_s),$$

and

$$h_n = C_n / (d_{n,k} N_k), \text{ and}$$

$$h_s = C_s / ((1 - d_{n,k})N_k).$$

For a given  $h_u$  and  $\theta_k$ , the line of integration through the joint distribution  $L(E'_n, E'_s | C_n, C_s, \theta_k, \phi_k)$  is illustrated in fig. 3.2.

Note that the likelihood calculations are presented as though the factors that affect the north and south migration routes are independent, and that actual harvest rate variability is independent of escapement error. The Monte Carlo simulations did not suggest a strong association between harvest rate variability and escapement error under the assumptions of chapter 2, but the impact of dependence between approach routes was not examined.

#### *SPECIFICATION OF PRIORS*

The prior probability distributions quantify the degree of prior belief in the parameters and can potentially have a large effect on the posterior distributions. The implications of some different priors are illustrated in example 3.1, scenarios A-C.

The approach taken with this problem initially involves assigning uniform distributions for all elements of  $\theta$  and  $\phi$  (scenario A, fig. 3.3A). The use of non-informative priors is recommended when there are no data available with which to generate informative priors (Walters and Ludwig 1994). It is conceivable that information from other systems could be used to constrain  $\phi$ , but it will become apparent

that the choice of  $\phi$  priors is not likely to have a big effect on the posteriors for  $d_n$ . The priors for  $N_i$  are informative, in so far as run-reconstruction provides some constraints. Clearly,  $N_i$  must be greater than the combined catch for each approach route, and  $N_i$  must be less than the total run size. In example 3.1, I assigned a uniform distribution:  $P_0(N_i) \sim U[C_{n,i} + C_{s,i}, C_{n,i} + C_{s,i} + 2 E'_{n+s,i}]$ . Since the escapement observations are large relative to catch (Table 3.2), this prior is likely to err on the side of not being restrictive enough. In a real application, good arguments could undoubtedly be made to further restrict this distribution.

Assuming that the relationships between harvest rates and effort are fairly stable among fisheries, it is expected that information from multiple fisheries can be combined to reduce uncertainty in  $\phi$ , and this can in turn be used to reduce uncertainty in  $\theta$ . This is accomplished by using the posterior probabilities of  $\phi$  (marginalized over  $\theta$ ) from fishery  $i$ , as the prior probability of fishery  $i+1$ , ( $P_0(\phi_{i+1}) = P(\phi_i)$ ). Since there is nothing special about the temporal order of the fisheries, the posteriors for  $\phi$  calculated over all fisheries provides the most informative prior for the calculation of each  $\theta$  posterior. However, this is a double accounting of data and amounts to a circular process of generating a posterior, and then using it as the prior for the same data (the greater the number of fisheries the smaller this error would be). To avoid this problem, the prior for fishery  $j$ ,  $P_0(\phi_j)$  should incorporate the information across all fisheries except  $j$ :

$$P_0(\phi_j) = \prod_{i=1, i \neq j}^I P_p(\phi_i),$$

where  $P_p(\phi_i)$  is the posterior for  $\phi_i$  (marginalized over  $\theta_i$ ) calculated with  $P_0(\phi_i) \sim U[]$ . The priors for example 3.1 scenario B, fishery  $j = 1$  are shown in fig. 3.3B. Within this framework, as new fisheries occur, the precision of parameter estimates from past fisheries is also improved.

The precision with which one can estimate  $d_n$  for any given fishery is ultimately limited by the migration dynamics. With a long informative time series,  $\phi$  could probably be estimated very precisely, but  $\theta$  remains relatively uncertain because the elements of  $\theta$  are independent among fisheries. Scenario C demonstrates the uncertainty that can be expected for  $d_n$  given perfect knowledge of  $\phi$  (priors shown in fig. 3.3C).

It is important to note that when the problem is formulated in this way, the selection of priors have implications that may not be immediately obvious because of the interdependence of the variables. The uniform priors for  $\theta$  and  $\phi$  imply non-uniform prior belief in the harvest rates  $h_n$  and  $h_s$  (fig. 3.4). I explored an alternative formulation of this problem, in which harvest rate priors were explicitly defined, and this resulted in implicit priors for  $N$  and  $d_n$ . It is not clear that either approach is better.

#### *POSTERIORES FOR EXAMPLE (3.1)*

The posteriors for example (3.1) were evaluated on a uniform parameter grid, and due to computation time constraints, the grid was rather coarse. Given the uncertainty in the system, though, it is unlikely that the coarse resolution seriously affected the results,

particularly for  $d_n$ . It would probably be appropriate to use a more efficient computational algorithm (e.g. metropolis, Gelman et al. 1995) for this problem. However, some of the initial results (not shown) indicated that bimodal posteriors could result, and these might not be described properly by stochastic algorithms.

In example 3.1, the precision of  $\phi$  has only a small effect on the uncertainty around  $d_n$ . Fig. 3.5A shows the  $d_n$  posteriors that result if the five fisheries (Table 3.2) are examined independently (i.e. scenario A, for all elements of  $\phi$ ,  $P_0(\phi) \sim U[]$ ). The variance in the posteriors is greatest when  $d_n$  is near 0.5, and decreases as  $d_n$  approaches 0 or 1, and this was a general feature common in other trials (not shown). The utilization of information across fisheries (scenario B,  $P_0(\phi_j) = \prod_{i=1, i \neq j}^L P_p(\phi_i)$ ) decreases the variance of the  $d_n$  posteriors, but the change is rather trivial (figure 3.5B). In fact, even perfect knowledge of  $\phi$  does not substantially reduce uncertainty in  $d_n$  (fig. 3.5C). This suggests that the information to be gained by combining across fisheries is not great under the given assumptions.

The uncertainty in the marginal posteriors for  $\phi$  decreases substantially from the single fishery case ( $i = 1$ , fig 3.6A) to the 5 fishery case (fig. 3.6B). However, in all the scenarios examined (example 3.1 and others not shown), there was a disturbing tendency for the marginal posteriors of individual parameters to converge toward incorrect values. This may result in part from the selection of relatively short time series of hypothetical data (due to computational time limits). However, the practical implications of this

problem may not be substantial because  $h$  is the more meaningful value for fisheries management. Depending on the fishery structure, uncertainty in  $\phi$  may have a relatively small effect on uncertainty in  $h$ . The joint posterior distribution for  $h_n$  and  $h_s$  (calculated from the joint posterior  $P(\theta, \phi | Y)$  for fishery  $i = 1$ , scenario A, is shown in fig. 3.7. The inverse relationship between plausible  $h_n$  and  $h_s$  combinations is clearly visible.

## DISCUSSION

The estimation of harvest rates and migration routes in a multiple approach salmon fishery is a complicated task if one attempts to explicitly account for the major sources of uncertainty that exist. The approach that I have presented admits uncertainty from what I consider to be the three most important sources. It is not clear that this approach would yield more accurate results than the *ad hoc* approach that has been used historically, but there are a number of attractive features to this method. This discussion provides a brief critique of the approach, and comments on some issues that I would address before applying it to actual fisheries.

Implementation of a formal estimation approach based on this framework would be advantageous for a number of reasons: 1) the estimation methodology would be standardized, 2) variability could be estimated within years (on a fishery-specific basis), and possibly among stocks for major stock-groupings, 3) the migration dynamics assumptions must be explicitly stated so that they are available for external evaluation, 4)

information from multiple fisheries across years is incorporated within a single cohesive framework, and updated with the addition of each new fishery, and 5) posterior probability distributions are generated, which indicate the (relative) uncertainty associated with each estimate.

A number of potential benefits could be expected from the resulting diversion rate and harvest rate estimates if this approach was implemented. Harvest rate uncertainty could be implemented in pre-season planning to develop robust management tactics, or demonstrate that complex allocation objectives are either not obtainable or represent substantial overfishing risk (see discussion of chapter (2)). A time series of fishery-specific (and conceivably stock-specific) northern diversion rate estimates could be useful for migration studies. Within year, and among-stock variation in migration routes has not been thoroughly examined to date, and would increase the temporal resolution with which to explore oceanographic mechanisms that influence migration variability. Admission of the uncertainty associated with migration route estimates would help to quantify the statistical properties of explanatory and predictive models.

The major problem that affects this estimation method (and all others) is the quantification of migration dynamics. The need to use Monte Carlo simulations to estimate harvest rate error distributions for particular fisheries and fish dynamics is cumbersome, but conceivably, general likelihood models of the form described in chapter (2) could be extended to account for the important factors. Treating all fisheries independently (within years) may not be entirely valid. The migration delays that



introduce an escapement underestimation error to one fishery are probably more likely to cause an escapement overestimation error in an immediately subsequent fishery as the aggregated fish eventually reach the river. Furthermore, migration dynamics are probably not independent between approach routes. Certainly, the northern and southern fish experience similar physical conditions in the mouth of the Fraser River, where substantial migration delays are known to exist.

There is considerable potential for simplifying the estimation approach. Example (3.1) suggests that the precision that can be attained by combining data among fisheries is not great. If this is shown to be the case in situations that have different migration dynamics assumptions and fishery structures, it could greatly simplify the estimation procedure. The uncertainty in  $d_n$  is not substantially reduced by increasing the precision of  $\phi$ , so most of this uncertainty results from the variable migration dynamics (fig. 3.5A-C). It seems likely that  $\phi$  could be reduced to one parameter for each of the north and south approach routes without a substantial loss in estimation precision, and this would reduce the total computation time (by about two orders of magnitude). Alternatively,  $\phi$  could be eliminated completely, and the estimation process could focus directly on  $h_n$  and  $h_s$  irrespective of effort. I would expect that there are conditions under which the precision to be gained from combining information across fisheries would be more substantial than indicated in example (3.1) (e.g. when total harvest rates are very high). However, if the noise around the relationship between fleet sizes and effort is great, or if effort contrast is limited, then the simpler approach is bound to perform well, and be computationally simpler and easier to interpret. Monte Carlo simulations of fisheries

under a range of conditions would be required to confirm the best approach to apply in the Fraser system.

Given that the northern diversion rate cannot be reliably predicted, fisheries managers should be attempting to deal with the uncertainty. I would recommend invoking harvesting strategies that are robust to migration route and harvest rate variation to the extent possible, or designing the assessment program to estimate the diversion rate as quickly and as frequently as possible in-season. Hydroacoustic estimates of escapement in each approach route would certainly help to define harvest rates, and would provide considerable information for in-season stock assessment. Of course, the value of the information generated from this extra assessment would have to be weighed against the expense of implementation. But irrespective of changes to the fishery structure, I think that steps should be taken to formalize the estimation process, and the approach presented here may provide a working template for that process.

Table 3.1. Temporal and spatial structure of northern and southern approach route fisheries defined in example (3.1). The northern fishery roughly corresponds to a Johnstone Strait sockeye purse seine fishery, while the southern fishery corresponds to a Juan de Fuca Strait fishery. Approximate distances to boundaries are from the in-river escapement monitoring site at Mission. Boxcar # indicates the number of boxcars from the outside boundary assuming migration rates of  $45 \text{ km} \cdot \text{d}^{-1}$  (i.e. 450-405 km = Boxcar #1, 45-0 km = boxcar # 10).

Fishery	Duration (d)	Inner Boundary		Outer Boundary	
		km	boxcar # ( <i>l</i> )	km	boxcar # ( <i>l</i> )
north	1	225	5	450	1
south	1	180	6	315	4

Table 3.2. Example (3.1) parameters and hypothetical observations from a time series of fisheries in a system with two approach routes. Catch from the north and south ( $C_n$ ,  $C_s$ ) and escapement ( $E_{n+s}$ , not shown) values are proportions of the total number of fish within the defined interval during the fishery,  $N$  ( $= C_n + C_s + E_{n+s} = 1$ ). The catch observations ( $C_n$ ,  $C_s$ ) are calculated from the mean of the harvest rate error distribution for each approach route, (equations (3.4) and (3.5)). Escapement,  $E'_{n+s}$  ( $= E'_n + E'_s$ ), is the sum of the mean of the escapement error distributions (calculated from equations (3.6) and (3.7)).  $E'_{n+s} > E_{n+s}$  due to estimation bias. Fleet sizes ( $F_n$ ,  $F_s$ ) describe standardized units of fishing effort (purse seine equivalents).

$i$	Parameters						Observations				
	$\theta$	$N$	$u_{100n}$	$u_{50n}$	$u_{100s}$	$u_{50s}$	$F_n$	$F_s$	$C_n$	$C_s$	$E'_{n+s}$
1	0.5	1	0.9	0.5	0.9	0.9	140	260	0.09	0.19	0.97
2	0.15	1	"	"	"	"	15	385	0.01	0.33	0.77
3	0.85	1	"	"	"	"	385	15	0.52	0.01	0.52
4	0.35	1	"	"	"	"	35	365	0.03	0.25	0.81
5	0.65	1	"	"	"	"	320	80	0.34	0.10	0.77

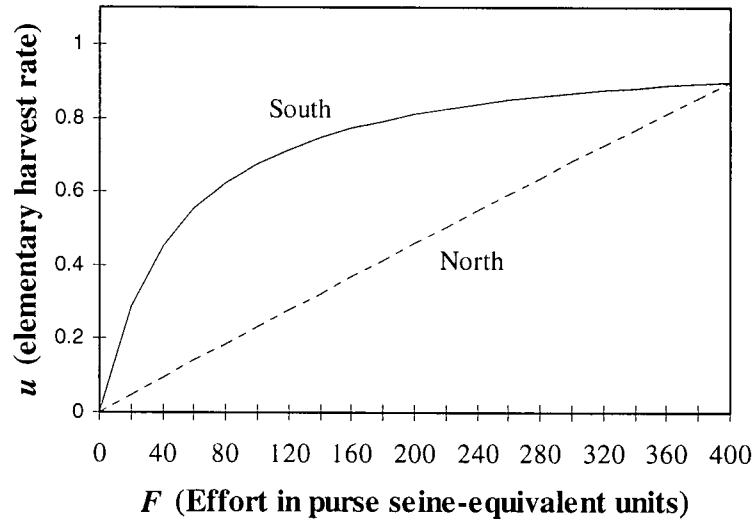


Fig. 3.1. The relationships (equation (3.3)) between fishing effort and elementary (single boxcar daily) harvest rate for the two hypothetical fisheries described in example (3.1), where  $u_{100n} = 0.9$ ,  $u_{50n} = 0.51$ ,  $u_{100s} = 0.9$ ,  $u_{50s} = 0.9$  and  $F_{max} = 400$ .

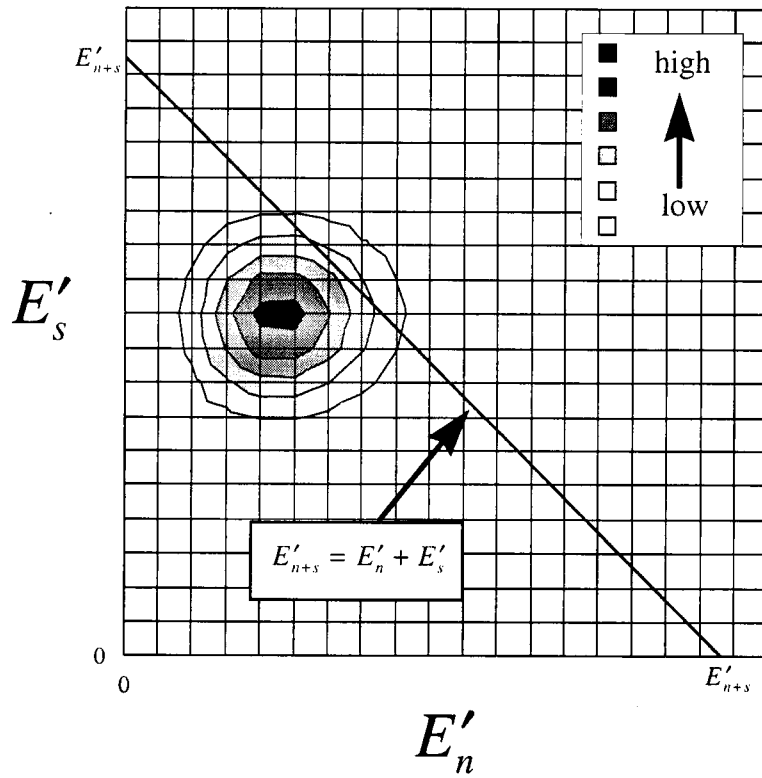


Fig. 3.2. Joint distribution for  $L(E'_n, E'_s | C_n, C_s, \theta_k, \phi_k)$  illustrating the calculation of  $L(E'_{n+s} | C_n, C_s, \theta_k, \phi_k)$ . Contours represent the likelihood of observing different escapement combinations for a given set of catch observations and parameter combination  $k$ . The line through the joint distribution corresponds to all possible combinations of (unobservable)  $E'_n$ , and  $E'_s$  which could yield the observed  $E'_{n+s}$  and the integrated likelihood along this line is proportional to  $L(E'_{n+s} | C_n, C_s, \theta_k, \phi_k)$ .

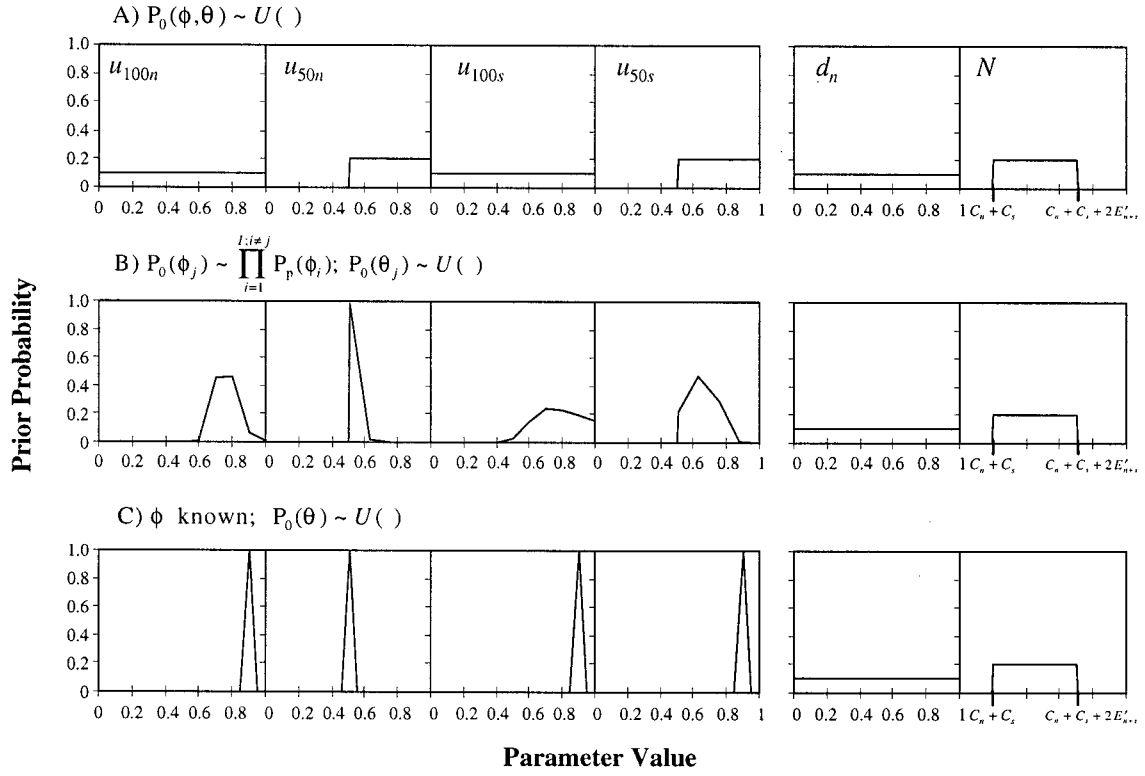


Fig. 3.3. Prior probability distributions for the parameters of example (3.1). In scenario A) each fishery is examined independently; B) information is combined across fisheries such that the prior for  $\phi$  for fishery  $i = 1$  is the posterior for  $\phi$  from all fisheries except  $i = 1$ ; and C) illustrates the priors for fishery  $i$  assuming  $\phi$  is known perfectly, but  $\theta$  is unknown.

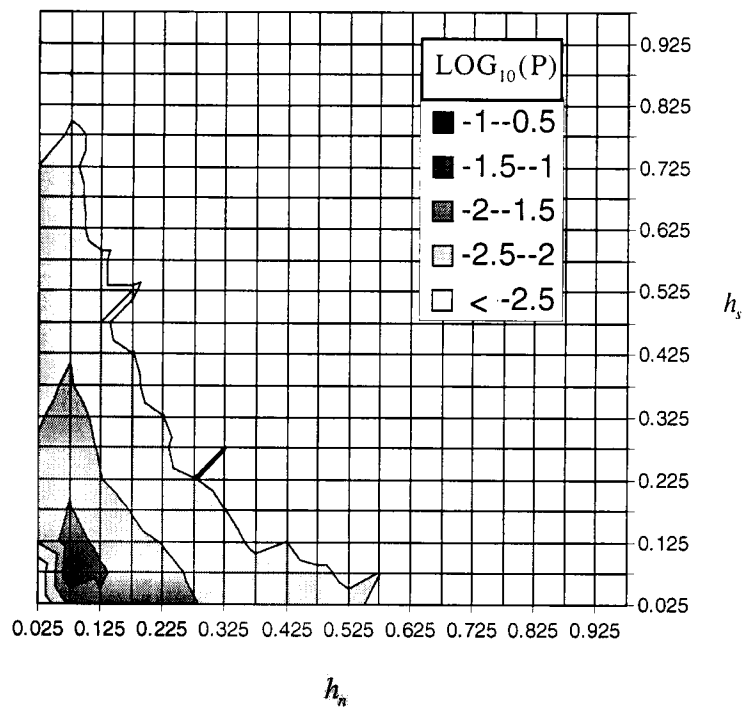


Fig. 3.4. The joint prior probability distribution for  $h_n$  and  $h_s$  that is implied by the uniform priors for  $\theta$  and  $\phi$  (scenario A) for example (3.1), fishery  $i = 1$ . The irregular pattern results from the coarseness of the parameter grids.



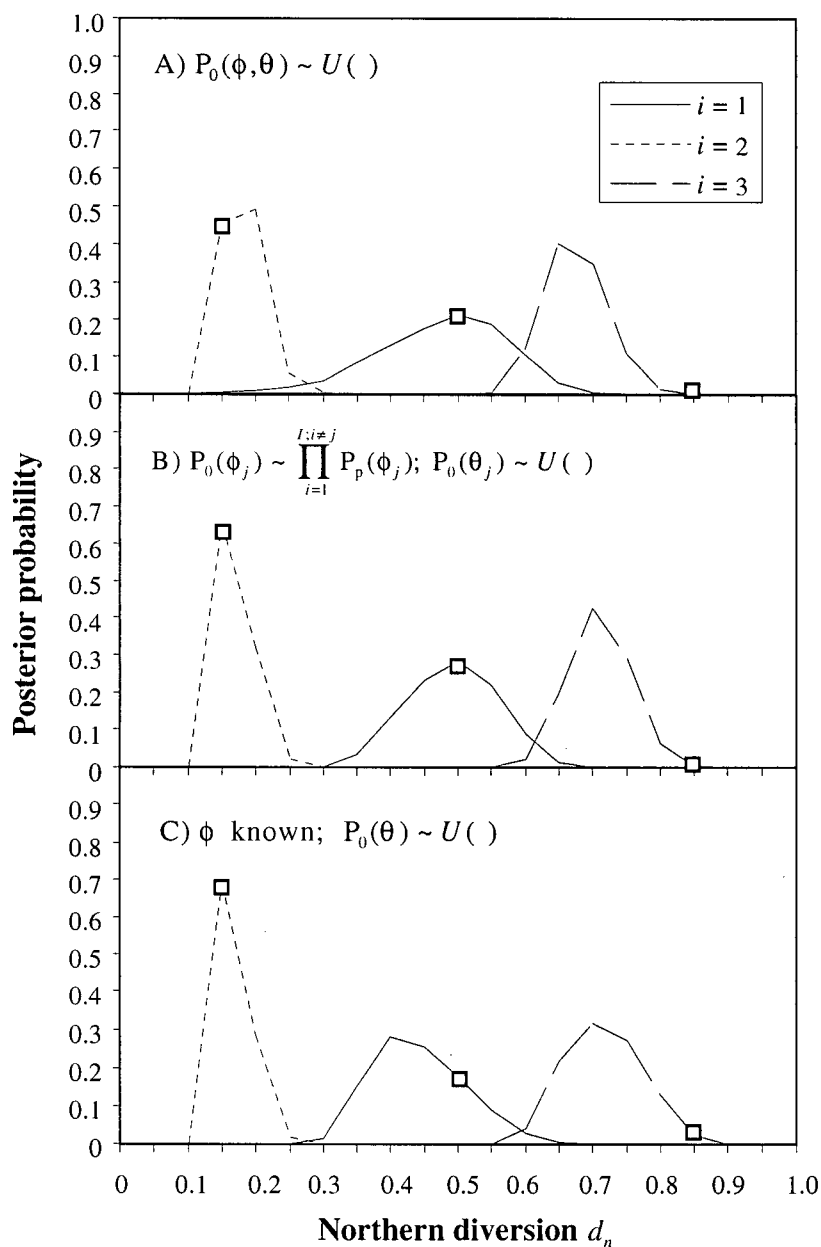


Fig. 3.5. Example (3.1) northern diversion rate ( $d_n$ ) marginal posterior distributions for fisheries  $i = 1, 2, 3$  calculated from the data in Table 3.2. Scenario A) illustrates the posteriors calculated independently; B) shows the posteriors which result when information is combined across all 5 fisheries (only the first 3 are shown for clarity); C) illustrates the posteriors which would result if  $\phi$  was known perfectly, but  $\theta$  was unknown. Squares indicate the actual value of  $d_n$  from Table 3.2.

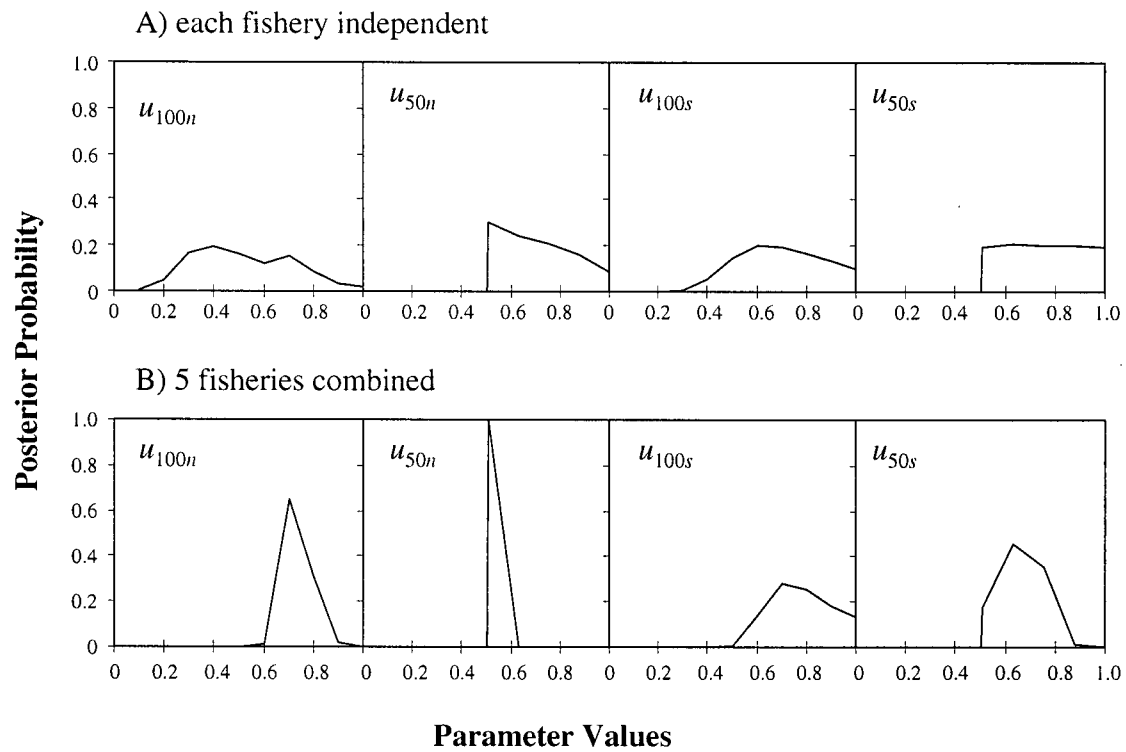


Fig. 3.6. Example (3.1) marginal posteriors for  $\phi$ . Scenario A) illustrates the posterior for fishery  $i = 1$  calculated independently of the other fisheries; scenario B) shows the posteriors for the same fishery when data is combined across all 5 fisheries of Table 3.2.

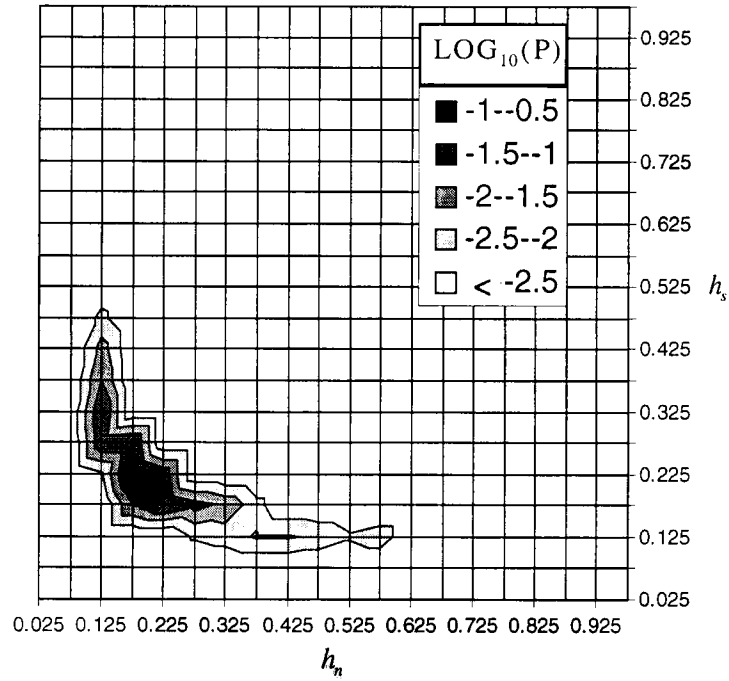


Fig. 3.7. The posterior probability distribution for  $h_n$  and  $h_s$  that is implied by the posteriors for  $N$  and  $d_n$  for example (3.1), scenario A, fishery  $i = 1$ . The irregular pattern results from the coarseness of the parameter grids.

## **CHAPTER 4: NUMERICAL SIMULATIONS OF FRASER RIVER SOCKEYE SALMON HOMING MIGRATION ROUTES IN A DYNAMIC MARINE ENVIRONMENT**

Chapter (4) is essentially a reproduction of Kolody and Healey (1998).

## ABSTRACT

A spatially-explicit individual-based model was used to simulate adult sockeye salmon return migration routes from the Gulf of Alaska to the Fraser River through temporally variable, spatially-explicit environmental fields. We wanted to examine whether coastal migration route variability could be explained by the interactions between simple behavior rules and a dynamic ocean environment described by historical temperature observations and estimated surface currents. Assuming that sockeye were broadly distributed throughout the central Gulf of Alaska prior to homeward migration, and that during homeward migration they oriented on a fixed compass bearing, the following mechanisms were invoked to produce migration route variations among years: 1) the distribution prior to homing was constrained by thermal limits, 2) sockeye were advected by surface currents during open ocean migration, and 3) sockeye tended to avoid high water temperatures. The behavioural component of the model was numerically optimized to maximize the fit between simulated and observed coastal migration routes, while maintaining swimming speeds and migratory timing consistent with the literature. The optimized model suggested that southern thermal limits and current advection could not explain much of the observed coastal migration route variability. The tendency to avoid high temperatures explained about 33% of the variation and suggested that coastal processes may be more important than offshore.

## INTRODUCTION

Adult sockeye salmon (*Oncorhynchus nerka*) can return from the Gulf of Alaska to the Fraser River by migrating around either the north or south end of Vancouver Island (fig. 1.1). The proportion of fish using the northern route (northern diversion rate) varies considerably among years (fig. 1.2), and it is not known what factors cause this variation. Chapter (1) summarizes the ecological significance, management implications and previous studies of the migration route variability.

As a new investigative approach for this system, we used a process-based model to explore explicit, testable hypotheses about the effects of oceanic conditions on Fraser sockeye coastal migration routes on temporal and spatial scales relevant to the decision processes of individuals. Specifically, we chose to explore how sockeye migration routes could be affected by 1) the initial distribution in the NE Pacific Ocean, 2) advection by open ocean surface currents, and 3) SST preference behaviours. Marine distributions and migration routes of sockeye salmon are not well known, but there is empirical evidence suggesting that temperatures and currents may affect the sockeye distribution prior to and during the homing migration. Mark and recapture studies have suggested that during the year prior to homing, Fraser sockeye are located throughout the Gulf of Alaska (French et al. 1976). Welch et al. (1995) observed that the southern limit of the offshore sockeye distribution is associated with SST. It is not known what effect SST has during the marine phase of the homing migration, but high river temperatures can delay salmon migration into and within rivers (e.g. Major and Mighell 1966, Alabaster 1990).

Presumably, avoidance of high temperature could also result in deflected trajectories of sockeye in marine areas. Similarly, Thomson et al. (1992) have shown that ocean currents in the Gulf of Alaska are strong enough and variable enough to have a substantial effect on the latitude at which homing sockeye reach the coast. The two years that they examined, 1982 and 1983, corresponded to low and high diversion years, respectively. A small sample of Fraser River sockeye tagged on the north coast of British Columbia during these years also suggested that the Fraser sockeye were less abundant in northern coastal waters in 1982 relative to 1983 (Groot and Quinn 1987).

We used a spatially-explicit, individual-based model to explore the potential effects of these three factors on coastal migration routes. Numerical optimization of behavioural parameters was used to maximize the fit between modelled and observed diversion rate time series, subject to external constraints that were imposed to maintain consistency with other biological observations. The potential importance of individual and combined mechanisms is examined.

## METHODS

### *NUMERICAL REPRESENTATION OF THE PHYSICAL OCEANOGRAPHY OF THE NORTH-EAST PACIFIC OCEAN*

The model domain covered the NE Pacific Ocean from 44-61° N and 123-160° W and incorporated temporal and spatial variability of observed SST and estimated surface currents in the open ocean region. The land mask was approximated on a 0.18 X 0.18 degree grid corresponding to the SST grid resolution, and the coastal region was defined as all areas within approximately 50 km of the land mask.

Gulf of Alaska SST was described by weekly Advanced Very High Resolution Radiometry (AVHRR) images (1982-94), obtained from the Physical Oceanography Distributed Active Archive Center at Jet Propulsion Laboratory/California Institute of Technology. Calibration and image processing details are provided at the web site [http://podaac.jpl.nasa.gov:2031/DATASET\\_DOCS/avhrr\\_wkly\\_mcsst.html#17](http://podaac.jpl.nasa.gov:2031/DATASET_DOCS/avhrr_wkly_mcsst.html#17) (3 Oct 1997). Images were archived on an equal-angle grid with spatial resolution of approximately 0.18 X 0.18 degrees (19.5 X 19.5 km on the equator). Each weekly (approximately) image was a composite of numerous images produced during a week, and often considerable spatial interpolation was required to estimate temperatures beneath cloud cover. In our model, linear interpolation was used to estimate SST between the available image dates.



Surface currents within the model were approximated by hindcast output from the Ocean Surface CURrent Simulations (OSCURS) model described by Ingraham and Miyahara (1988, 1989). OSCURS currents are calculated as the vector sum of long term mean baroclinic geostrophic flow and daily wind driven surface flow. Sea level pressure fields are used to generate the wind driven current estimates over a rectangular grid of approximately 90 km resolution across the north Pacific Ocean. To reduce data storage requirements for our individual-based model, daily hindcast current observations (1982-94) were converted to monthly averages and interpolated onto a 1 degree grid. During simulations, bilinear spatial interpolation and linear temporal interpolation were used to estimate currents at specific points in time and space. Currents were reduced to 0 in coastal areas, because OSCURS does not account for coastal geometry or tidal effects. There is at present no satisfactory means of hindcasting British Columbia coastal currents for the period of interest.

#### *NUMERICAL REPRESENTATION OF SOCKEYE SALMON HOMING MIGRATION BEHAVIOUR*

Sockeye salmon homing migrations were simulated from the central Gulf of Alaska to the coastal approaches of the Fraser River. Fish that arrived at Queen Charlotte Strait or Juan de Fuca Strait were removed from the model and committed to either the northern or southern migration routes respectively. Fish that wandered out of the model domain or failed to reach Queen Charlotte Strait or Juan de Fuca Strait by the end of the simulation were not included in annual diversion rate calculations, but were recorded for homing success rate calculations. A complete run of the model involved simulating

homing trajectories for years 1982-94 and calculating time series of annual diversion rates and homing success rates.

The model required a large number of parameters to describe behavioural interactions with the ocean environment and ensure reasonably successful homing rates (Table 1). These parameters contributed to one of the following roles: 1) establishing the initial sockeye distribution, 2) defining general orientation behaviour, 3) helping to avoid trapping in complex coastal geometry, or 4) describing interactions between sockeye and local SST.

The initial Fraser River sockeye distribution in the NE Pacific Ocean was described by the latitude, longitude and spread of the distribution. We assumed that the distribution was of uniform density and circular, roughly covering the central Gulf of Alaska as indicated by the French et al. (1976) summary of tagging studies. During the optimization procedure, the parameters describing the location and spread of the initial distribution were not constrained. However, one model scenario involved using seasonally-varying thermal limits to constrain the initial distribution. We assumed a simplified version of the seasonal thermal limits defined by Welch et al. (1998). Prior to Day-Of-Year (DOY) 170, the limit was 8 ° C, between DOY 170 - 190, the limit increased linearly to 12 ° C, and between DOY 190 and 250, the limit remained at 12 ° C. In the thermal limit scenario, fish were established according to the location and spread parameters, but as each simulation year was initialized, fish located in regions with SST exceeding the thermal limit were eliminated. The initial temperatures and thermal limits

were averaged over the preceding 21 days under the assumption that fish take some time to react to changing temperatures and redistribute themselves.

During a simulated homeward migration, all sockeye used the same fixed compass bearing (which differed between open ocean and coastal regions) as the primary direction finding mechanism. Swim speeds were confined to limits suggested by tagging studies (French et al. 1976, Quinn 1988) and migration initiation dates were determined by the requirement for sockeye to return to the Fraser River during the interval DOY 170-250 (Killick and Clemens 1963).

A number of parameters were invoked largely to help fish migrate through complex coastal geometry that would trap individuals if they migrated on a compass bearing with perfect accuracy. These included: 1) a probability of reorienting to the compass bearing during a given time step, 2) an inertial directional component, which describes the tendency to keep migrating in the same direction, and 3) a coefficient of directedness, describing directional precision. These parameters provided a stochastic element to the orientation similar to those invoked by Pascual and Quinn (1991).

The interactions between fish and local SST consisted of a simple decision; whether or not to enter an adjacent SST box (0.18 X 0.18 degree AVHRR SST grid unit). On any given timestep, the fish had an initial migration direction. If the fish reached the border with an adjacent SST box, it either entered the box and continued swimming in the same direction, or it rebounded off the adjacent box like an elastic particle (if the fish

struck land it always rebounded). The decision to enter or rebound was based on the relative difference in preference values between adjacent boxes. If the fish was moving from a lower preference value to a higher preference value it would always proceed, however, if it was moving from higher to lower preference, the fish may have rebounded, depending on whether the magnitude of the difference exceeded a minimum detection threshold plus a stochastic decision element. All temperatures below the seasonally-varying thermal limit threshold were considered to be of equally high baseline preference value. Preference values for temperatures exceeding the thermal limit were lower than the baseline value by a factor proportional to the squared difference between the local SST and the thermal limit. The direct biological interpretation of this decision process was: fish detected physical conditions where they were at any given time, and could remember physical conditions experienced an average of  $\approx 10$  km prior. The fish assessed water quality only in water masses that it directly experienced, and could only distinguish gradients over distances of  $\approx 18$  km or less, and then only if a minimum detection threshold difference was exceeded. In this way, net migration from lower to higher preference water masses resulted from reactive movement away from undesirable areas, rather than a proactive movement into favourable areas.

#### *OPTIMIZATION WITH A FLOATING POINT GENETIC ALGORITHM*

The migration model required many parameters, most of which could not be directly quantified from the literature. Therefore an objective optimization scheme was needed to test parameter combinations that potentially included all reasonable values. We

used a floating point genetic algorithm (e.g. Michalewicz 1994) as a computationally intensive numerical method of fitting simulated and observed time series. This technique is merely an optimization tool, and we are not using it to imply anything about salmon genetics or evolution. However, the floating point genetic algorithm is most easily described by functional analogy with genetic evolution. A single parameter is analogous to a gene, a complete set of model parameters is analogous to a genotype, and the superset of all genotypes can be thought of as the genepool. Genotype fitness in this case was calculated as the goodness of fit ( $R^2$ , coefficient of determination) between modelled and observed coastal migration routes described below. The genetic algorithm calculated a fitness value for all genotypes from an initial arbitrary genepool, and then selected genotypes with highest fitness for the next generation, while low fitness genotypes were removed from the genepool. The genotypes in the new generation were subjected to random perturbations of parameters (mutations) and switching of groups of parameters (crossovers). Fitness values of the new genotypes were then calculated and the whole process was repeated until maximum fitness values no longer increased from one generation to the next.

Genotype fitness was calculated as the goodness of fit between modelled and observed coastal migration routes, subject to the following constraints: 1) swimming speeds had to be consistent with tagging studies, 2) arrival timing in coastal fisheries had to fall within the period from late June to early September, and 3) homing success rates had to exceed 70%. While there is no way of knowing what the actual homing success rate is, a navigational failure rate of 30% is probably much too high. However, without

introducing more complex navigational behaviour, we were not able to produce both consistently high success rates, and substantial interannual migration route variation. We felt that a 70% success rate represented a trade-off between describing trajectories of the majority of the fish, and allowing us to explore potential effects of interannual oceanographic variations by not overly constraining the initial positions and orientation behaviour of the fish.

The coefficient of determination ( $R^2$ ), was used as a comparative index of the goodness of fit between simulated and observed migration route time series:

$$R^2 = 1 - \text{ESS} / \text{TSS}$$

where:

ESS = Error Sums of Squares

$$= \sum_{i=1982}^{1994} (\hat{y}_i - y_i)^2,$$

TSS = corrected Total Sums of Squares

$$= \sum_{i=1982}^{1994} (y_i - \bar{y})^2,$$

$\hat{y}_i$  = simulated northern diversion rate in year  $i$ ,

$y_i$  = observed northern diversion rate in year  $i$ , and

$\bar{y}$  = mean observed northern diversion rate 1982-94.

This value is equal to the familiar  $R^2$  in least squares linear regression. However, in this case, predicted and observed values of  $y$  are not related by a least squares linear regression fit, so the properties of  $R^2$  are slightly different.  $R^2 = 1$  indicates that the modelled and observed time series are identical,  $0 < R^2 \leq 1$  indicates that some of the variation around the mean diversion rate can be explained by the model, and  $R^2 < 0$  indicates that the mean diversion rate is a better fit to the time series than the model result. The coefficient of determination was used as a relative measure to evaluate and compare alternative models, but we did not attempt to assess the statistical significance of these models.

The genetic algorithm may not find a global optimum solution, because parameter combinations may become trapped in local optima, and the stochastic behaviour of the fish may obscure the true optimum. However, this method should identify solutions that are reasonably close to the global optimum if it exists over a reasonably large parameter space. Substantially different parameter combinations may yield similar goodness of fit values because two parameters may have offsetting effects. For example, a late initiation date and fast swimming speed may yield essentially the same result as an early initiation date and a slow swimming speed. In this study, the role of the numerical optimization was to quantify (approximately) how much coastal migration route variability could be explained by each behavioural/oceanographic mechanism. Thus, the relative explanatory

power of each mechanism is of primary importance, while the actual parameter values are of secondary interest and not reported.

This method of optimization raises two important concerns: 1) because there are so many parameters in the model, the genetic algorithm may be able to produce good, but spurious, coherence between modelled and observed coastal migration routes using any mechanism, or conversely 2) the genetic algorithm may not be able to optimize the model adequately, so that the explanatory power of one or more mechanisms could be severely underestimated. If the first situation occurred, it would be obvious. If the second situation occurred, it would not be detectable, and the apparent effects of the different mechanisms would be the result of random events during optimization. We attempted to address this concern by using the migration model as a reference model. An arbitrary set of parameters was selected to produce a time series of coastal migration routes with substantial interannual variability. Then the genetic algorithm was used to optimize the model from random initial conditions. This process was repeated a number of times and we found that the optimized model could consistently explain a substantial amount of the migration route variability ( $0.75 < R^2 < 0.97$ ). Individual parameters often varied substantially between the reference model and the optimized model, but the relative contribution of the different mechanism changed relatively little. This gives us some confidence that the optimization procedure performs as we hoped, but we cannot be certain that it is effective in all situations.



The effects of three mechanisms on coastal migration route variability were explored:

- 1) the Fraser sockeye distribution prior to migrating is constrained by thermal limits
- 2) sockeye salmon are advected by offshore surface currents in the Gulf of Alaska
- 3) sockeye tend to avoid water temperatures that are bioenergetically unfavourable.

The model was optimized several times, first to examine the effects of each mechanism independently, and then to examine the mechanisms in combination. The SST constraints and high SST avoidance behaviours were removed to optimize the model for current variability alone. To optimize the model for either SST constraints or high SST avoidance alone, year-specific monthly currents were replaced by monthly mean currents averaged over the years 1982-94.

## **RESULTS**

Sockeye orientation in the optimized models always included a somewhat eastward directional preference in offshore waters, and a south-eastward directional preference in coastal waters. Thus, successful sockeye always arrived at the coast somewhere north of Juan de Fuca Strait and then followed the coast south.

*EFFECTS OF THERMAL CONSTRAINTS ON THE SOCKEYE DISTRIBUTION PRIOR TO HOMING*

Thermal constraints on the sockeye initial distribution did not explain very much of the northern diversion rate variability ( $R^2 = 0.07$ ). In the optimized model, thermal limit constraints had the greatest effect on the initial distribution in 1983, and no effect in several other years (fig. 4.1). In a few years, the distributions were marginally affected on the southern and eastern boundaries, while northern and western boundaries were always unaffected.

The model is not able to produce both high and low diversions with a single parameter combination because constraints essentially affect only the south-east boundary. As the distribution contracts along this boundary, the number of southern migrants decreases, resulting in an increase in the proportion of northern migrants. As the boundary extends southward, the number of southern migrants increases, but the number of northern migrants remains the same. Without a concurrent decrease in the number of northern migrants, the northern diversion rate cannot reach very low values. Of course, the northern diversion rate could take very low values if the preferred compass bearing was shifted to the south, but then the problem would be reversed and very high diversion rates would not be attainable.

#### *EFFECTS OF CURRENT ADVECTION*

Current advection in the offshore oceanic region did not explain any of the observed coastal migration route variability ( $R^2 = 0$ ). Mean migration trajectories of salmon in offshore waters (fig. 4.2) indicate that currents do not produce large route deviations relative to the width of the optimized initial distribution. Since offshore currents are the only mechanism introducing variability in this case, variability in the latitude of arrival in coastal waters determines the diversion rate. All fish are affected by interannual current variation, but when the initial distribution is broad, only a small proportion are positioned so that the current displacement causes them to switch between northern and southern routes. If the initial distribution is very narrow, then the proportion of fish that change routes may be much greater. However, the genetic algorithm could not identify any broad or narrow initial distributions that would indicate that current variability was consistent with the diversion rate time series.

#### *EFFECTS OF A BEHAVIOURAL TENDENCY TO AVOID HIGH SST DURING HOMING MIGRATION*

The behavioural tendency to avoid high SST explained the most northern diversion rate variability ( $R^2 = 0.33$ ). The optimal parameter set was unexpected in that the initial distribution was essentially a point source (20 km diameter) and open ocean migration precision was essentially perfect (coefficient of directedness = 0.98). This resulted in a single mass of fish arriving simultaneously in the coastal waters north of

Vancouver Island (fig. 4.3). The open ocean trajectories did not differ much among years, and the fish rapidly dispersed in coastal waters (only 10 trajectories from a single year are shown because the overlapping paths are confusing and uninformative). The comparison of modelled and observed diversion rates (fig. 4.4) indicates that the model did not produce much diversion variability. The model did simulate higher than average diversions in the four high diversion years (1983, 1992-94), but not nearly as high as observed. Only 1990 appeared as a very low diversion year in the simulations, similar to the observed value. The highest and lowest diversion years in the simulations (1983 and 1990 respectively), were also two of the warmest years along the British Columbia coast. This demonstrates that the high SST avoidance behaviour can result in both high and low diversions depending on the fine scale SST spatial distribution. Thus, defining the appropriate scale of interaction between salmon and SST may be critical for understanding migration routes.

We also optimized this model with the additional constraint that the initial distribution had to be greater than 500 km in diameter, but in this case, much less diversion rate variability could be explained ( $R^2 = 0.12$ ).

#### *EFFECTS OF COMBINED MECHANISMS*

The northern diversion rate variability explained by individual and combined mechanisms is summarized in Table 2. Combined mechanisms did not result in any increased explanatory power. When high SST avoidance and thermal limit constraints

were combined, the thermal limits did not actually have any effect in the optimized models because the initial distribution was essentially a point source as described above. The slight decrease in explained variation resulting from the addition of currents to thermal limits or high SST avoidance further suggests that current variability does not covary with diversion rates, but may also indicate imperfect optimization.

## DISCUSSION

Our model was unable to reproduce the Fraser sockeye northern diversion rate time series well enough to demonstrate the viability of a causal hypothesis, or to be a useful predictive tool for fisheries management. The failure of the model to explain more of the northern diversion rate variability was most likely due to two main factors: 1) inappropriate representation of salmon behaviour, and 2) inappropriate representation of the NE Pacific oceanography. Incomplete optimization and errors in the observed northern diversion rate time series are probably of lesser importance. However, the model has provided insight into the workings of the system and the results suggest directions for additional modelling and field studies.

Our representation of salmon behaviour was obviously simplistic. We ignored interactions between behaviour and all environmental stimuli except for SST (and the static stimuli required for salmon to distinguish open ocean and coastal regions, land, and compass directions). Our representation of navigation behaviour was the simplest that we

could conceive of, such that fish could reach the coastal approaches to the Fraser River from vastly different initial positions. However, the low homing success rates attained in some years (approaching 70 %), suggests that additional behaviours are likely important. Some kind of longer term memory could help fish avoid becoming trapped in coastal geometry or prevent substantial delays in regions of high water temperature that could be handled most efficiently with more directed swimming. With simple compass navigation, fish may bypass their coastal target, and fail to return home because there is no provision for turning around (but we do not know if this is a problem in reality). The assumptions that the initial distribution was uniform, and that all stocks began migrating at the same time is also likely unrealistic. Different coastal migratory timing observed for different stocks (Clemens and Killick 1963) suggests that either the stocks occupy different areas of the ocean, they start migrating at different times, they swim at different rates or they follow different routes. The model would have to be optimized separately for each stock to account for this variability, but the biological data are not sufficient to describe stock-specific variations in any of these features.

Our results suggested that the offshore processes that we defined could not explain as much northern diversion rate variability as coastal processes. If all salmon orient on a similar compass bearing, and offshore distributions are as broad as field studies have suggested (French et al. 1976, Welch et al. 1995), then it is unlikely that thermal limits and offshore currents could produce both very high and very low diversion rates. Broad initial distributions also prevented SST avoidance behaviour from reproducing observed diversion rates, but we did not explore whether this behaviour was

capable of producing arbitrarily high and low diversions. However, if all fish arrive north of Vancouver Island in a tight spatial distribution and narrow time window, then SST preference behaviours can reproduce a substantial amount of northern diversion rate variability. This supports the notion that initial conditions prior to migrating do not necessarily influence diversion rates. If the migration route decision is made at essentially the same coastal location by all fish, then offshore processes may be largely irrelevant. For this to occur, there would have to be some mechanism aggregating the fish. The most obvious aggregation occurs as sockeye swim eastward and 'pile up' on the coast. If the majority of the fish arrive on the coast north of Vancouver Island, they will all migrate through a relatively narrow corridor in the Queen Charlotte Sound area, although the timing will not be synchronous. In this manner, the coastal migration route decision process could be determined in a very confined area despite a broad and variable open ocean distribution.

We did not expect to explain much coastal migration route variability with coastal processes because the model timestep and physical oceanographic representation were more appropriate for open ocean processes. The AVHRR SST images probably provided adequate resolution in time and space for the offshore processes that we were describing. These images do not resolve mesoscale SST variability very well, and this is probably a more serious problem in coastal areas. Relative to offshore waters, British Columbia coastal oceanography is characterized by steep SST gradients, and complex tidal, wind driven, and buoyancy-driven currents. This coastal heterogeneity was not well represented in our model, so we cannot confidently describe the potential interactions

between salmon and oceanographic variability in the region north of Vancouver Island. Our model results demonstrated that high SST avoidance behaviours could explain some of the interannual migration route variability, and suggested that the system might be very sensitive to the scale of interaction. High annual temperatures could produce both high and low diversions, depending on the SST spatial distribution. If the important temporal and spatial patterns are not described with the appropriate resolution, substantial errors will likely eventually result from any predictive model, even if the underlying processes are essentially understood. In this system, predictive correlation models based on annual indices and vague understanding of important processes are probably doomed to predictive failure.

Our results suggest that further research into the mechanisms driving migration route variability should be focused on the coastal region, particularly around the north end of Vancouver Island. Seemingly small interannual variations in coastal SST distributions or Fraser River northward flow patterns may have a large effect on coastal migration routes. Simulation modelling of fine scale interactions between coastal oceanographic variability and fish behaviour may help to further define critical decision points in the migration route, however, the mechanisms that drive migration route variability will never be adequately described without additional field studies. Detailed observations of sockeye migration trajectories may help to quantify the important behaviours. It may be informative to observe how trajectories of individuals around the north end of Vancouver Island relate to mesoscale oceanographic variability, especially SST and salinity gradients. Although if the important factors are difficult to measure (e.g. Fraser River



odours), individual trajectories may not be informative. If consistent behaviours could be identified, and quantitatively described, we could work toward understanding the spatial and temporal scales of interaction, and modify our migration models accordingly.

Table 1. Range of valid parameter values in the spatially-explicit individual-based migration model.

Parameter	min.	max.
latitude of initial distribution centre	48	55 ° N
longitude of initial distribution centre	140	150 ° W
radius of distribution	0	1000 km
initiation date for homing migration	150	190 DOY
swimming speed	20	60 km / d
open ocean compass bearing	0	360 °
coastal compass bearing	0	360 °
(inertial / compass) open ocean directional weighting	0	100
(inertial / compass) coastal directional weighting	0	100
open ocean directional precision	0	1
coastal directional precision	0	1
probability of reorienting to the compass (per timestep)	0	1
SST difference detection threshold	0	5 ° C
SST preference random factor	0	10 ° C
thermal limit adjustment factor	-4	4 ° C

Table 2. Goodness of fit between modelled and observed Fraser River sockeye salmon coastal migration routes (1982-94). Behavioural parameters were optimized independently for each individual mechanism and each combination of mechanisms.

Mechanism	$R^2 \times 100$
(1) thermal limit constraints on the initial distribution	7
(2) offshore current advection	0
(3) behavioural avoidance of high SST	33
(1) & (2)	5
(1) & (3)	33
(2) & (3)	29
(1) & (2) & (3)	29

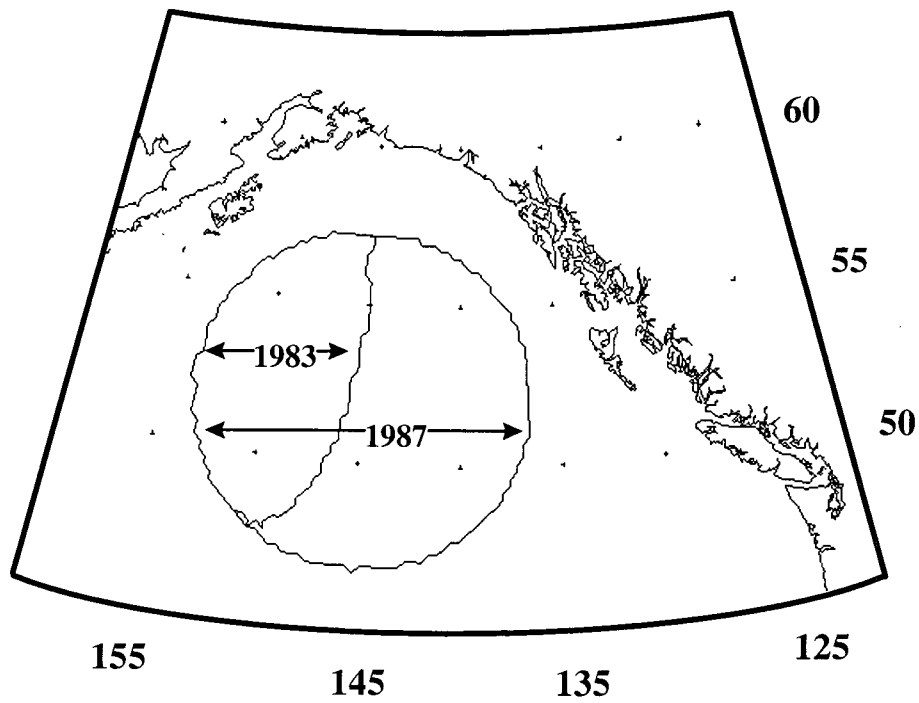


Fig. 4.1. Range of sockeye salmon initial distributions that resulted when the migration model was optimized with thermal limit constraints on the initial distribution. 1983 demonstrated the most restricted distribution, while 1987 (and some other years) were not affected by thermal limits.

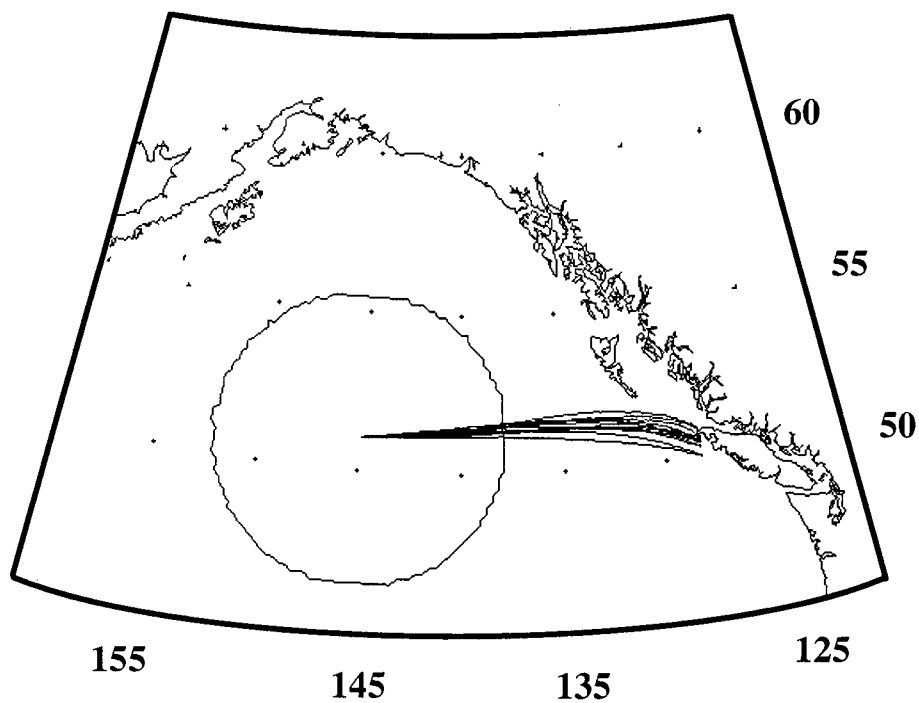


Fig. 4.2. Initial distribution and mean migration trajectories that resulted when the model was optimized with offshore current variability. The large circle outlines the initial distribution; each line connecting the distribution centre to the coast represents the mean open ocean trajectory of all individuals from a single year (1982-94).

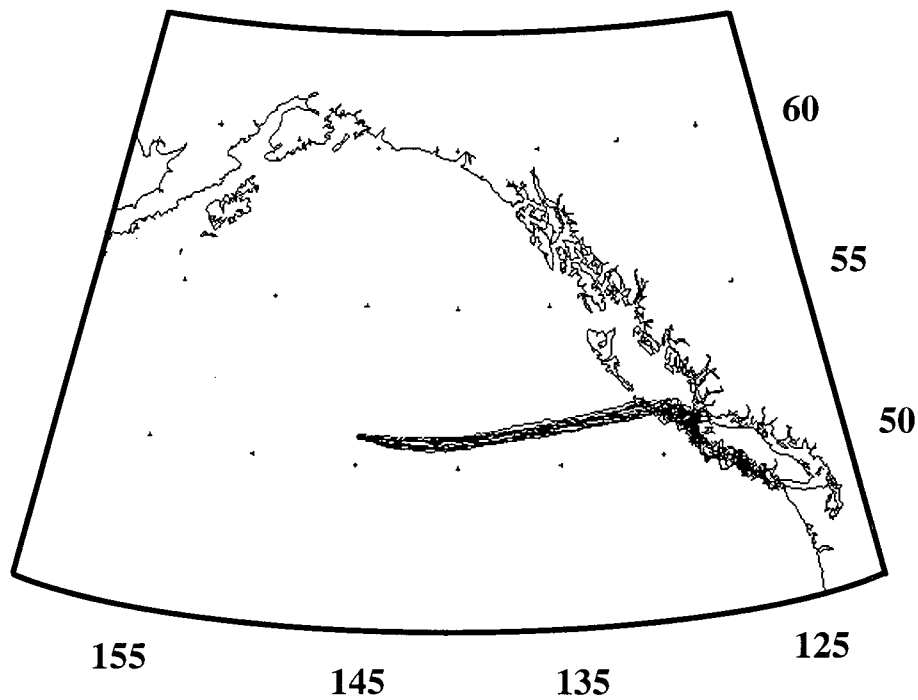


Fig. 4.3. Typical trajectories that resulted when the model was optimized with a behavioural tendency to avoid high SST. Ten trajectories from 1982 are shown, and are representative of the precise open ocean migration and more dispersed coastal migration observed in all years. The initial distribution was essentially a point source.

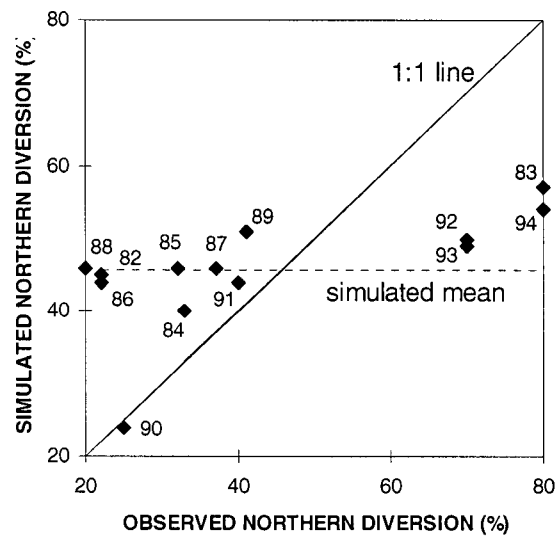


Fig. 4.4. Comparison of simulated and observed annual northern diversion rates (1982-94) generated when the model was optimized with a behavioural tendency to avoid high SST. Individual years are labeled.

## **CHAPTER 5: GENERAL DISCUSSION**



The three studies described in this thesis are all linked by the common objective of attempting to understand Fraser River sockeye salmon coastal migration route variability. The first two projects, chapters (2) and (3), examined the estimation of fishery harvest rates and developed methods for estimating fishery-specific migration routing. These studies have potential for increasing the amount of useful information that can be extracted from fisheries data, and can be used to help bound the uncertainty of the existing migration route time series. This general discussion summarizes how these methods can be applied in future studies of migration research, while potential implications for fisheries management are described in the respective chapter discussions, and not repeated here. The third study, chapter (4), described my attempt to explain Fraser sockeye coastal migration route variation by simulating explicit interactions between migrating individuals and a dynamic marine environment. The simulation modelling approach is examined in relation to other methods that could be applied to this system, and the results of chapter (4) are used to prioritize future studies.

Salmon migration is a complex biological event that can be decomposed into processes that operate on a range of temporal and spatial scales. A satisfactory understanding will only emerge as studies are integrated across numerous scientific disciplines. The sensory and navigational processes that guide migration will probably remain poorly understood for the foreseeable future (probably forever if the reductionist goal of understanding is carried to the level of brain function which underlies the decision processes). In the study of Fraser sockeye coastal migration routes, it would be a substantial achievement if one could 1) identify and quantify the sources of

oceanographic and/or biological variation which cause migration route variability, and 2) describe how fish distributions change in response to this variation. This level of understanding would represent a dramatic improvement over the current state, and would probably resolve many outstanding problems in stock assessment and management. The pursuit of deeper levels of understanding (e.g. the neuro-endocrine regulation of migratory timing) may have considerable theoretical appeal to particular disciplines, but extend beyond the scope of my discussion.

Most hypotheses about the mechanisms that influence migration route variability fall into a general classification in which adult homing behaviour remains fairly constant among years, while variability in the spatial/temporal distribution of physical and/or biological factors introduces interannual variability to the sockeye distribution prior to and/or during the homing migration. This general classification can be distinguished from at least two other mechanistic classifications: 1) adult migration behaviour could vary substantially among years because of genetic or developmental factors (e.g. migration routes could be learned as juveniles as disproved by Groot and Cooke (1987)), or 2) observed migration routes could represent among-year variability in survival patterns (e.g. fisheries off SE Alaska and the Queen Charlotte Islands catch substantial numbers of Fraser sockeye in some years and it is not known whether removal of these fish affects the resulting northern diversion rate). The latter two classes of mechanisms are more difficult to investigate because any part of the marine life history could be affected. I also consider these mechanisms to be less likely, and in the interest of focusing research along the most productive paths, I do not consider them further.

Additional work along several lines will be required before the mechanisms driving coastal migration route variability are conclusively revealed, if in fact they ever are. There must be additional description of marine spatial distributions. Ideally, this would include field sampling and tagging studies, but there is also additional information that can be extracted from existing fisheries data. Behavioural experiments and modeling studies will be required to relate observed distributions to potentially important environmental factors.

The relative importance of offshore and coastal processes in determining coastal migration routes is not known, but I would recommend more detailed sampling of spatial distributions and/or trajectories in the Queen Charlotte Sound area. The results of chapter (4) suggest that offshore temperatures and currents might be less important than high temperature avoidance behaviour in Queen Charlotte Sound. This region represents a reasonable point where the coastal migration route could bifurcate, as the commitment to migrate along the east or west side of Vancouver Island must be established in this vicinity (at least for fish that arrive in this area). In terms of logistics, this region is also the most accessible location in which there is a high probability that the migration route choice is still undetermined.

Observations of individual salmon trajectories will probably be essential to understanding coastal migration route variation. Two types of tags are presently available for tracking individuals. Ultrasonic tags have been used to generate high resolution

observations of salmon movements in both coastal (e.g. Stasko et al. 1976, Quinn and terHart 1987, Madison et al. 1972) and offshore (Ogura and Ishida 1992, 1995) regions. However, these observations have been limited to a few days because of the difficulty of tracking fish 24 hours per day. Archival tags can be used to monitor fish movements for much longer periods, but at a much lower spatial resolution than ultrasonic tags (e.g. DeLong et al. 1992), however these tags have not yet been used on salmon and must be recovered to download the data. To infer interactions between behaviour and the oceanographic environment, there would have to be concurrent monitoring of the appropriate oceanographic variables. Measurement of currents, temperature and salinity is feasible on small scales, but large scale sampling is problematic. Other potentially important factors are difficult or impossible to measure, including predator and prey distributions and odour concentrations. Assuming that the appropriate environmental factors could be measured, there would likely have to be representative sampling of the salmon distribution in space and time, and replication of the tagging over a number of years to describe the correct interactions. It is conceivable that these types of studies would not necessarily discriminate the proximal mechanisms of migration route variation, but these observations would provide a substantial contribution toward understanding mesoscale behaviour in general.

Fisheries observations provide opportunistic collection of migratory timing and coastal migration route data that is useful for migration studies, however, the data quality must be carefully examined. Chapters (2) and (3) examined the statistical properties of harvest rate and coastal migration route estimates generated from fisheries data, and

described how migration route estimates could be calculated with relative measures of uncertainty. If these methods were applied to specific fisheries, then variation in migration routes could be described within years and possibly even among stocks. Stock-specific estimates of migratory timing through coastal fisheries already exist. As with the existing northern diversion rate time series, migratory timing estimation is dependent on run-reconstruction and its assumptions, but the uncertainty in timing has never been explored. The methods of chapters (2) could be easily modified to estimate the relative error associated with timing estimates. Migration route and timing estimates can be used to make inferences about spatial distributions prior to the fisheries. The arrival of a fish in a particular fishery will depend on many previous factors, including the location prior to embarking on the homeward migration, the date of initiation of the homeward migration, the choice of migration route (both offshore and coastal), and the migration rate. Time series of stock-specific migration routes and timing would increase the resolution at which interactions between migration behaviour and environmental variability could be examined. These observations could also be used as behavioural constraints in process-based migration models such as the individual-based model of chapter (4).

Experimental work will ultimately be required to sort out which factors are important for migrating salmon, particularly if observable quantities co-vary, as they tend to in oceanographic systems. There have been experiments conducted to test the magnetic and visual sensory abilities of sockeye for orientation (e.g. Groot et al. 1986, Quinn and Brannon 1982), and responses to water properties (e.g. Piercey et al. 1993).

These experimental manipulations are crucial to understanding migration behaviour and provide the only means of confidently distinguishing among hypotheses. However, it is not possible to conduct experiments on all the potentially important migration mechanisms, and it is difficult to extrapolate from small experimental systems to the whole of the NE Pacific Ocean.

Focusing on the northern diversion rate as the annual proportion of salmon migrating through Johnstone Strait results in a tendency to simplify discussion of mechanisms that may be driving the variability. The northern diversion rate is a cumulative result from migratory decision processes of millions of individuals distributed throughout large parts of the NE Pacific Ocean over a period of years. Perhaps there are very few factors influencing migration variation that actually propagate through to affect the observed coastal approach route, but the potential for complicated non-linear dynamics is enormous. If multiple factors are important, several years of measuring the appropriate factors, waiting for informative contrast, would likely be required to sort out the importance of each. And one could never be certain that additional important factors would not arise in the future.

The most frequently used quantitative method of examining coastal migration route variability has been the correlation of annual migration route estimates with environmental indices. While this approach has resulted in a large number of publications, the proposed mechanisms are vaguely defined. This approach is criticized because of the high probability of generating spurious relationships (e.g. Walters and

Collie 1988), and the lack of movement toward defining mechanisms. I do believe that the approach has a role if used cautiously within a larger framework of study (e.g. Tyler 1992). However, in this system, correlations have not provided much guidance for additional fieldwork and are not likely to advance the understanding of this particular system any further. If temporal and spatial variations in multiple factors are affecting the diversion rate, then non-linear dynamics probably dominate, and cannot be adequately described by simple indices.

I believe that dynamic, spatially-explicit models will remain the most useful tool for exploring assertions about the mechanisms that drive Fraser River sockeye coastal migration rate variation, but these models can only evolve with input from field observations and experiments. One might be justified in criticizing the individual-based model complexity (chapter (4)), since it was arguably no more enlightening than the correlation approach. However, by admitting enough complexity to explore explicit, field-testable mechanisms, these types of models establish a framework within which additional information can be integrated. Poorly quantified, but biologically meaningful parameters reflect uncertainty about the state of knowledge of the system, and define issues that must be resolved to attain the desired level of understanding. Process-based modelling cannot prove that a mechanism is correct (e.g. Oreskes et al. 1994), but does provide a framework with which observations and experimental results can be merged, and updated as additional information becomes available. In this way, the evolution of our understanding of the system can progress with internal consistency, even though system dynamics are too complicated to follow in detail without the aid of computers.

## REFERENCES

- Alabaster, J. S. 1990. The temperature requirements of adult Atlantic salmon, *Salmo salar* L., during their upstream migration in the River Dee. J. Fish. Biol. 37: 659-661.
- Barber, F. G. 1983. Inshore migration of adult Fraser sockeye, a speculation. Can. Tech. Rep. Fish. Aquat. Sci. 1162: iv +14 p.
- Cave, J. D., and W. J. Gazey. 1994. A preseason simulation model for fisheries on Fraser River sockeye salmon (*Oncorhynchus nerka*). Can. J. Fish. Aquat. Sci. 51: 1535-1549.
- Cooper, J. C. and A. T. Scholz. 1976. Homing of artificially imprinted steelhead (rainbow) trout, *Salmo gairdneri*. J. Fish. Res. Board Can. 33: 826-829
- Dat, C. G., P. H. LeBlond, K. A. Thomson, and W. J. Ingraham. 1995. Computer simulations of homeward-migrating Fraser River sockeye salmon: is compass orientation a sufficient direction-finding mechanism in the north-east Pacific Ocean?
- DeLong, R. L., B. S. Stewart, and R. D. Hill. 1992. Documenting migrations of northern elephant seals using day length. Marine Mammal Science 8(2): 155-159.
- Favorite, F. 1961. Surface temperature and salinity of the Washington and British Columbia coasts, August, 1958 and 1959. J. Fish Res. Board Can. 18: 311-319.
- Fraser, J. A. 1995. Fraser River Sockeye 1994: Problems and Discrepancies. Report of the Fraser River Sockeye Public Review Board. Public Works and Government Services Canada. 131 p.
- French, R. R., H. Bilton, M. Osako, and A. Hartt. 1976. Distribution and origin of sockeye salmon (*Oncorhynchus nerka*) in offshore waters of the north Pacific Ocean. International North Pacific Fisheries Commission Bulletin 34.
- Gelman, A., J. B. Carlin, H. S. Stern, and D. B. Rubin. 1995. Bayesian Data Analysis. Chapman and Hall. London, UK. 526 p.
- Gilhausen, P. 1960. Migratory behaviour of adult Fraser River sockeye. Int. Pac. Salmon Fish. Comm. Progr. Rep. No. 7.
- Gillis, D. M., R. M. Peterman, and A. V. Tyler. 1993. Movement dynamics in a fishery: application of the ideal free distribution to spatial allocation of effort. Can. J. Fish. Aquat. Sci. 50: 323-333.
- Griffin, D. R. 1955. Bird navigation. pp. 154-197. In: A. Wolfson (ed.) Recent studies in



avian biology. University of Illinois Press, Urbana.

- Groot, C., and K. Cooke. 1987. Are the migrations of juvenile and adult Fraser River sockeye salmon (*Oncorhynchus nerka*) in near-shore waters related? p. 53-60. In H.D. Smith, L. Margolis, and C.C. Wood led. Sockeye salmon (*Oncorhynchus nerka*) population biology and future management. Can. Spec. Publ. Fish. Aquat. Sci. 96.
- Groot, C. and T. P. Quinn. 1987. Homing migration of sockeye salmon to the Fraser River. Fish. Bull. 85: 455-469.
- Groot, C., T. P. Quinn and R. J. Hara. 1986. Responses of migrating adult sockeye salmon (*Oncorhynchus nerka*) to population-specific odours. Can. J. Zool. 64: 926-932.
- Hamilton, K. 1985. A study of the variability of the return migration route of Fraser River sockeye salmon (*O. nerka*). Can. J. Zool. 63: 1930-43.
- Hawryshyn, C. W. and A. E. Bolger. 1990. Spatial orientation of trout to partially polarized light. Journal of Comparative Physiology A. 167: 691-697.
- Healey, M. C., and C. Groot. 1987. Marine migration and orientation of ocean-type chinook and sockeye salmon. Am. Fish. Soc. Symp. 1: 298-312.
- Hsieh, W. W., W. G. Lee, and L. A. Mysak. 1991. Using a numerical model of the Northeast Pacific Ocean to study the interannual variability of the Fraser River sockeye salmon (*Oncorhynchus nerka*). Can. J. Fish. Aquat. Sci. 48: 623-630.
- Ingraham, W. J. and R. K. Miyahara. 1988. Ocean surface current simulations in the North Pacific and Bering Sea (OSCURS - numerical model). U.S. Dep. Commer. NOAA Tech. Memo. NMFS F/NWC - 130: 155p.
- Ingraham, W. J. and R. K. Miyahara. 1989. Tuning the OSCURS numerical model to ocean surface current measurements in the Gulf of Alaska. U.S. Dep. Commer. NOAA Tech. Memo. NMFS F/NWC - 168: 67p.
- Killick, S. R., and W. A. Clemens. 1963. The age, sex ratio and size of Fraser River sockeye salmon 1915-1960. Int. Pac. Salmon Comm. Bull. XIV.
- Kolody, D. and M. Healey. 1998. Numerical simulations of Fraser River sockeye salmon homing migration routes in a dynamic marine environment. N. Pac. Anadr. Fish. Comm. Bull. No. 1: 118-128.
- Leblond, P. H., D. A. Griffin and R. E. Thomson. 1994. Surface salinity variations in the Juan de Fuca Strait: test of a predictive model. Continental shelf Research. 14 1:37-56.

- Lohman, K. L. and C. M. F. Lohman. 1996. Detection of magnetic field intensity by sea turtles. *Nature* 380: 59-61.
- Leggett, W. C. 1977. The ecology of fish migrations. *Annu. Rev. Ecol. Syst.* 8: 285-308.
- Madison, D. M., R. M. Horrall, A. B. Stasko and A. D. Hasler. 1972. Migratory movements of adult sockeye salmon (*Oncorhynchus nerka*) in coastal British Columbia as revealed by ultrasonic tracking. *J. Fish. Res. Board Can.* 21: 995-1018.
- Major, R. L. and J. L. Mighell. 1966. Influence of Rocky Reach dam and the temperature of the Okanogan River on the upstream migration of sockeye salmon. *Fish. Bull.* 66: 131-147.
- Michalewicz, Z. 1994. Genetic Algorithms + Data Structures = Evolution Programs, second, extended edition. Springer - Verlag. Berlin. 340 p.
- Moore, B. R. 1980. Is the pigeon's map geomagnetic? *Nature*. 285: 69-70.
- Ogura, M. and Y. Ishida. 1995. Homing behavior and vertical movements of four species of Pacific salmon (*Oncorhynchus* spp.) in the central Bering Sea. *Can. J. Fish. Aquat. Sci.* 52: 532-540.
- Ogura, M. and Y. Ishida. 1992. Swimming behavior of coho salmon, *Oncorhynchus kisutch*, in the open sea as determined by ultrasonic telemetry. *Can. J. Fish. Aquat. Sci.* 49: 453-457.
- Oreskes, N., K. Shrader-Frechette, and. Belitz. 1994. Verification, validation, and confirmation in the Earth sciences. *Science*. 263: 641-646.
- Pascual, M. A., and T. P. Quinn. 1991. Evaluation of alternative models of the coastal migration of adult Fraser River sockeye salmon (*Oncorhynchus nerka*). *Can. J. Fish. Aquat. Sci.* 48: 799-810.
- Patten, B. C. 1964. The rational decision process in salmon migration. *J. Cons. Int. Explor. Mer.* 28: 410-417.
- Piercy, G. E., I. K. Birtwell, J. S. Korstrom, G. M. Kruzynski, C. M. Langton and S. Spohn. 1993. Behavioural responses of adult sockeye salmon (*Oncorhynchus nerka*) under simulated estuarine conditions and salt water hypoxia. *Can. Data Rep. Fish. Aquat. Sci.* 906: 276p.
- PSC. 1995. Pacific Salmon Commission run-size estimation procedures: an analysis of the 1994 shortfall in escapement of late-run Fraser River sockeye salmon. Pacific Salmon Commission technical report no. 6.

- Quinn, T. P. and E. L. Brannon. 1982. The use of celestial and magnetic cues by orienting sockeye salmon smolts. *J. Comp. Physiol.* 147: 547-552.
- Quinn, T. P. 1980. Evidence for celestial and magnetic compass orientation in lake migrating sockeye salmon fry. *J. Comp. Physiol.* 137: 243-248.
- Quinn, T. P. 1988. Estimated swimming speeds of migrating adult sockeye salmon. *Can. J. Zool.* 66: 2160-2163.
- Quinn, T. P. and B. A. terHart. 1987. Movements of adult sockeye salmon (*Oncorhynchus nerka*) in British Columbia coastal waters in relation to temperature and salinity stratification: ultrasonic telemetry results, p. 61-77. In H. D. Smith, L. Margolis, and C.C. Wood (ed.) Sockeye salmon (*Oncorhynchus nerka*) population biology and future management. *Can. Spec. Publ. Fish. Aquat. Sci.* 96.
- Royal, L. A. and J. P. Tully. 1961. Relationships of variable oceanographic factors to migration and survival of Fraser River salmon. *Cal. Coop. Ocean. Fish. Invest. Rep.* 8, Dep. Fish Game, CA, USA.
- Saila, S. B., and R. A. Shappy. 1963. Random movement and orientation in salmon migration. *J. Cons. Int. Explor. Mer.* 28: 153-166.
- Shimuzu, M., H. Kudo, H. Ueda, A. Hara, K. Shimakazi, and K. Yamauchi. 1993. Identification and immunological properties of an immunological-specific protein in kokanee salmon (*Oncorhynchus nerka*). *Zoological Science* 10: 287-294.
- Starr, P. J., A. T. Charles, and M. A. Henderson. 1984. Reconstruction of British Columbia sockeye salmon (*Oncorhynchus nerka*) stocks: 1970-1982. *Can. MS Rep. Fish. Aquat. Sci.* 1780: 123 p.
- Starr, P., and R. Hilborn. 1988. Reconstruction of harvest rates and stock contribution in gauntlet salmon fisheries: application to British Columbia and Washington sockeye (*Oncorhynchus nerka*). *Can. J. Fish. Aquat. Sci.* 45: 2216-2229.
- Stasko, A. B., R. M. Horrall and A. D. Hasler. 1976. Coastal movements of adult sockeye salmon (*Oncorhynchus nerka*) observed by ultrasonic tracking. *Trans. Am. Fish. Soc.* 105: 64 - 71.
- Thomson, K. A., W. J. Ingraham, M. C. Healey, P. H. Leblond, C. Groot, and C. G. Healey. 1992. The influence of ocean currents on latitude of landfall and migration speed of sockeye salmon returning to the Fraser River. *Fish. Oceanogr.* 1(2): 163-179.
- Thomson, R. E. 1981. Oceanography of the British Columbia coast. *Can. Spec. Publ. Fish. Aquat. Sci.* 56: 291p.

- Tully, J. P., A. J. Dodimead, and S. Tabata. 1960. An anomalous increase of temperature in the ocean off the Pacific Coast of Canada through 1957 and 1958. *J. Fish. Res. Board Can.* 17: 61-80.
- Tyler, A. 1992. A context for recruitment correlations: why marine fisheries biologists should still look for them. *Fisheries Oceanography* 1:97-107.
- Tyler, J. A. and K. A. Rose. 1994. Individual variability and spatial heterogeneity in fish population models. *Reviews in Fish Biology and Fisheries*. 4: 91-123.
- Verhoeven, L. A. and E. B. Davidoff. 1962. Marine Tagging of Fraser River sockeye salmon. *Int. Pac. Salmon Fish. Comm. Bull.* 13: 132 p.
- Walters, C. J. and Collie, J. S. 1988. Is research on environmental factors useful to fisheries management? *Can. J. Fish. Aquat. Sci.* 45: 1848-1854.
- Walters, C., and D. Ludwig. 1994. Calculation of Bayes posterior probability distributions for key population parameters. *Can. J. Fish. Aquat. Sci.* 51: 713-722.
- Ware, D. M. and G. A. McFarlane. 1989. Fisheries production domains in the Northeast Pacific Ocean, p. 359-379. *In* R. J. Beamish and G. A. McFarlane [ed.] *Effects of ocean variability on recruitment and an evaluation of parameters used in stock assessment models*. *Can. Spec. Publ. Fish. Aquat. Sci.* 108.
- Welch, D. W., A. I. Chigirinsky, and Y. Ishida. 1995. Upper thermal limits on the oceanic distribution of Pacific Salmon (*Oncorhynchus* spp.) in the spring. *Can. J. Fish. Aquat. Sci.* 52: 489-503.
- Welch, D. W., Y. Ishida, and K. Nagasawa. 1998. Thermal limits and ocean migrations of sockeye salmon (*Oncorhynchus nerka*): long term consequences of global warming. *Can. J. Fish. Aquat. Sci.* 55: 937-948.
- Wickett, W. P. 1977. Relationship of coastal oceanographic factors to the migration of Fraser River sockeye salmon (*Oncorhynchus nerka* W.) *Int. Comm. Explor. Mer. CM* 1977/M.26: 18pp.
- Woodey, J.C. 1987. In-season management of Fraser River sockeye salmon (*Oncorhynchus nerka*): meeting multiple objectives, p. 367-374. *In* H.D. Smith, L. Margolis, and C.C. Wood led. *Sockeye salmon (Oncorhynchus nerka) population biology and future management*. *Can. Spec. Publ. Fish. Aquat. Sci.* 96.
- Xie, L. and W. W. Hsieh. 1989. Predicting the return migration route of the Fraser River sockeye salmon (*Oncorhynchus nerka*). *Can. J. Fish. Aquat. Sci.* 46: 1287-1292.